Semiconductor detectors

- Tracking detectors in High Energy Physics
- Energy measurement of charged particles and gammas in nuclear physics

Semi-conductors

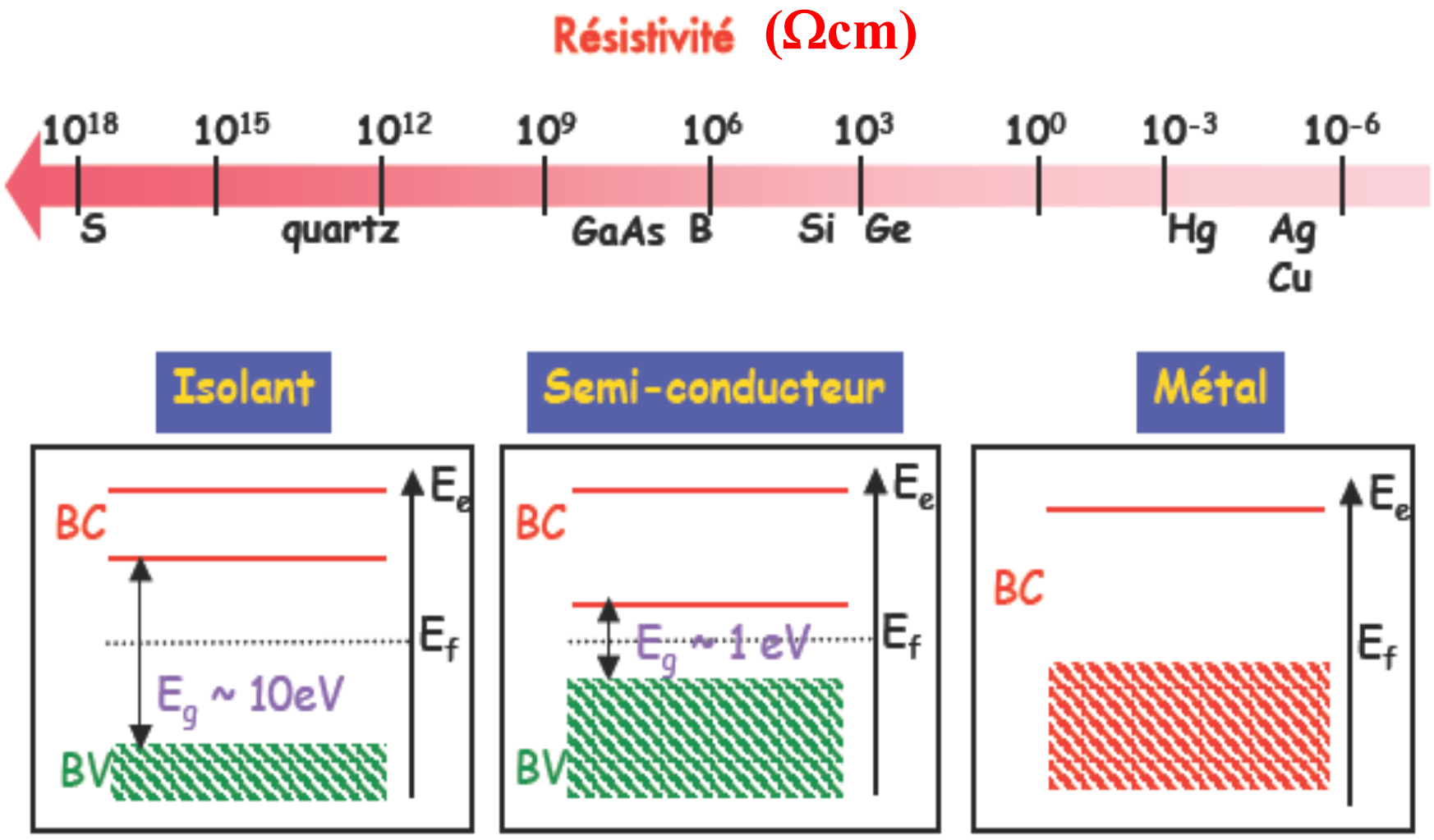

„Doped“ Semi-conductors

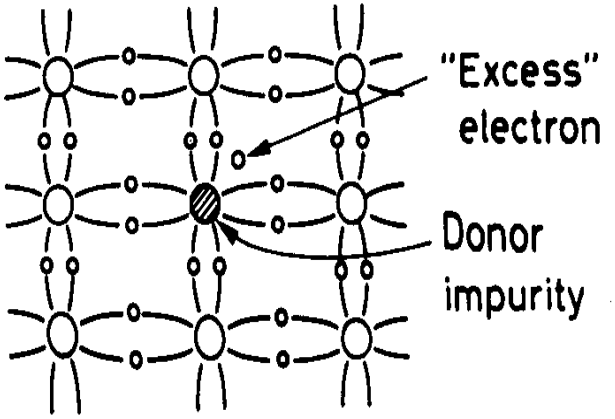

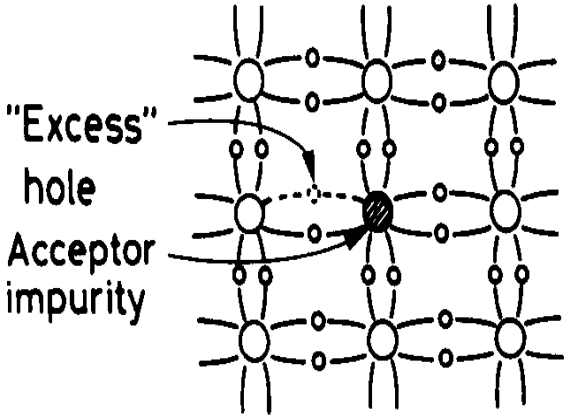

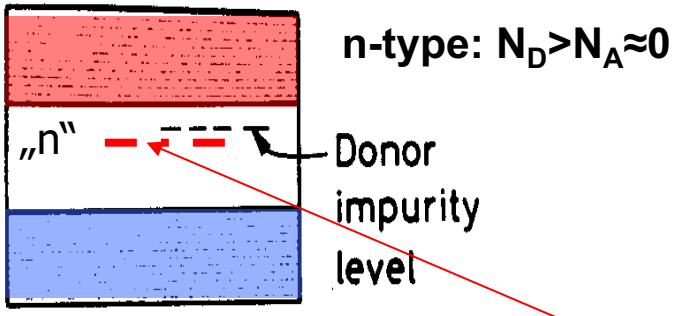

n-type: $N_D > N_A \approx 0$

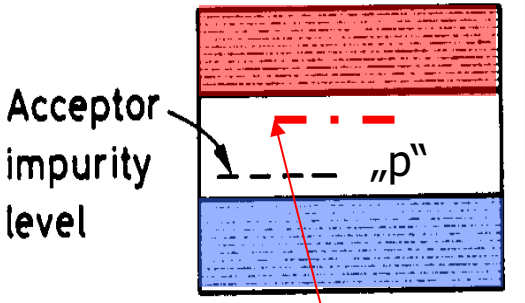

p-type: $N_A > N_D \approx 0$

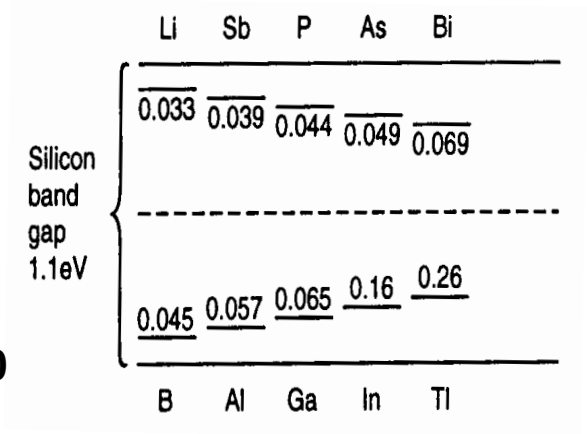

Energy levels within the band gap corresponding to various n- and p-type dopants [6]

Intrinsic: 1.5 10^{10}/cm³ (N_A = 6.022 10^{23}/cm³ !!)

n, p : 10^{13}/cm³

n^+, p^+ : 10^{20}/cm³

Impurities

- **traps**
- **recombination**

W.Dulinski

Semi-conductor detectors

Material	E_g [eV]	w [eV]	Mobility (velocity/E)		τ_e [s]	τ_h [s]	density	Z [a.m.u]
			μ_e [cm^2/Vs]	μ_h [cm^2/Vs]			g/cm^3	
C (diamond)	5.5	13	1800	1200	$2\ 10^{-9}$	$2\ 10^{-9}$	3.515	6
Si	1.12	3.61	1350	480	$5\ 10^{-3}$	$5\ 10^{-3}$	2.33	14
Ge	0.67	2.98	3900	1900	$2\ 10^{-5}$	$2\ 10^{-5}$	5.32	32
GaAs	1.42	4.70	8500	450	$5\ 10^{-8}$	$5\ 10^{-8}$	5.32	31,33
CdTe	1.56	4.43	1050	100	$1\ 10^{-6}$	$1\ 10^{-6}$		48,52
HgI_2	2.13	4.20	100	_	$1\ 10^{-6}$	$2\ 10^{-6}$		53,80

$$\frac{dN}{N} = \frac{1}{\sqrt{N}} \; ; \; E \sim N; \quad N = \text{numb. of (e,h)}$$

Parameters Values for Materials Used in Fabricating Semiconductor Radiation Sensors [3]

W.Dulinski

Junction p-n

Formation of a depletion zone

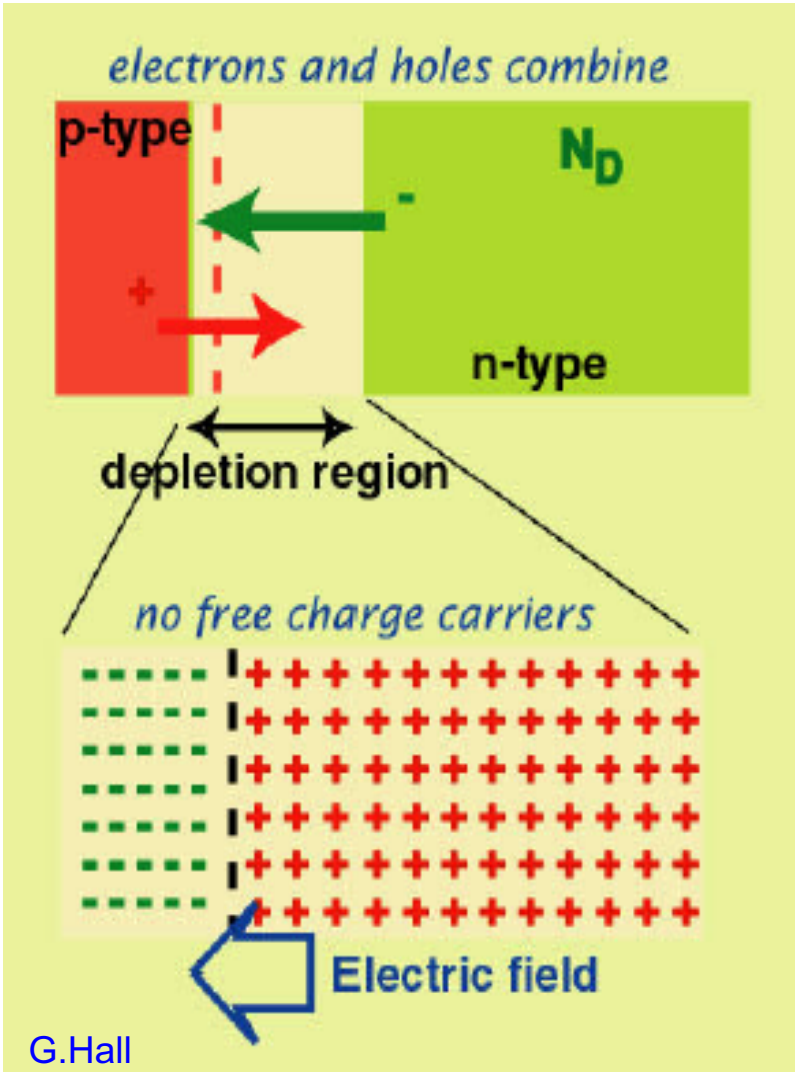

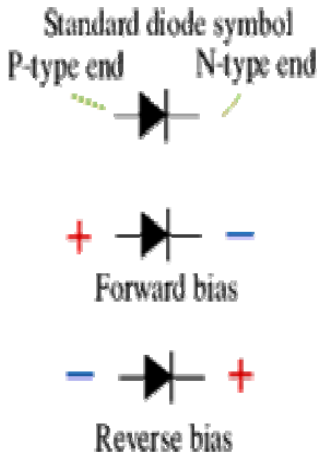

Direct Polarisation

- conduction
- $I \sim I_0[\exp(qV/kT) - 1]$

Inverse Polarisation

- increase of depletion zone
- reduction of capacitance

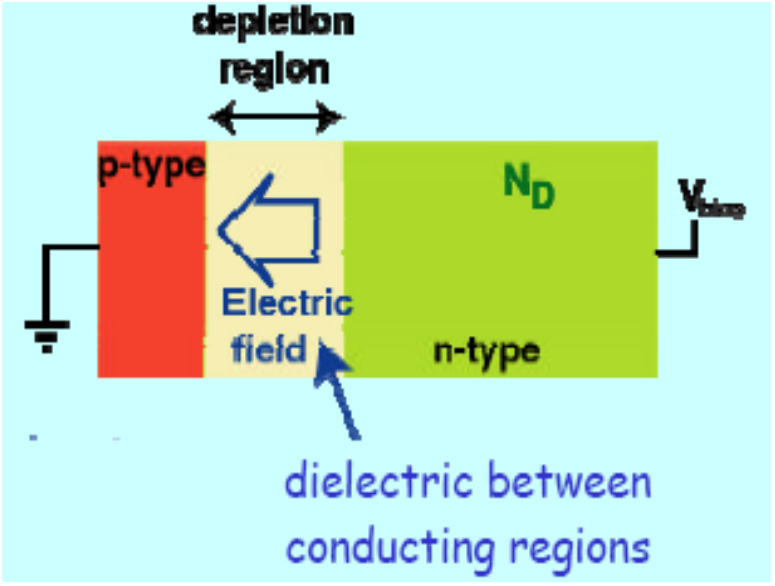

Depth of the depletion zone

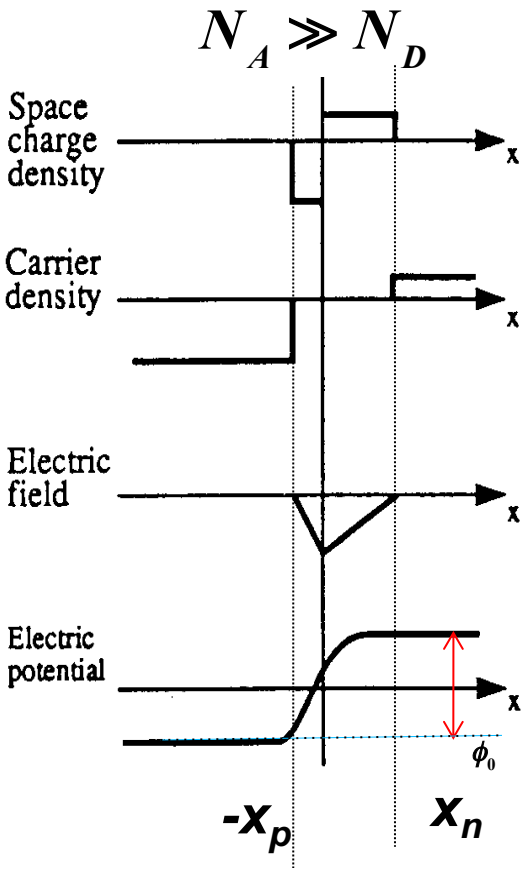

$$\frac{d^2\phi}{dx^2} = -\rho(x)/\varepsilon\ ;\ \ \rho(x) = \begin{cases} eN_D & 0 < x < x_n \\ -eN_A & -x_p < x < 0 \end{cases}$$

$$N_A x_p = N_D x_n$$

$$-E(x) = \frac{d\phi}{dx} = \begin{cases} -\dfrac{eN_D}{\varepsilon}x + C_n\ ; \\ \dfrac{eN_A}{\varepsilon}x + C_p\ ; \end{cases} \Rightarrow \begin{cases} -\dfrac{eN_D}{\varepsilon}(x - x_n)\ ;\ 0 < x < x_n \\ \dfrac{eN_A}{\varepsilon}(x + x_p)\ ;\ -x_p < x < 0 \end{cases}$$

$$\left[d\phi/dx = 0 \ \ à \ \ x = x_n \ \ \ et \ \ à \ \ x = -x_p \right]$$

$$\phi(x) = \begin{cases} -\dfrac{eN_D}{\varepsilon}\left(x^2/2 - x \cdot x_n\right) + C\ ;\ 0 < x < x_n \\ \dfrac{eN_A}{\varepsilon}\left(x^2/2 + x \cdot x_p\right) + C'\ ;\ -x_p < x < 0 \end{cases}$$

Exercise !!!!

continuity à $x = 0 \Rightarrow\ C = C'$;

à $x = x_n, \phi(x) = \phi_0 =$ **contact potentiel;** $\phi(x = -x_p) = 0$

$$\phi_0 = \frac{eN_D}{2\varepsilon}x_n^2 + C \ \ et \ \ 0 = -\frac{eN_A}{2\varepsilon}x_p^2 + C$$

$$\phi_0 = \frac{e}{2\varepsilon}\left(N_D x_n^2 + N_A x_p^2\right)$$

Depth of the depletion zone

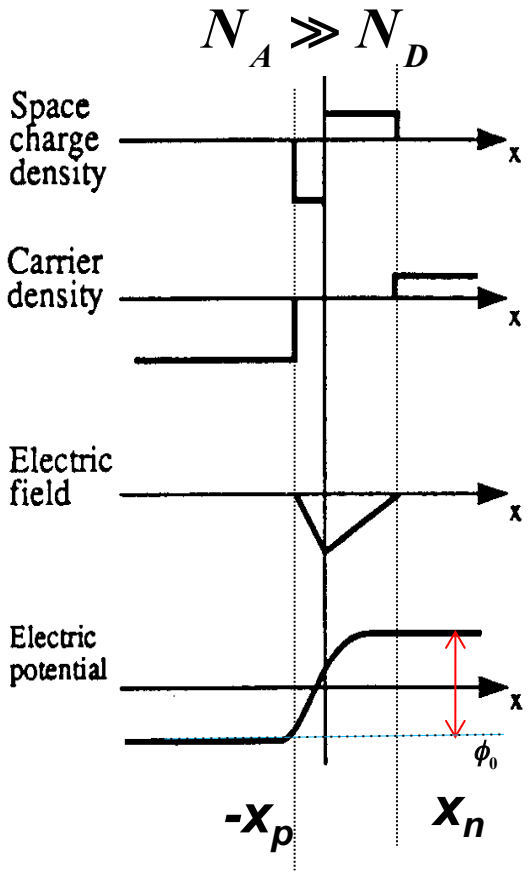

$$\phi_0 = \frac{e}{2\varepsilon}\left(N_D x_n^2 + N_A x_p^2\right); \qquad N_A x_p = N_D x_n$$

$$x_n = \sqrt{\frac{2\varepsilon\phi_0}{eN_D\left(1+N_D/N_A\right)}}\ ;\ x_p = \sqrt{\frac{2\varepsilon\phi_0}{eN_A\left(1+N_A/N_D\right)}}\ ;$$

$$d = x_n + x_p = \sqrt{\frac{2\varepsilon\phi_0}{e}\frac{\left(N_A+N_D\right)}{N_A N_D}}$$

$N_D \gg N_A\ (x_p \gg x_n) \Rightarrow$ depletion in p

$$x_n = \frac{1}{N_D}\sqrt{\frac{2\varepsilon\phi_0}{e}N_A}\ ;\ x_p = \sqrt{\frac{2\varepsilon\phi_0}{eN_A}}\ ;$$

$$d \simeq x_p \simeq \sqrt{\frac{2\varepsilon\phi_0}{eN_A}} = \sqrt{2\varepsilon\rho_p\mu_h\phi_0} \approx 0.32\sqrt{\rho_p\phi_0}\,\mu m \quad (Si)$$

$N_A \gg N_D\ (x_n \gg x_p) \Rightarrow$ depletion in n

$$x_n = \sqrt{\frac{2\varepsilon\phi_0}{eN_D}}\ ; \qquad x_p = \frac{1}{N_A}\sqrt{\frac{2\varepsilon\phi_0}{e}N_D}\ ;$$

Exercise !!!!

$$d \simeq x_n \simeq \sqrt{\frac{2\varepsilon\phi_0}{eN_D}} = \sqrt{2\varepsilon\rho_n\mu_e\phi_0} \approx 0.53\sqrt{\rho_n\phi_0}\,\mu m \quad (Si)$$

$\rho \sim 20000\,\Omega cm,\ \phi_0 \sim 1 Volt \Rightarrow d \sim 75\,\mu m$

Inverse Polarisation

$$d\big|_{V_{bias}} = x_n + x_p = \sqrt{\frac{2\varepsilon\left(\phi_0 + V_{bias}\right)}{e}\frac{\left(N_A + N_D\right)}{N_A N_D}}$$

Holes move to « - »

electrons move to contact "+"

$N_A \gg N_D$

depletion in n-type

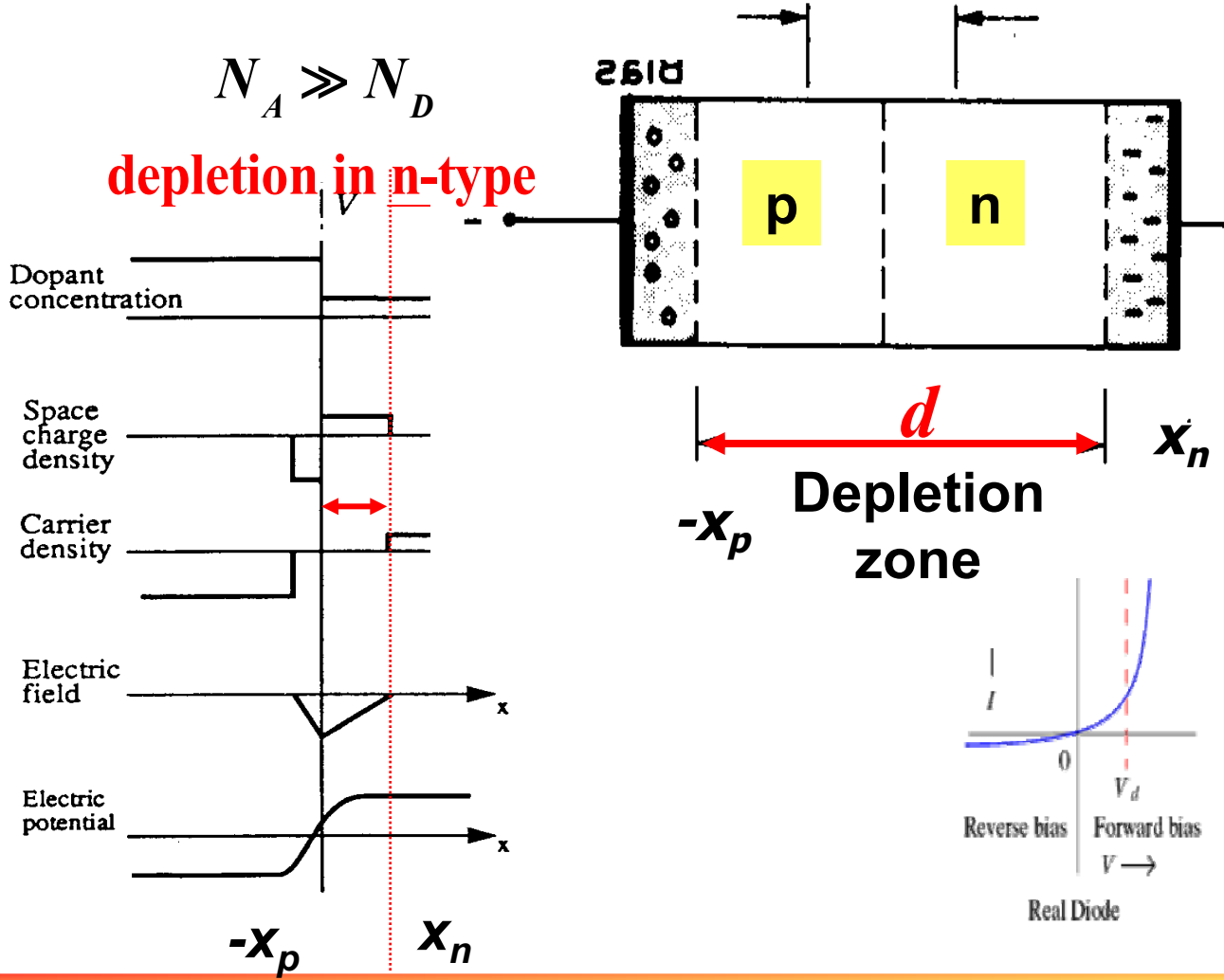

$d \simeq x_n \approx 0.53\sqrt{\rho_n \phi_0}\ \mu m$

$\rho \sim 2 \cdot 10^4\ \Omega cm,\ \phi_0 \sim 1V$

$\Rightarrow d \sim 75\,\mu m$

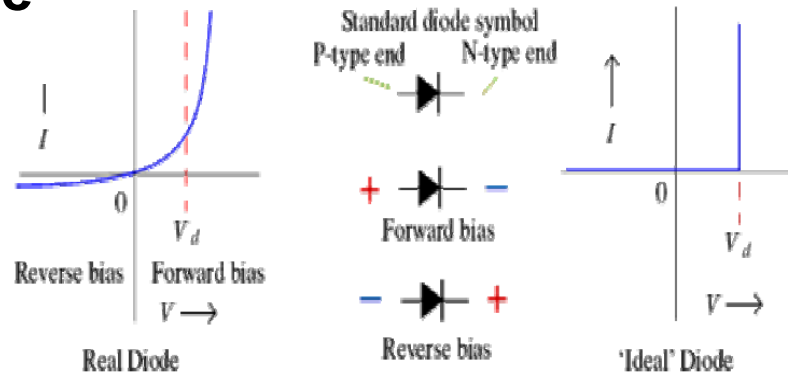

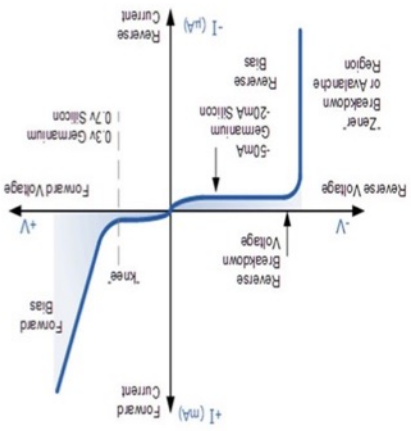

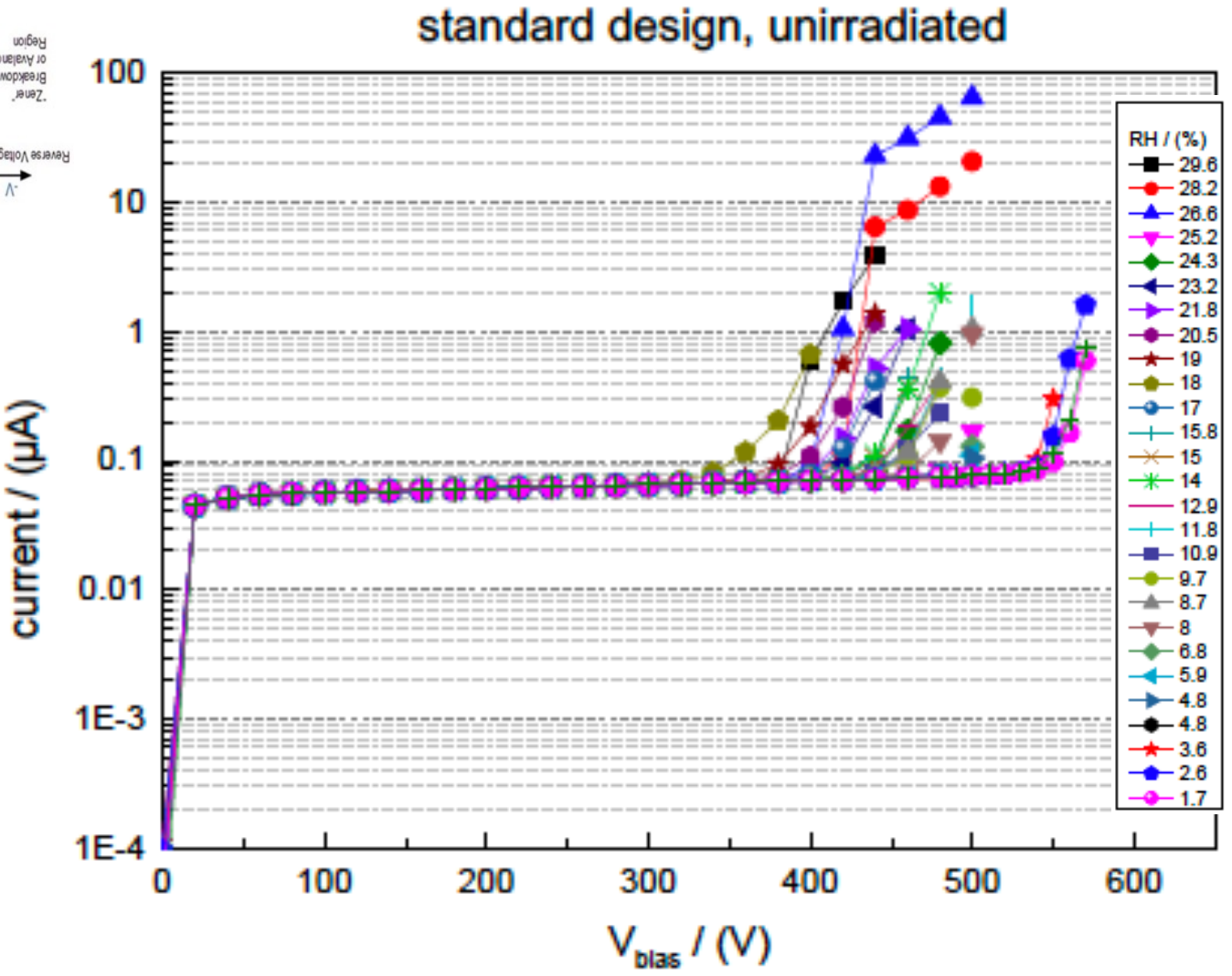

Figure 8.15: IV characteristics for the standard MaPSA light sensor of variant 2 (p-stop conc.= 1×10^{16} cm^{-3} and 2.5 μm deep) in dependence on the humidity RH.

Surface barrier detectors

Junction p-n

0.1-2µm ⇒ perte d'énergie

Diffused or Ion implanted

Diffused & Ion implanted[a]

oxide window

robust, flexible geometry

Shottky barrier

Shottky barrier

metal-silicon junction[b]

thin metal contact more fragile

20 nm ⇒ small energy loss

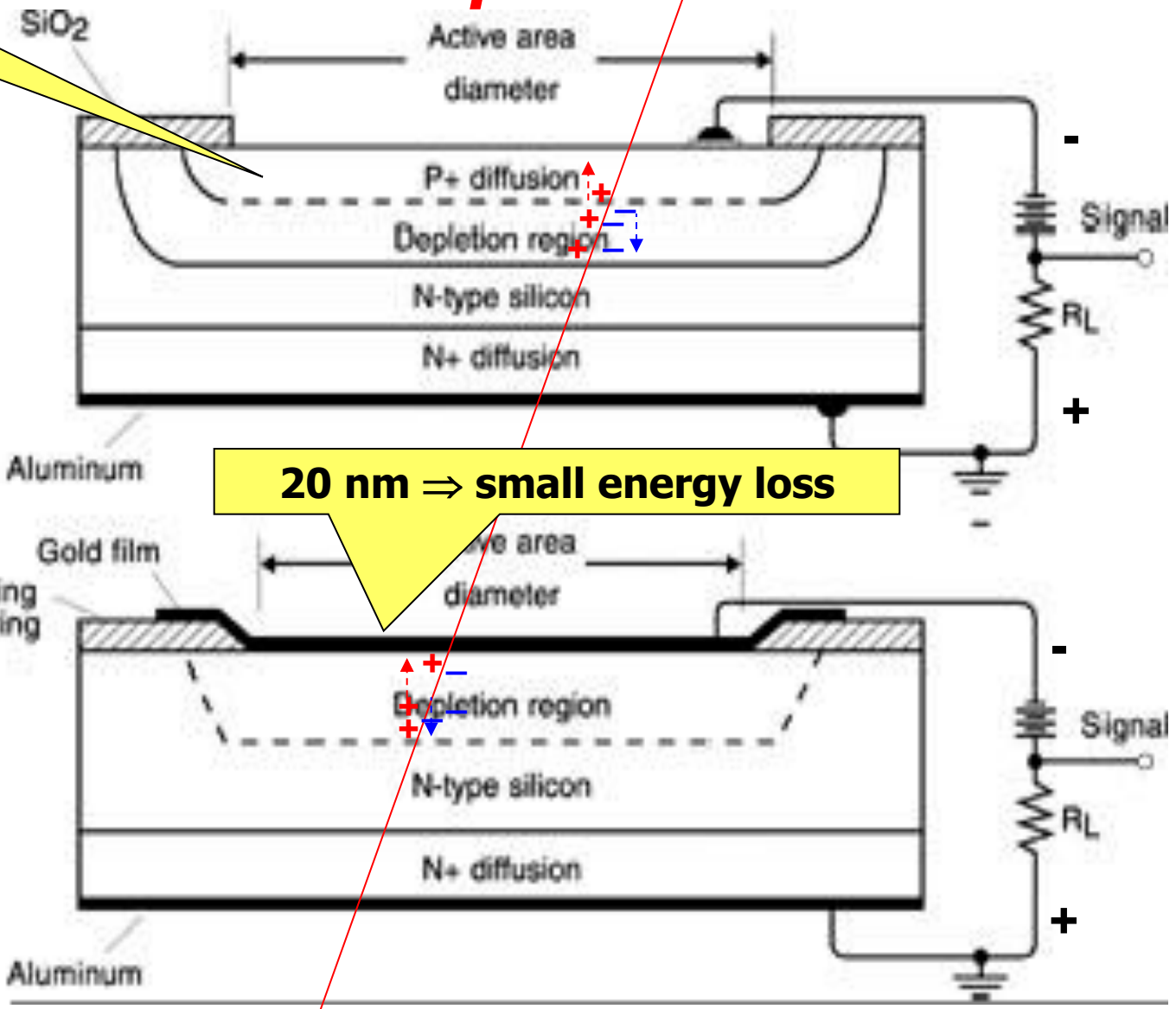

G.Hall

Interaction of charged particles in silicon

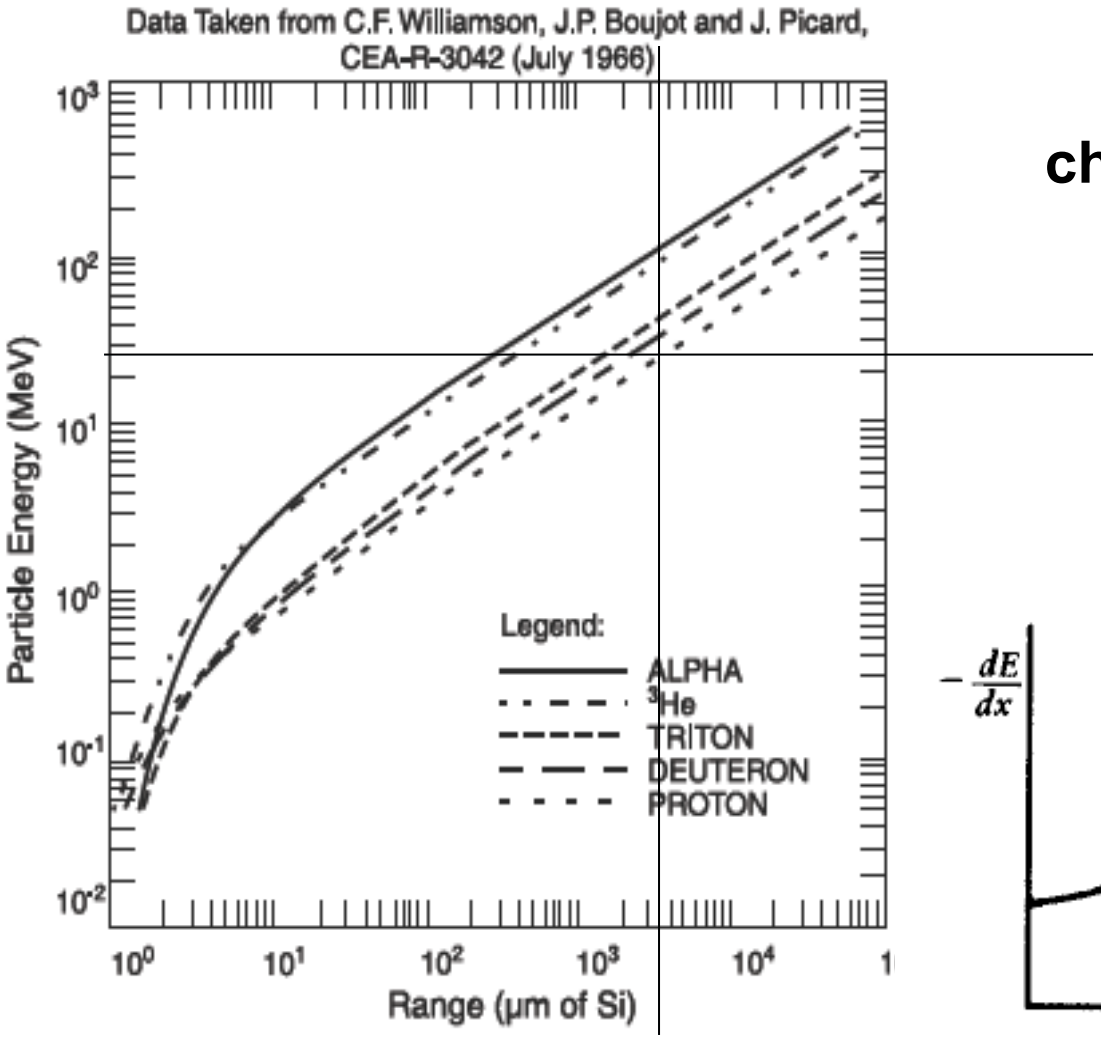

Figure 1.10 Range-Energy Curves in Silicon

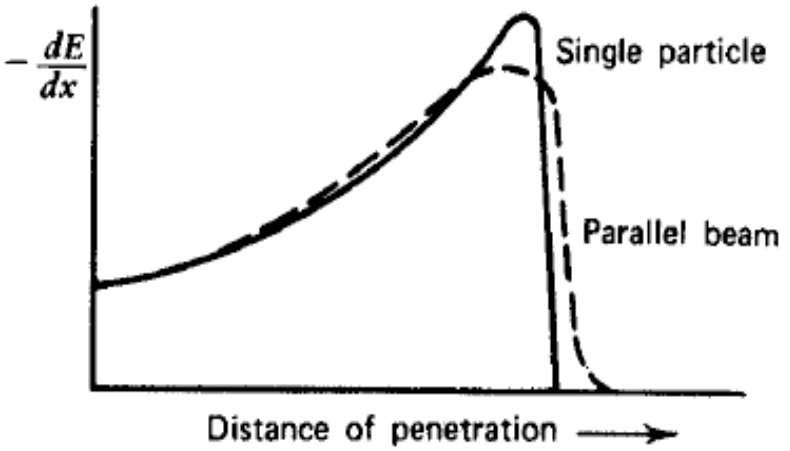

Identification of masses

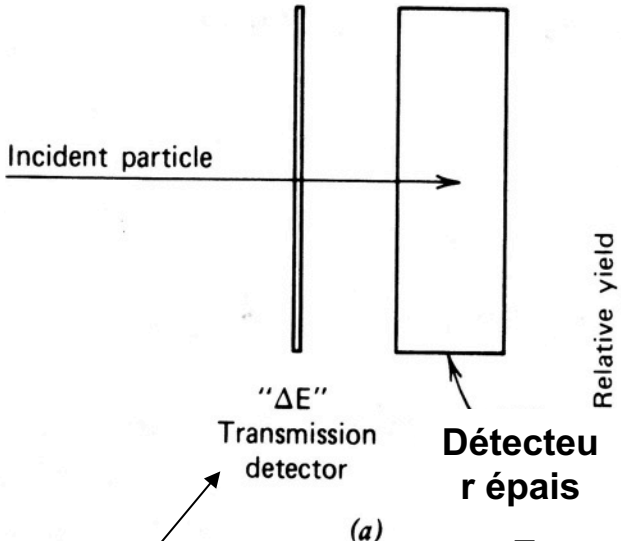

Détecteur épais

E

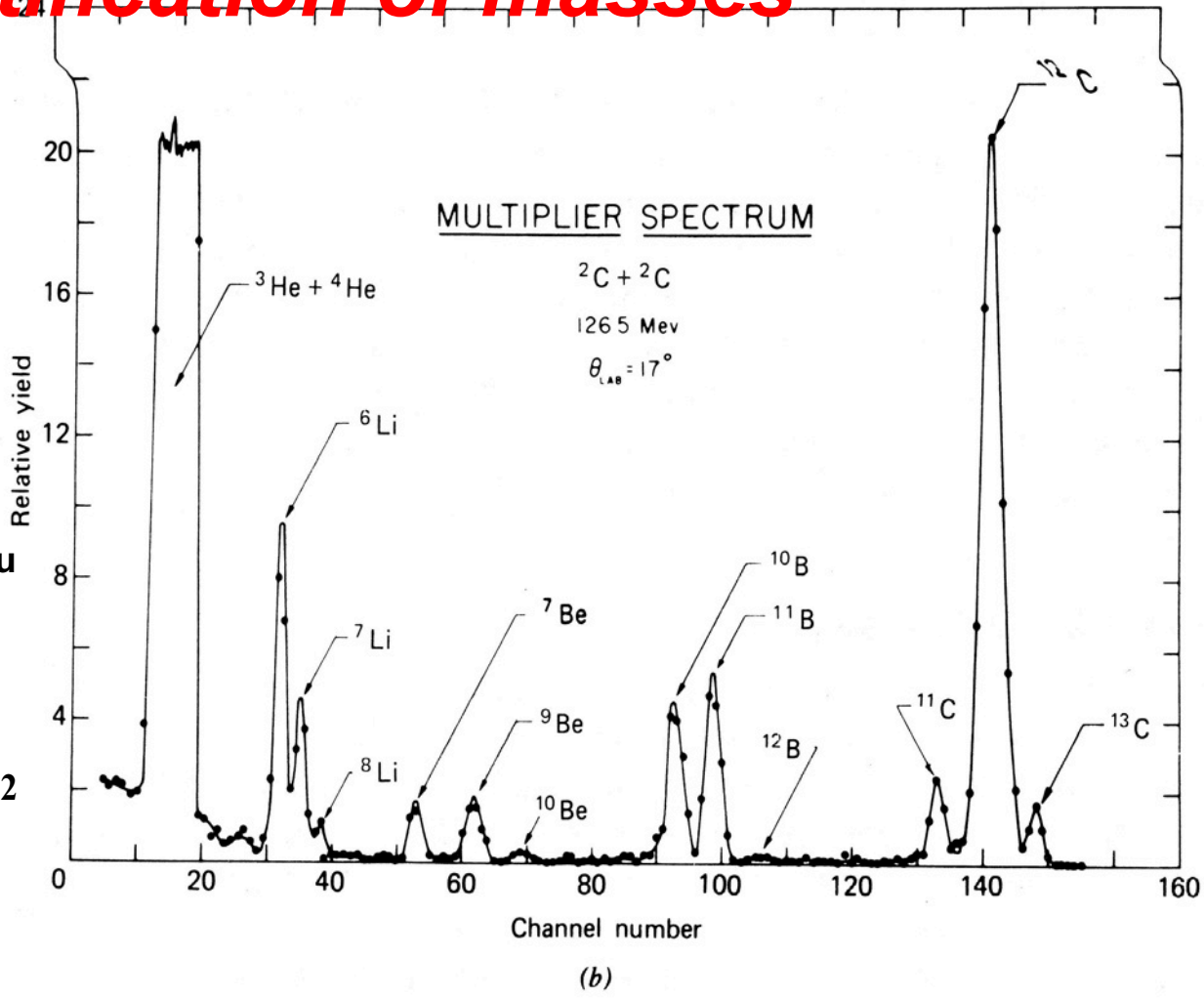

$$\frac{dE}{dx} \propto \frac{1}{v^2}; \quad E_{cin} = \frac{1}{2}mv^2$$

$$\Rightarrow$$

$$\frac{dE}{dx} \times E_{cin} \propto m$$

Figure 11-16 (a) A particle identifier arrangement consisting of tandem ΔE and E detectors operated in coincidence. (b) Experimental spectrum obtained for the $\Delta E \cdot E$ signal product for a mixture of different ions. (From Bromley.[90])

High energies

- SIlicon Tracking Detectors

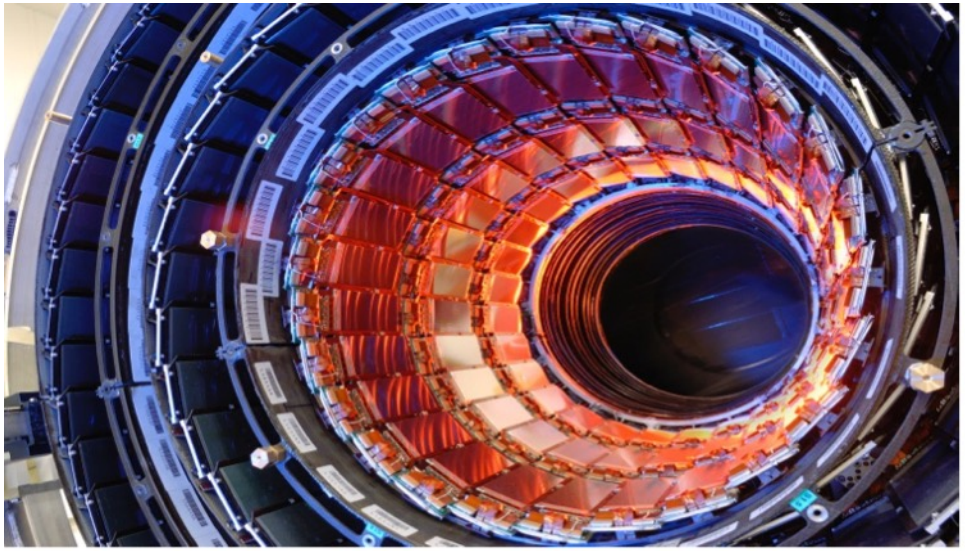

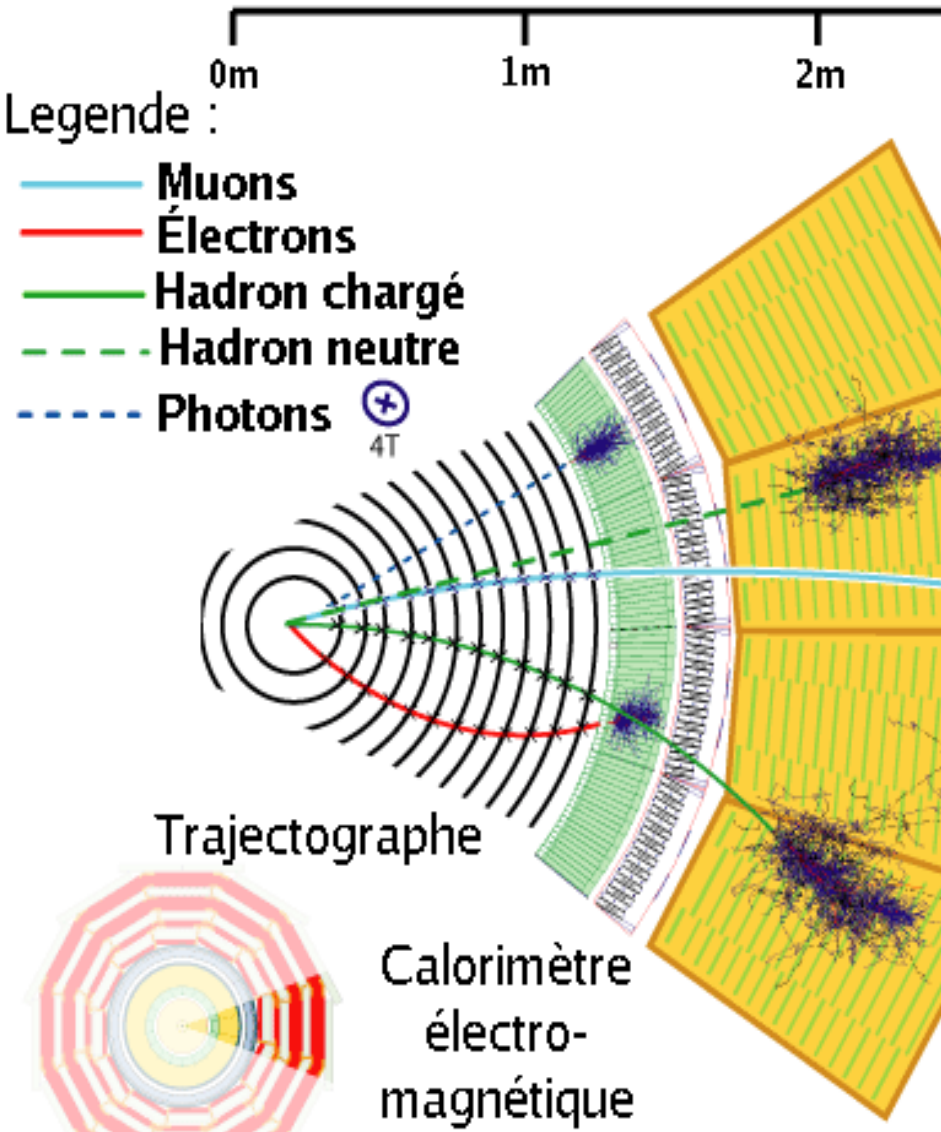

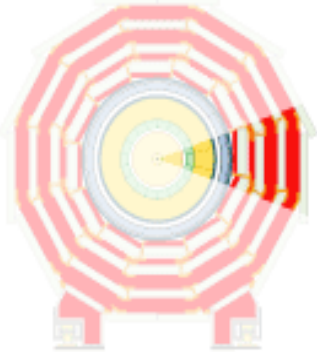

Vue transverse de CMS

Silicon Detector

Every electrode is connected to an amplifier →

Highly integrated readout electronics.

CMS Outer Barrel Module

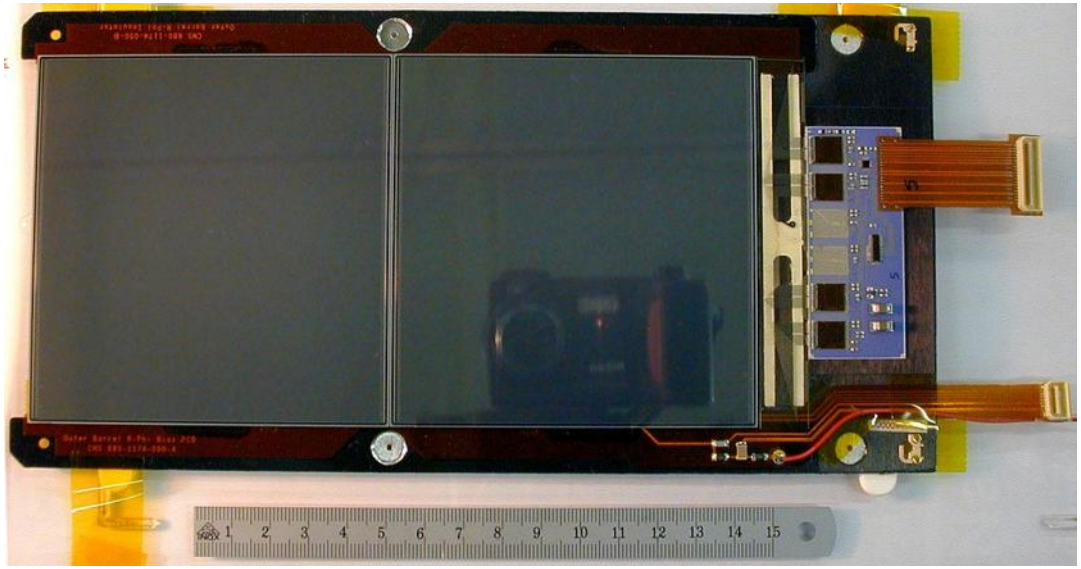

CMS Tracker

Charge Collection time

- Drift velocity of charge carriers $v \approx \mu E$, so drift time, $t_d = d/v = d/\mu E$

Typical values: d=300 μm, E= 2.5 kV/cm,
with μ_e= 1350 cm² / V·s and μ_h= 450 cm² / V·s

$\Rightarrow$ $t_d(e)$= 9ns , $t_d(h)$= 27ns

Micros strip silicon detectors to measure the trajectory of charged particles in a magnetic field

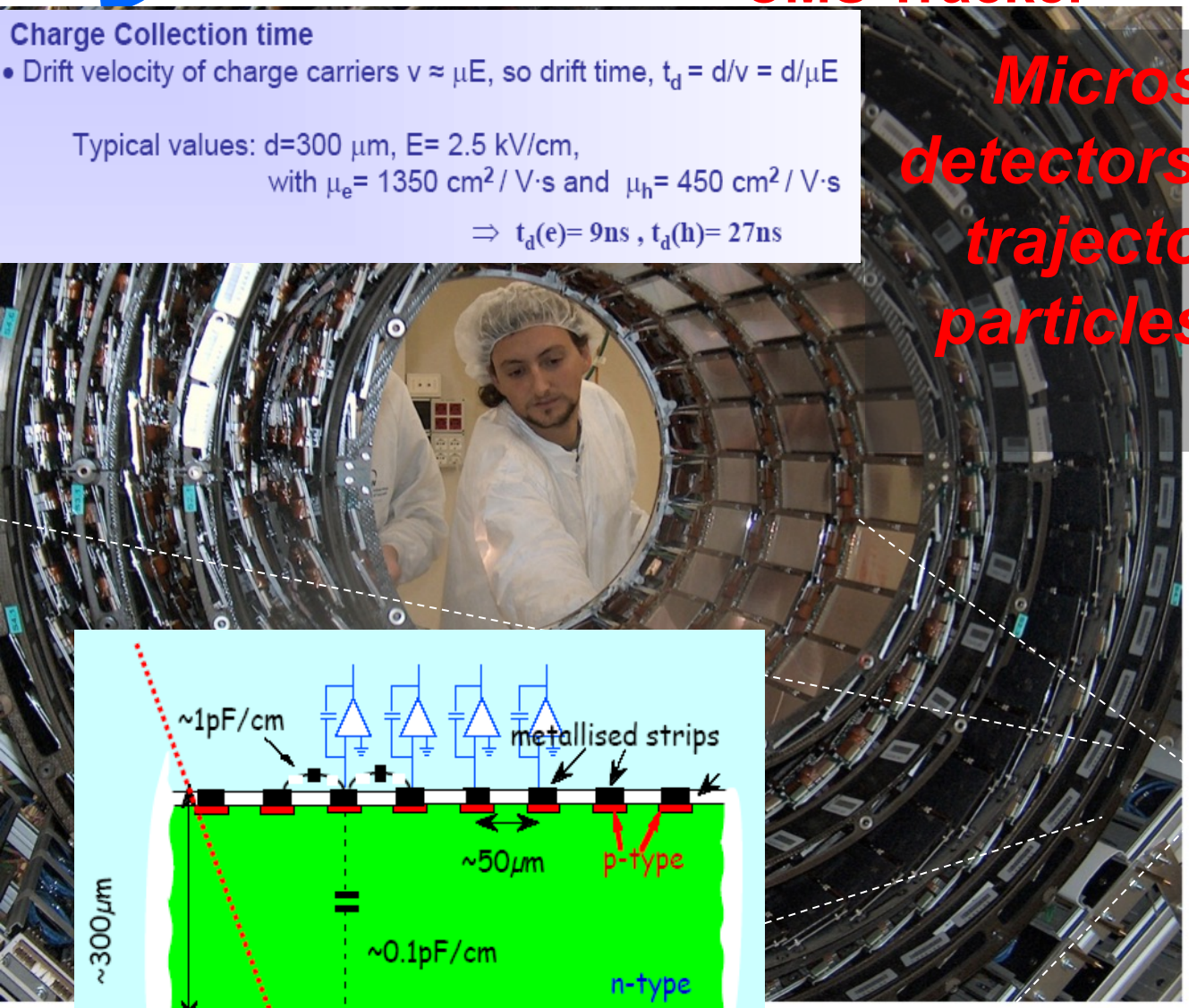

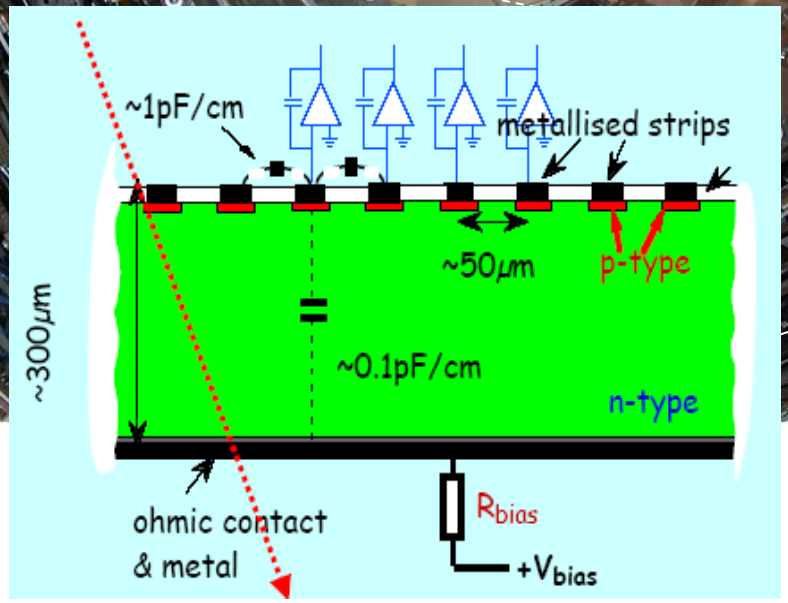

Pixel detectors

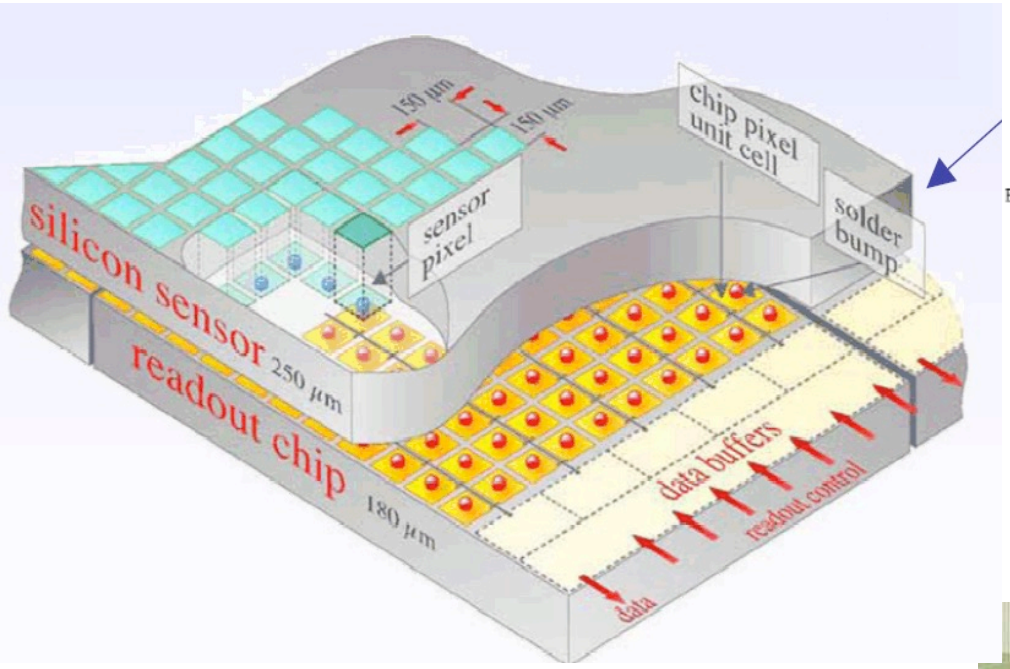

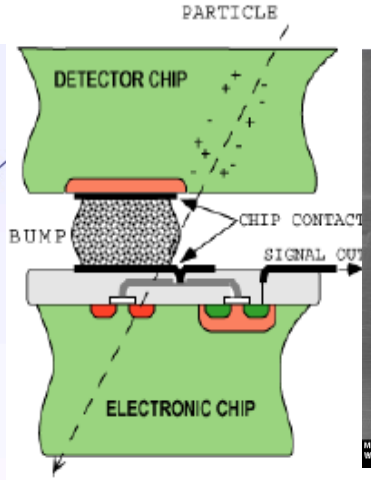

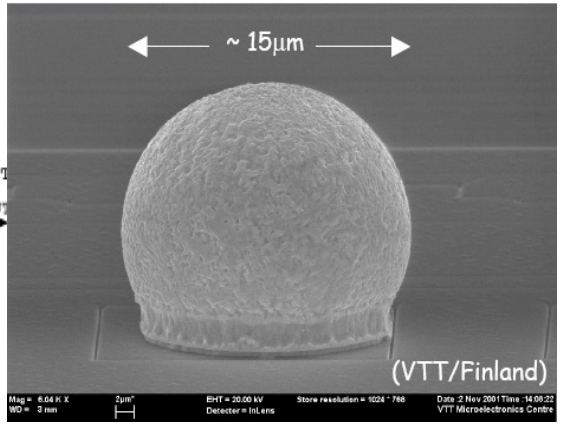

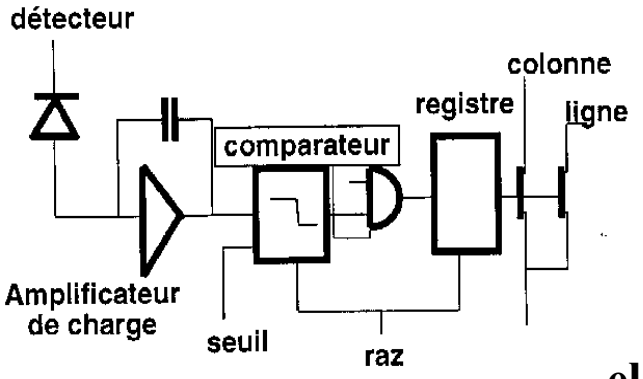

Pixel electronics: complex!

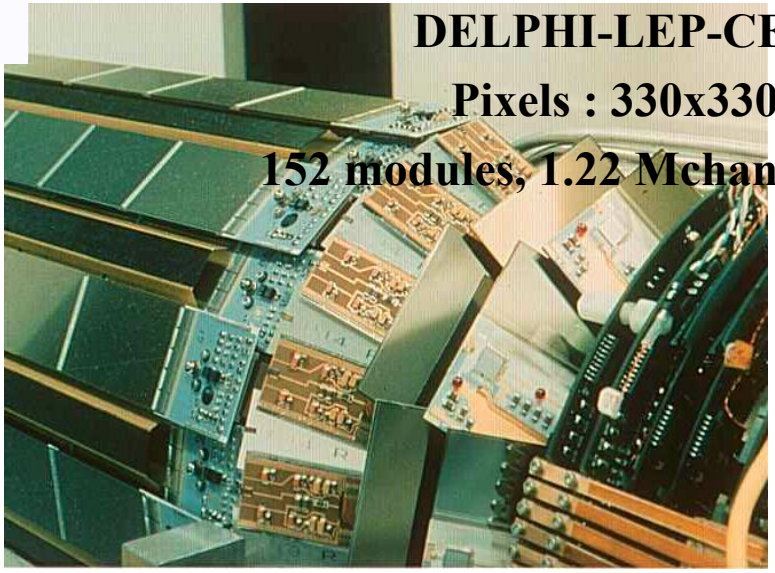

DELPHI-LEP-CERN

Pixels : 330x330 µm

152 modules, 1.22 Mchannels

CMS Pixels

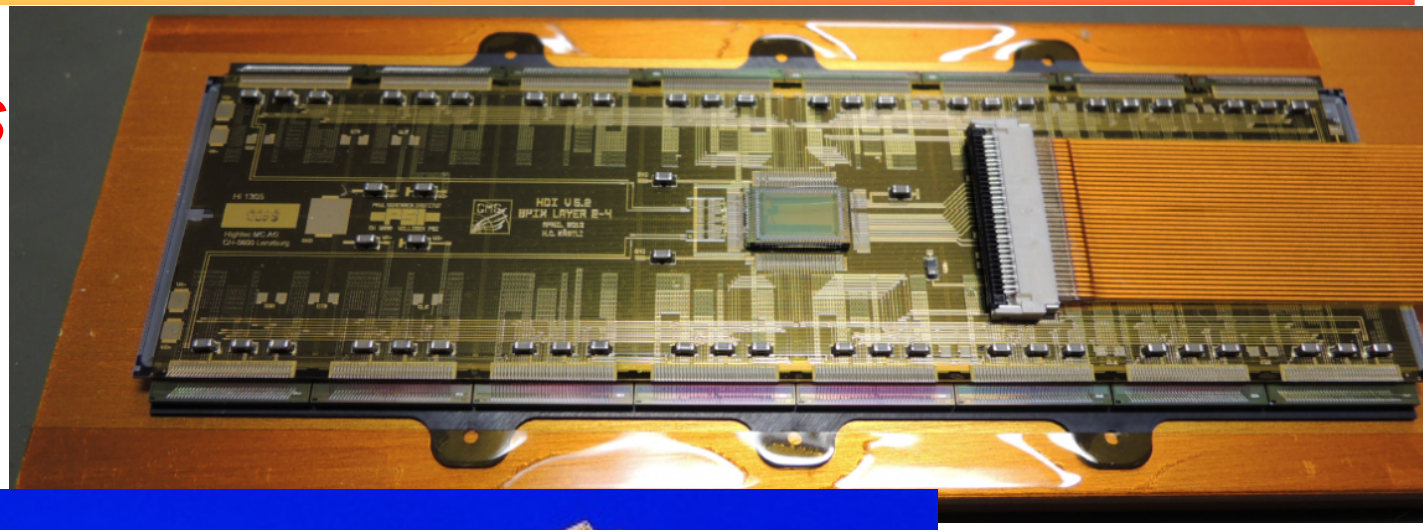

ATLAS Pixels

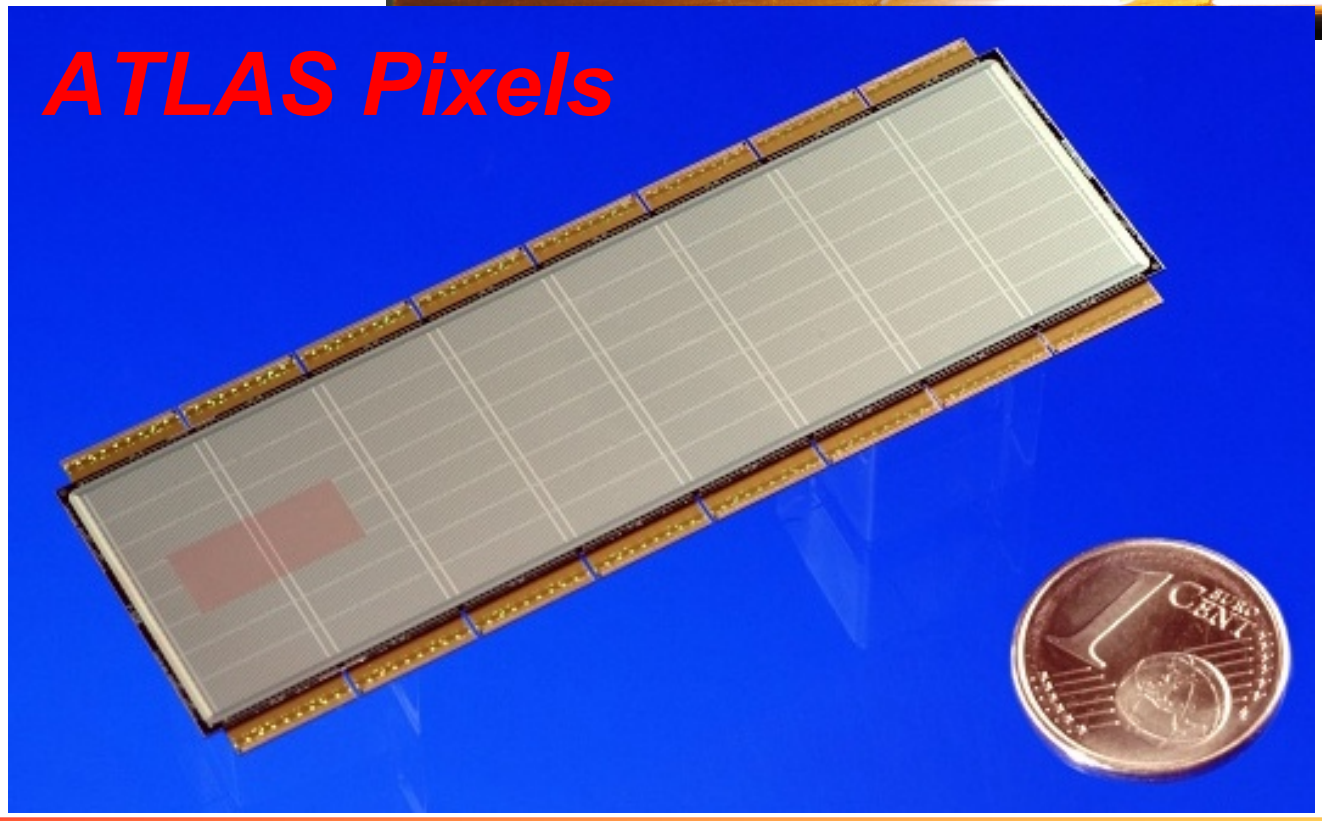

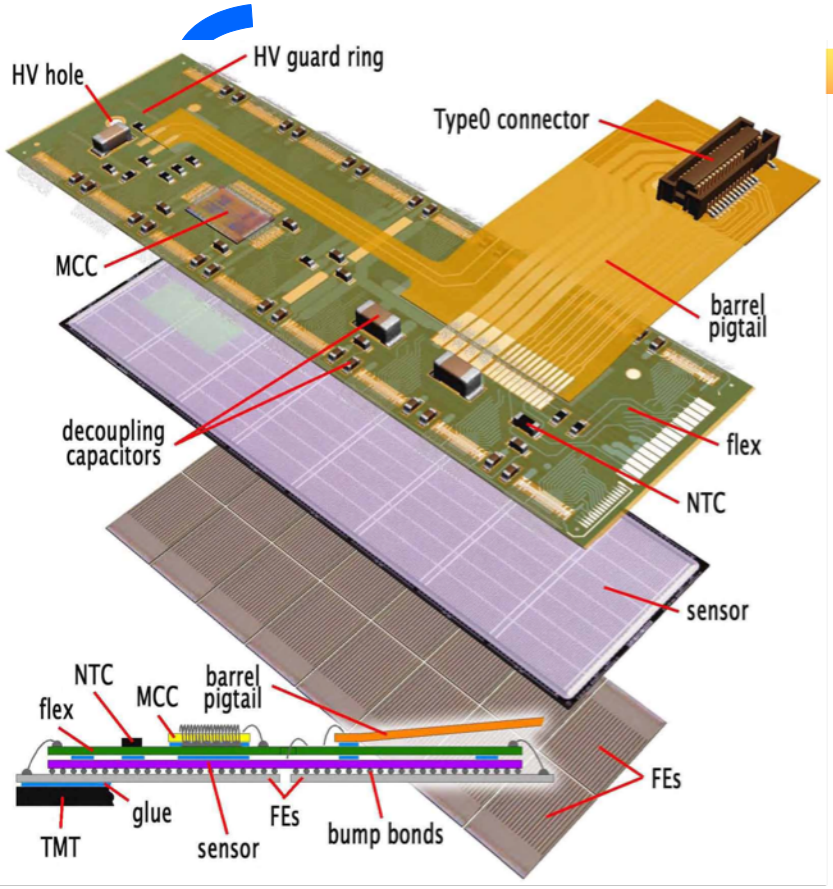
HV hole
HV guard ring
Type0 connector
MCC
barrel pigtail
decoupling capacitors
flex
NTC
sensor
NTC
flex
MCC
barrel pigtail
FEs
glue
FEs
TMT
sensor
bump bonds

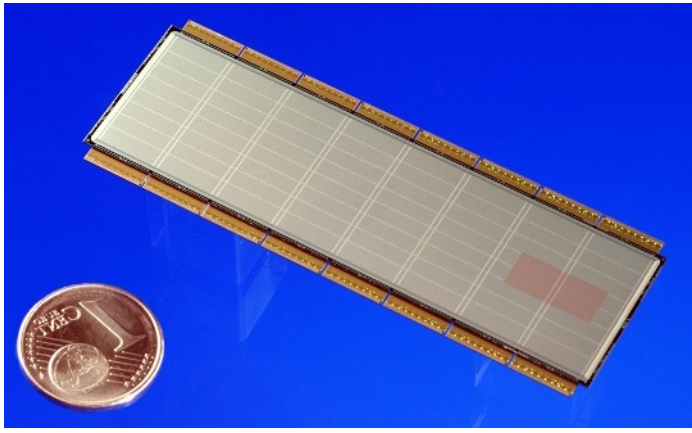

Many more types of silicon detectors

- Photo diodes
- Avalanche photo diodes
- Silicon photo diodes
- CCD
- CMOS Pixel detectors
- Silicon drift chambers
- …..
- No time in this lecture

Scintillators

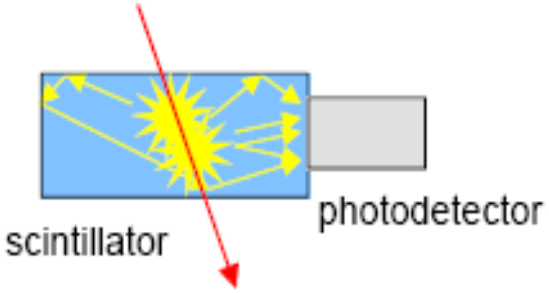

- Organic scintillators (molecules)
- Inorganic scintillators (crystals)
- Gas scintillators (atoms)

A good scintillator :

1. Number of produced photons should be high
2. And should be proportional to the deposited energy.
3. Transparent.
4. Short signals.
5. Good optical properties.
6. Refraction close to 1.5 .

Photomultiplier

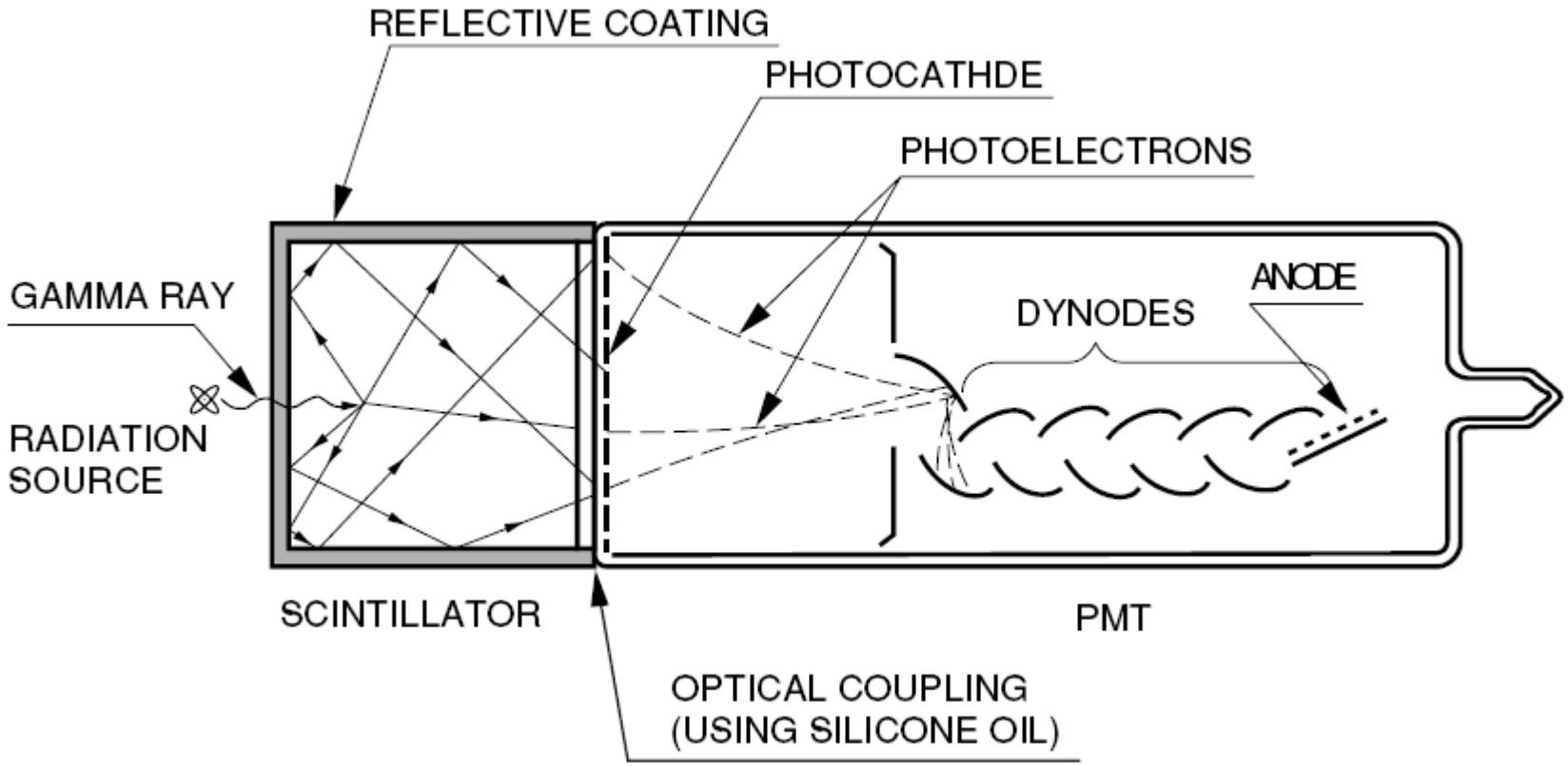

The gain

$$G = \eta \cdot \delta^N$$

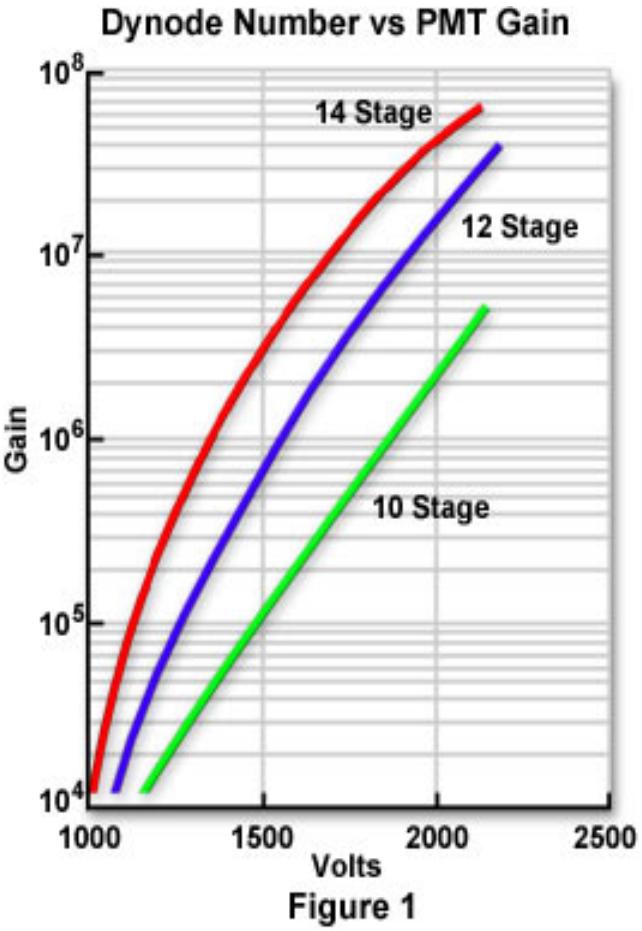

Figure 1

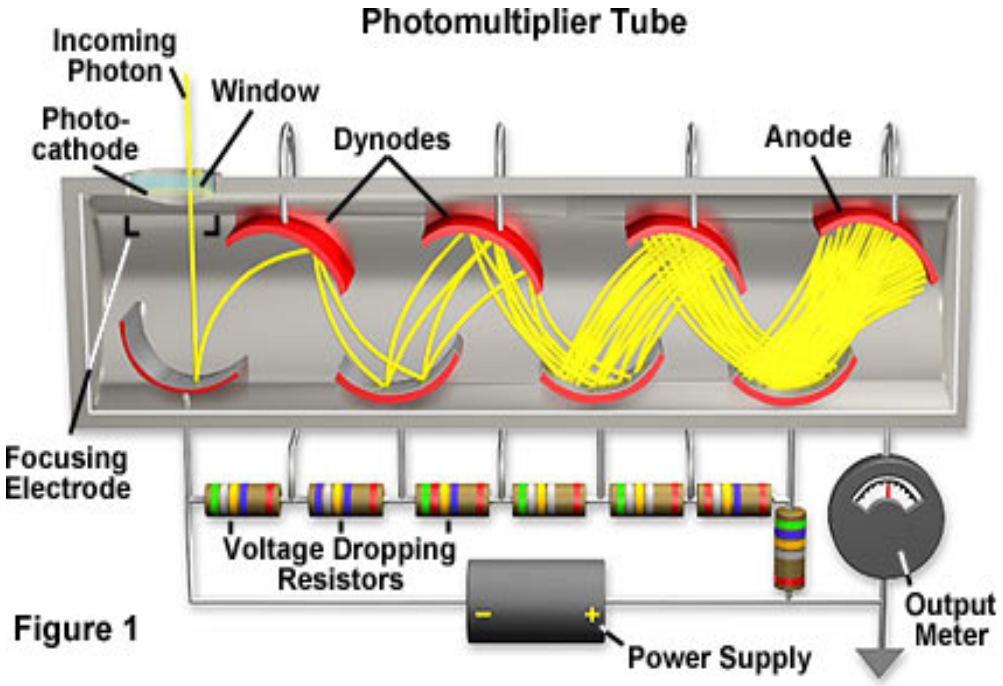

Figure 1

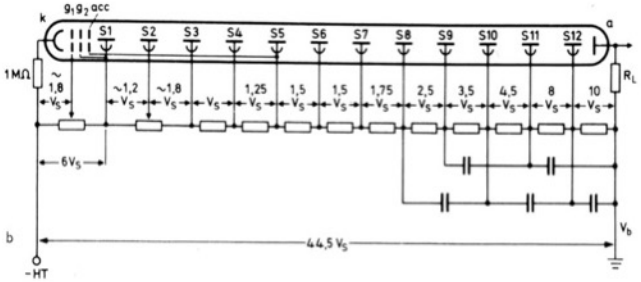

Fluorescence : < 10 ns
Phosphorescence >> 10 ns

Scintillators

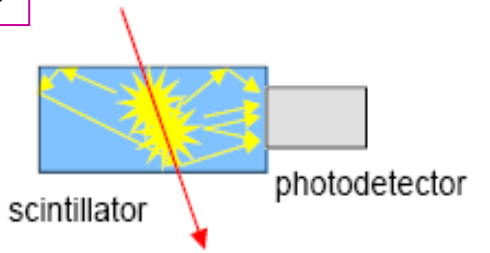

→generation
→transmission
→detection
} of scintillation light

- **Inorganic Scintillators**
  Crystal structure
  - → 40 000 *hν*/MeV
  - High Z material,
  - High density
  - Time constants of ns - µs
  - High price!
  - ~ radiation hard

  Used for
  - Gamma detection
  - Medical imaging
  - Electromagnetic calorimeters

- **Organic scintillator**
  plastic or liquid
  - → 10 000 *hν*/MeV
  - low Z,
  - Low density ≈ 1g/cm³
  - Large choice of emission spectra
  - Time constants of typically ns
  - "low" price
  - Sensitive to radiation

  Used for
  - Charged particle detection
  - TOF, Veto counters, calorimeters

Scintillator crystal

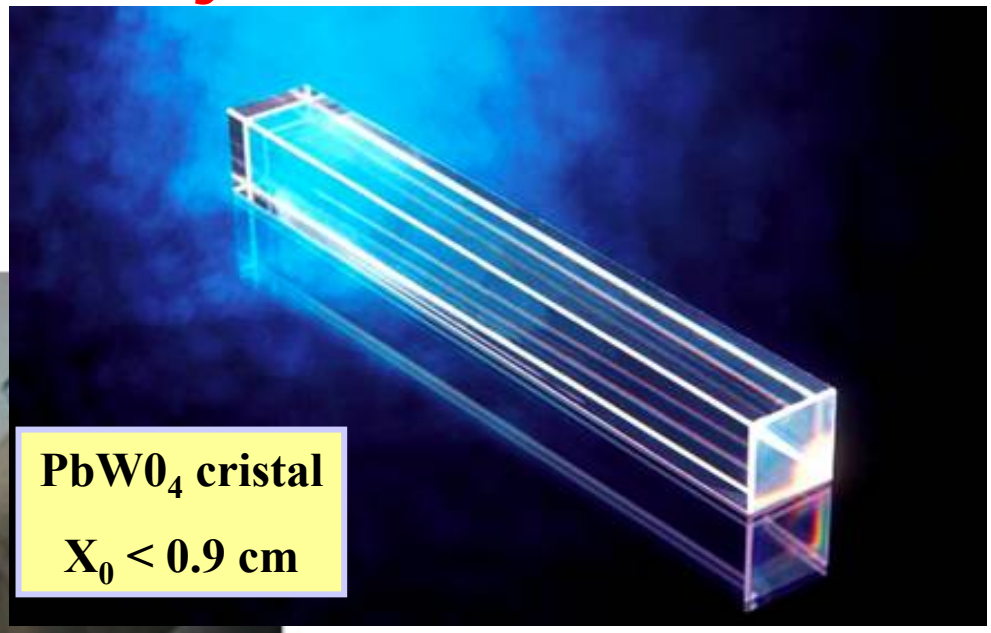

$PbW0_4$ cristal

$X_0 < 0.9$ cm

CMS

Scintillator - crystals

Three steps!
1. Absorption ⇒excitons/ionisation
2. Transfer to activator
3. Fluorescence of the activator

Excitons:

Pairs (e-,hole) (⇒ band below conduction band), but mobile within the crystal, will hit the activator atoms :

Transfer of energy

→ Excitation of activator atom

→ Radiative transition: light

→ Non-radiative transitions: vibrations (phonons) of the whole crystal, (energy loss)

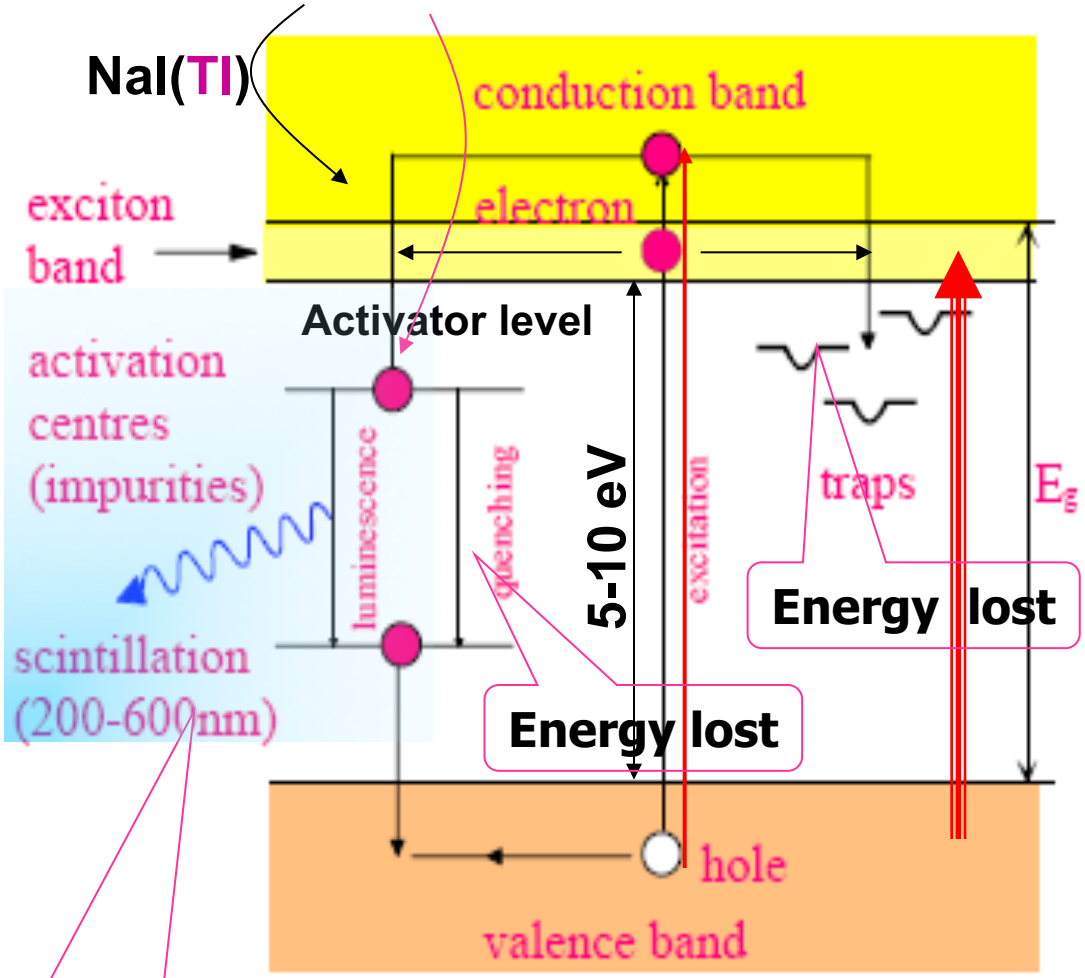

Light emission of energy $E = h\nu$

$$E = h\nu \; < \; E_{gap}; \; \tau_d \; = \; 0.02\text{-}1 \; \mu s$$

$$\frac{dN(t)}{dt} = \frac{N_0}{\tau_d} \exp\left(-t/\tau_d\right)$$

$$\lambda_{max} \; \approx \; 410 - 600 \text{ nm}$$

Scintillator composition	Density (g/cm^3)	Index of refraction	Wavelength of max.Em. (nm)	Decay time Constant (µs)	Scinti Pulse height[1)]	**Photons per Mev**
NaI(Tl)	3.67	1.9	410	0.25	100	38 000
CsI	4.51	1.8	310	0.01	6	
CsI(Tl)	4.51	1.8	565	1.0	45	52 000
CaF_2(Eu)	3.19	1.4	435	0.9	50	24 000
BaF_2	4.88	1.5	190/220 310	0,0006 0.63	5 15	10 000
BGO	7.13	2.2	480	0.30	10	8 200
$CdW0_4$	7.90	2.3	540	5.0	40	
$PbWO_4$	8.28	2.1	440	0.020	0.1	1 900
CeF_3	6.16	1.7	300 340	0.005 0.020	5	
GSO	6.71	1.9	430	0.060	40	
LSO	7	1.8	420	0.040	75	
YAP	5.50	1.9	370	0.030	70	

1) Relative to NaI(Tl) in %; 2) Hygroscopic; 3) Water soluble

Emission spectra of inorganic scintillators

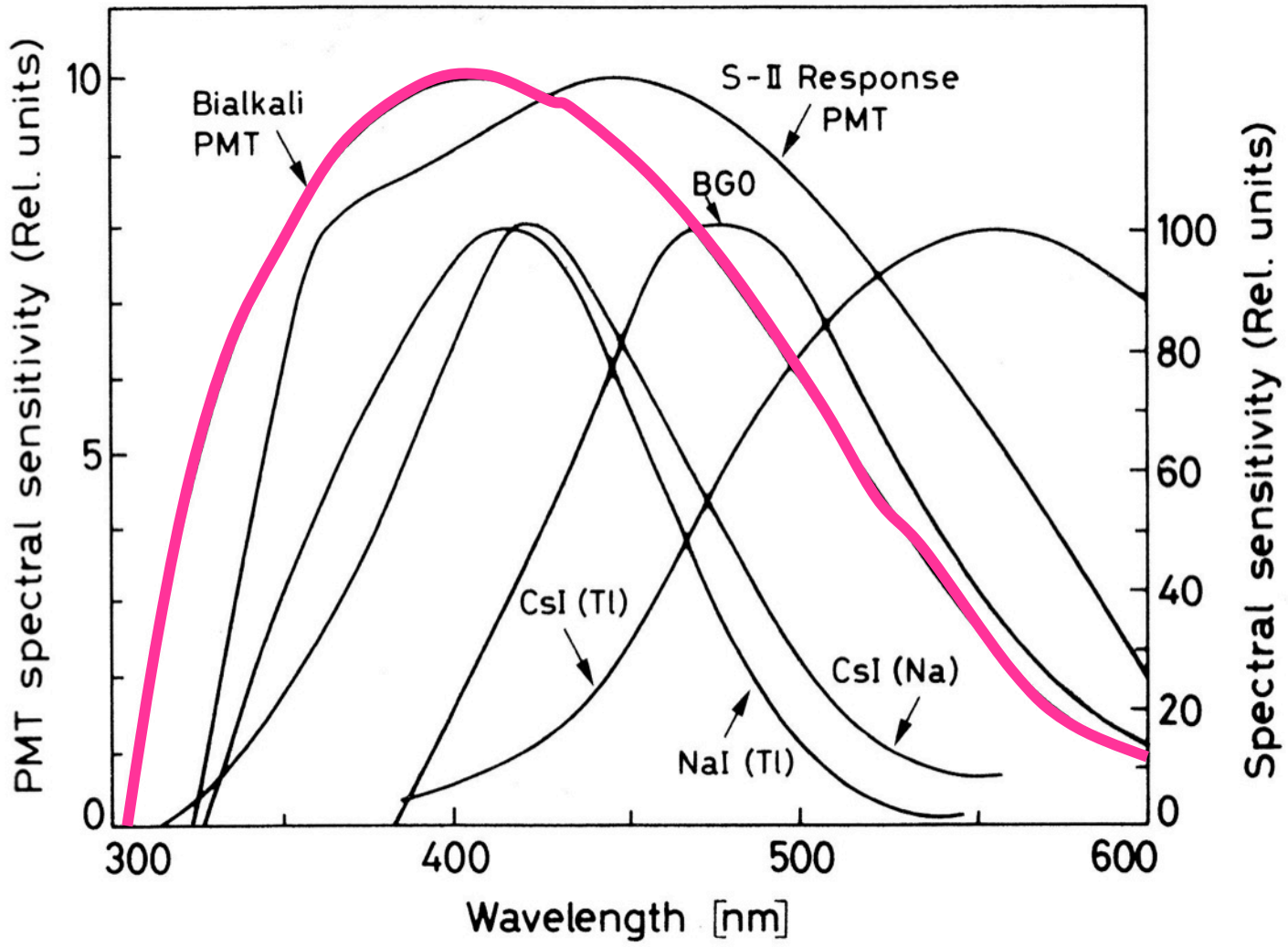

Respone of NaI

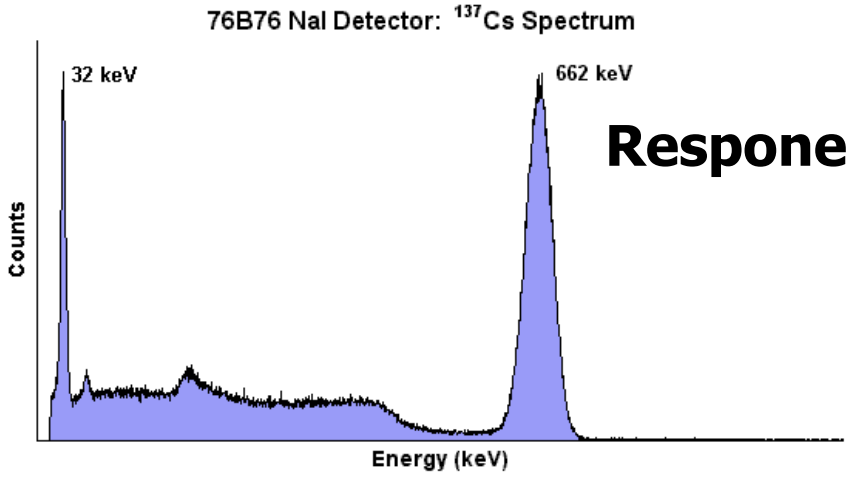

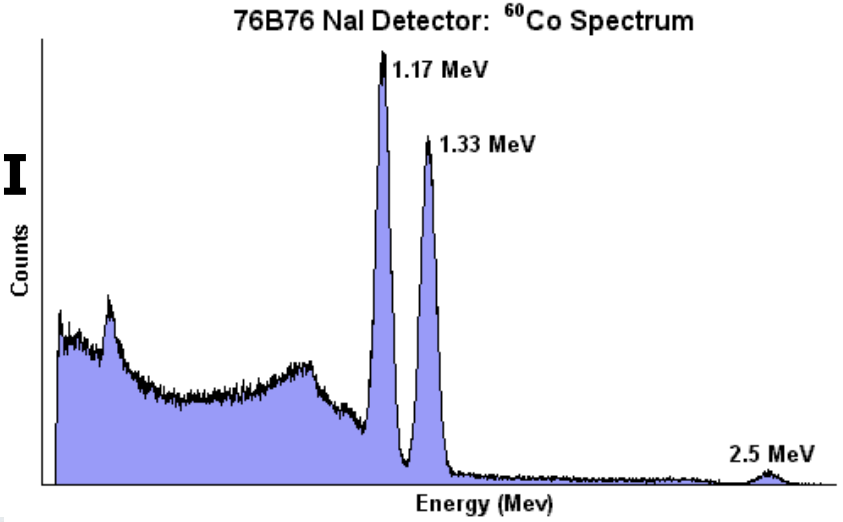

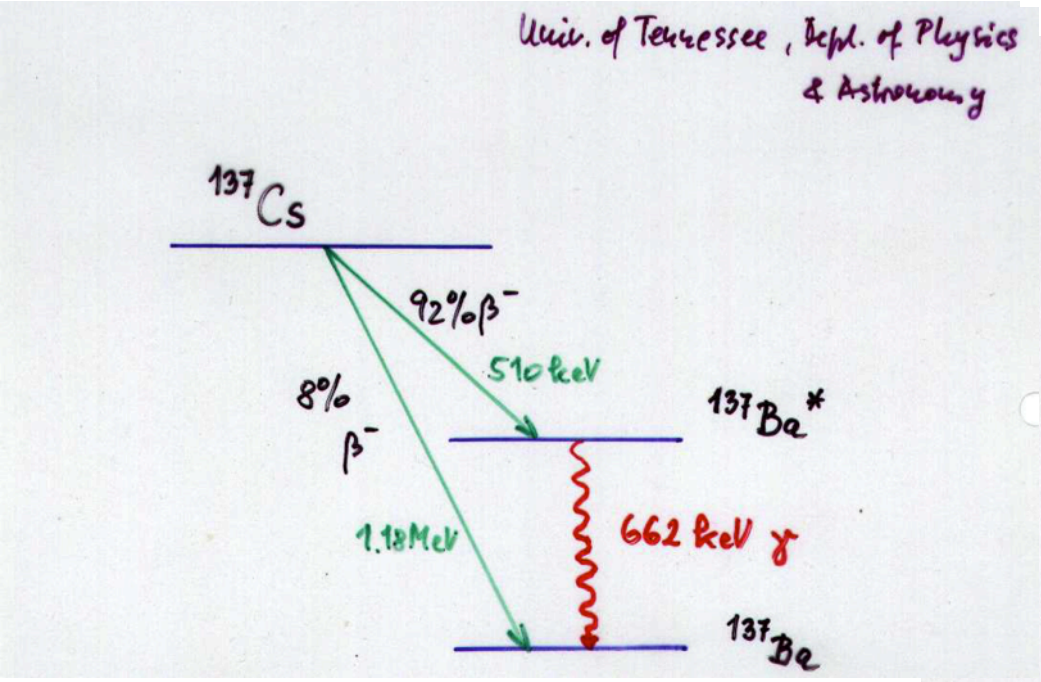

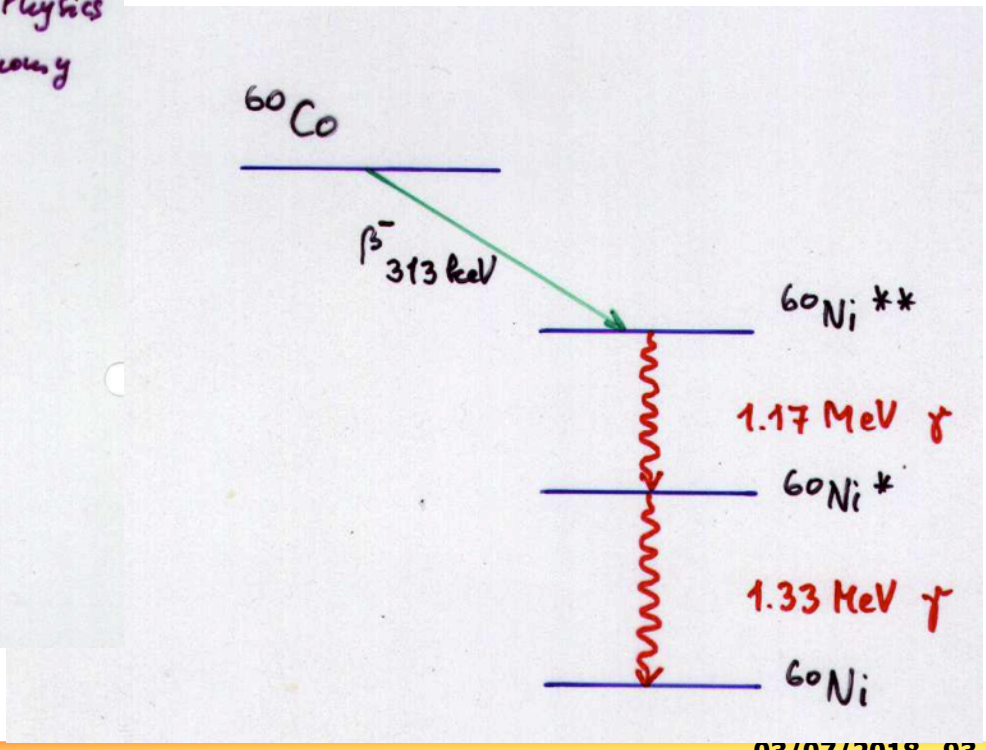

Energy Resolution

Detector response :

- For a fixed energy the detector will respond each time slightly different (also around the photo peak)
- All measurements will be distributed around a mean value with a certain width
- This distribution can be approximated by a Gaussian with
  - Mean μ and
  - A width FWHM
- The resolution *R* is defined by

$$R := \frac{\text{FWHM}}{\mu} = 2.35\frac{\sigma}{\mu}$$

μ, σ^2 = mean and variance of the distribution

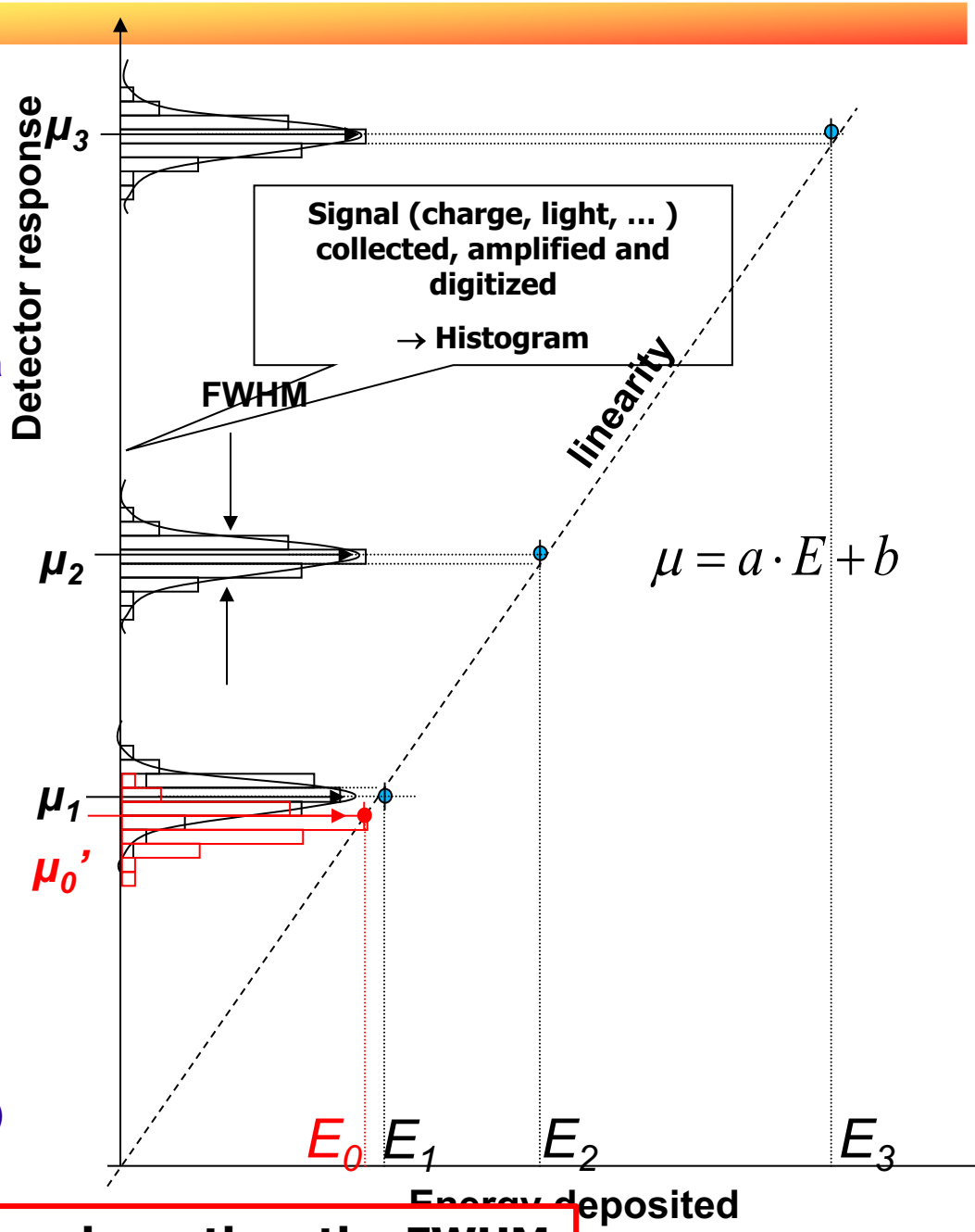

However, please note :

very often people talk about the resolution of their detector and what they (including myself) really mean or quote is σ/μ and NOT "*R*"

You cannot distinguish two energies closer than the FWHM

Gaussien or normal distribution

$\pm 1\sigma$ = 68.3% confidence level

$\pm 2\sigma$ = 95.5%

$\pm 3\sigma$ = 99.7%

$$P(x)=\frac{1}{\sigma\sqrt{2\pi}}\exp\left(-\frac{(x-\mu)^2}{2\sigma^2}\right);$$

μ = *mean*

σ^2 = variance;

FWHM =2.35 σ

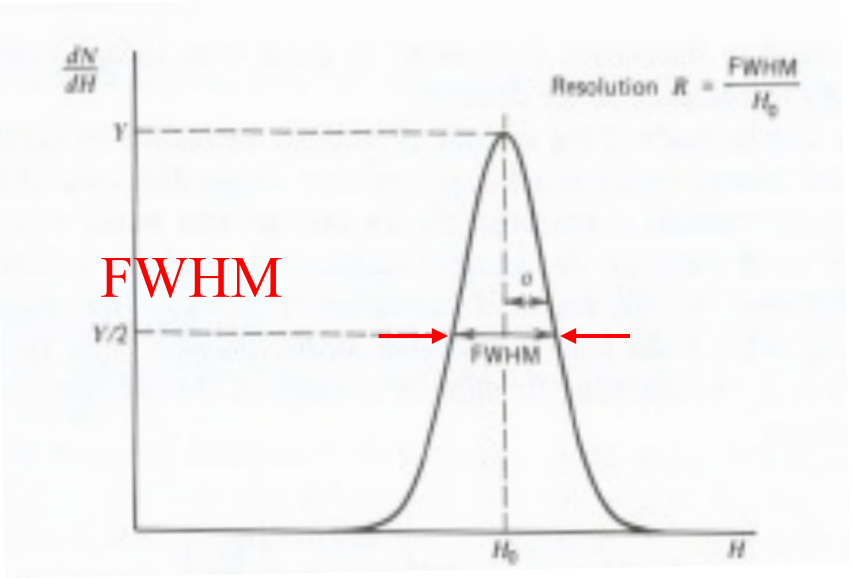

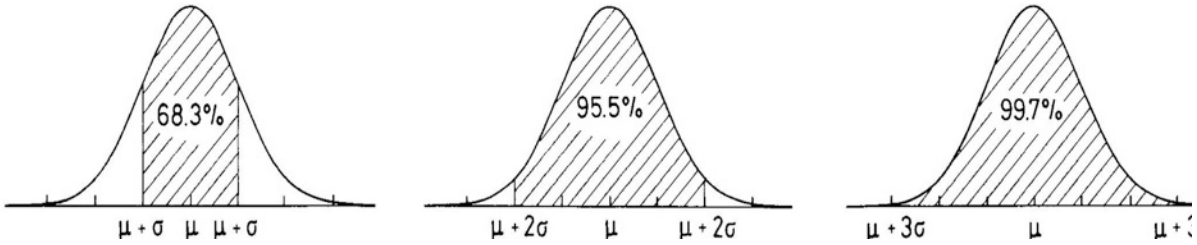

Resolution

$$R := \frac{\text{FWHM}}{\mu}$$

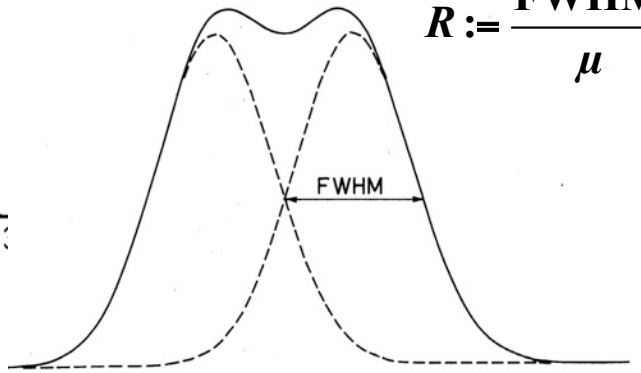

Impossible to separate two signals closer than FWHM

NaI-Resolution

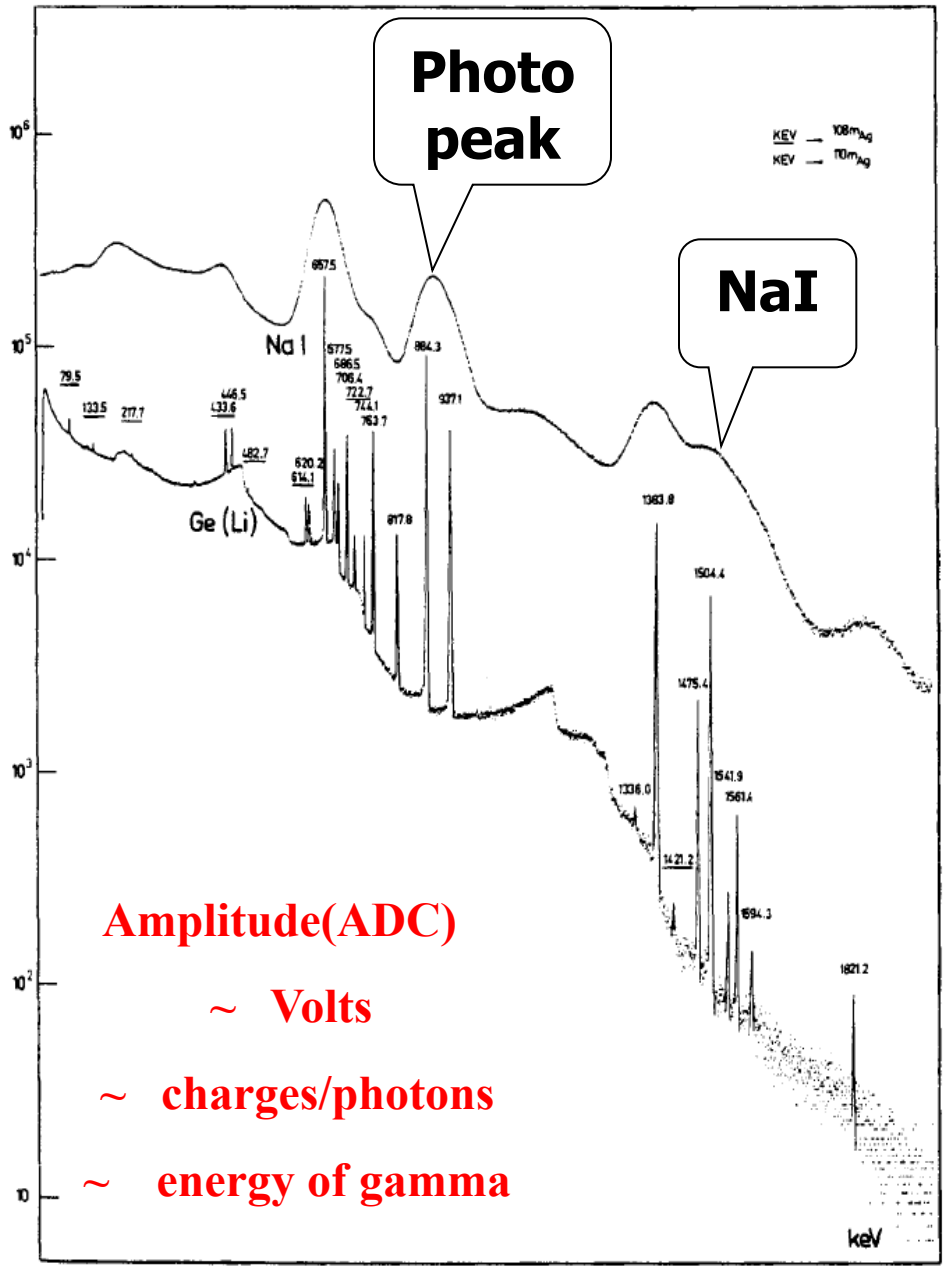

$$N_{h\nu} = \frac{E}{w};\ dN_{h\nu} = \sqrt{N_{h\nu}} = \sqrt{\frac{E}{w}}$$

Statistics strictly Poisson $\Rightarrow \sigma^2 = \mu;$

$$dE / E = dN_{h\nu} / N_{h\nu} \sim \frac{1}{\sqrt{N_{h\nu}}}$$

$NaI: w \approx 25\,eV / photon_{\text{scint}} \Rightarrow 40000\,h\nu / MeV$

Incomplete collection of scintillation photons and finite quantum efficiency will reduce the mean number of photo-electrons

$$N_{pe} = N_{h\nu} \times \varepsilon_{collection} \cdot \varepsilon_{quantic};$$

$$dN_{pe} = \sqrt{N_{pe}} = \sqrt{N_{h\nu} \times \varepsilon_{coll.} \cdot \varepsilon_{quant.}}$$

$$\varepsilon_{coll.} \approx 0.2 - 0.8;\ \varepsilon_{quant.} \approx 0.2\,(PM)$$

$$dE / E = dN_{pe} / N_{pe} \cong \frac{1}{\sqrt{N_{pe}}} = \frac{1}{\sqrt{N_{h\nu} \times \varepsilon_{coll.} \cdot \varepsilon_{quant.}}}$$

$$F \approx 1;\ \varepsilon_{coll.} \approx 0.4;\ \varepsilon_{quant.} \approx 0.2\,(PM)$$

$$\Rightarrow dE / E = \sigma_E / E \approx 1.5\% \text{ à } 1.333\ MeV$$

$$R = 2.35 \times 1.5\% = 3.6\% \xrightarrow{\text{experimental}} (5-8)\%$$

NaI (Tl)

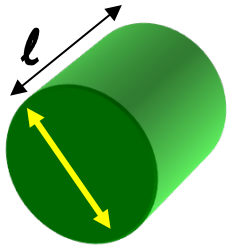

- Reference/standard of efficiency: $\varepsilon = 1{,}22 \times 10^{-3}$
  - Cylindrical detector NaI(Tl), 7,62(∅) x 7,62(ℓ) cm^3
  - Source of ^{60}Co (1,33 MeV) at 25 cm

Properties of NaI:

- Z = 53 high ⇒ good efficiency
- Relatively short decay time (230 ns)
- intense signal
- Relative good energy resolution
- But NaI is very hygroscopic!!

Exercise : verify efficiency!

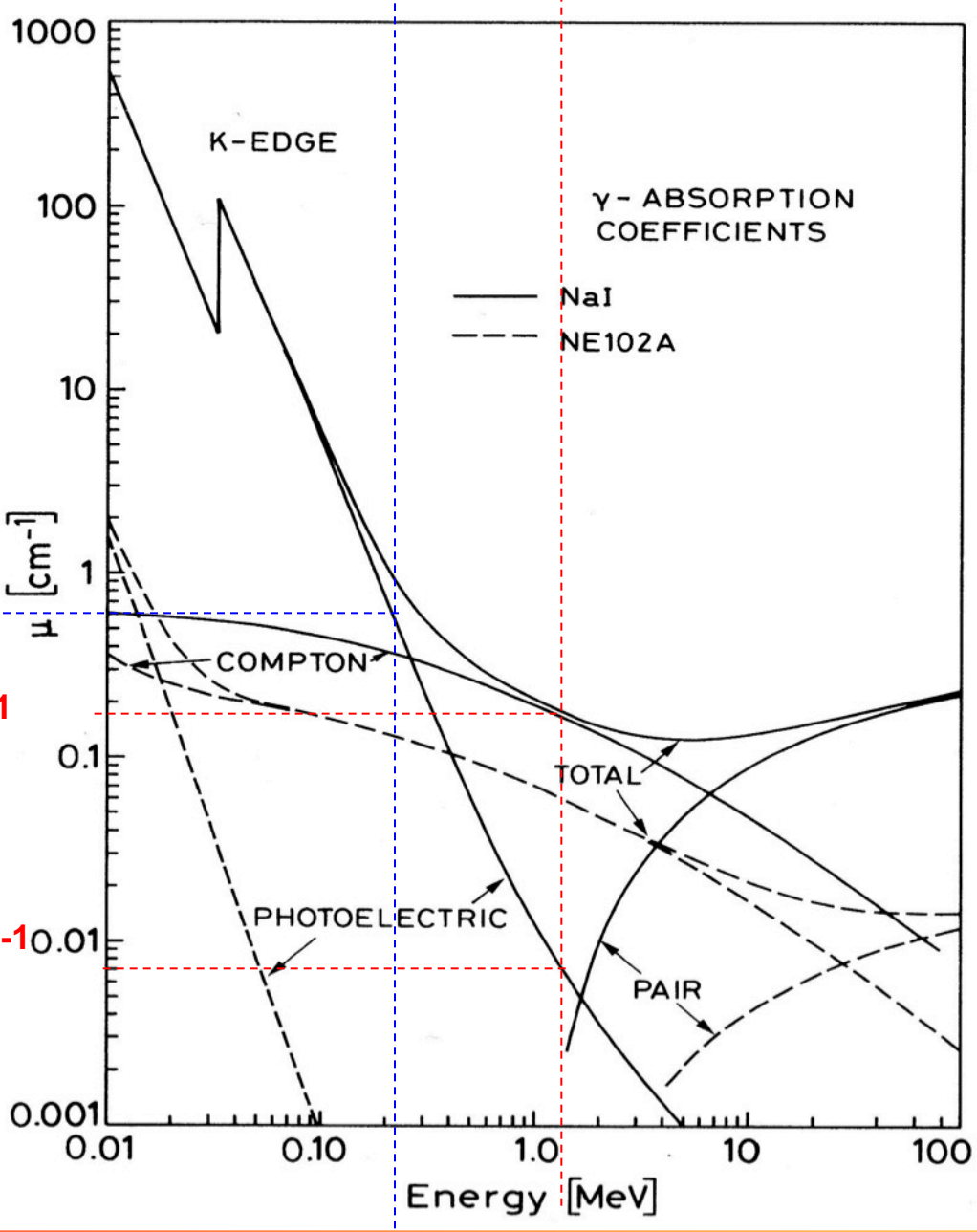

$\mu = 0.6\ cm^{-1}$

$\mu = 0.18\ cm^{-1}$

$\mu = 0.007\ cm^{-1}$

Organic scintillators

- Liquids and plastics
- Solvent which absorbs the energy
- The excitation energy of the solvent is transferred to the dopant
- Emission, reabsorption and re-emission of light
- Shift towards longer wave lengths
- Fast response, about <5ns
- Liquids :
  - Solvents liquids: xylene, tolene, benzene, phenylcyclohexane, triethylbenzene,decaline
  - Dopants for liquids: p-Terphenyl ($C_{18}H_{14}$), PBD($C_{20}H_{14}N_2O$), PPO($C_{15}H_{11}NO$), POPOP($C_{24}H_{16}N_2O_2$), ≈ 3g/l
- Solids:
  - Solvents plastics polyvinyltoluene, polyphenilbenzene, polystyrene.
  - Primary dopants for plastics : PBD, p-Terphenyl, PBO, 10g/l
  - Secondary dopant POPOP to shift the light to longer wavelengths.
- Quality depends largely on low level of impurities

Organic Scintillators

- fluorescence (durée ~ ns-μs)
- phosphorescence (durée ~ μs-min)

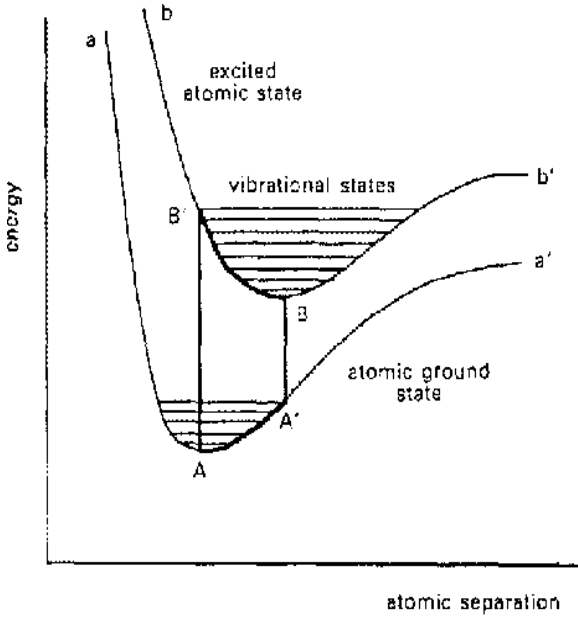

Valence electrons of the π-molecular orbitals

Radiation less transitions

(Förster)

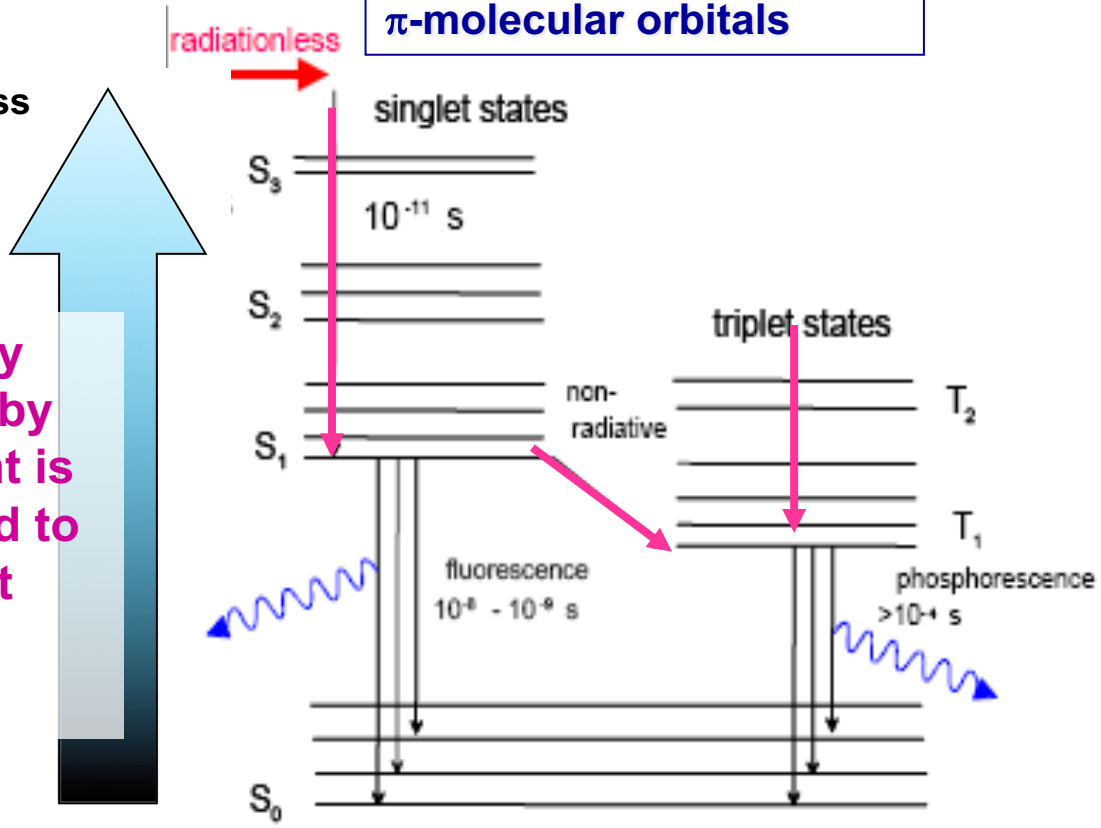

The energy absorbed by the solvent is transferred to the dopant without radiation

Phosphorescence : Slow emission

Organic Scintillators

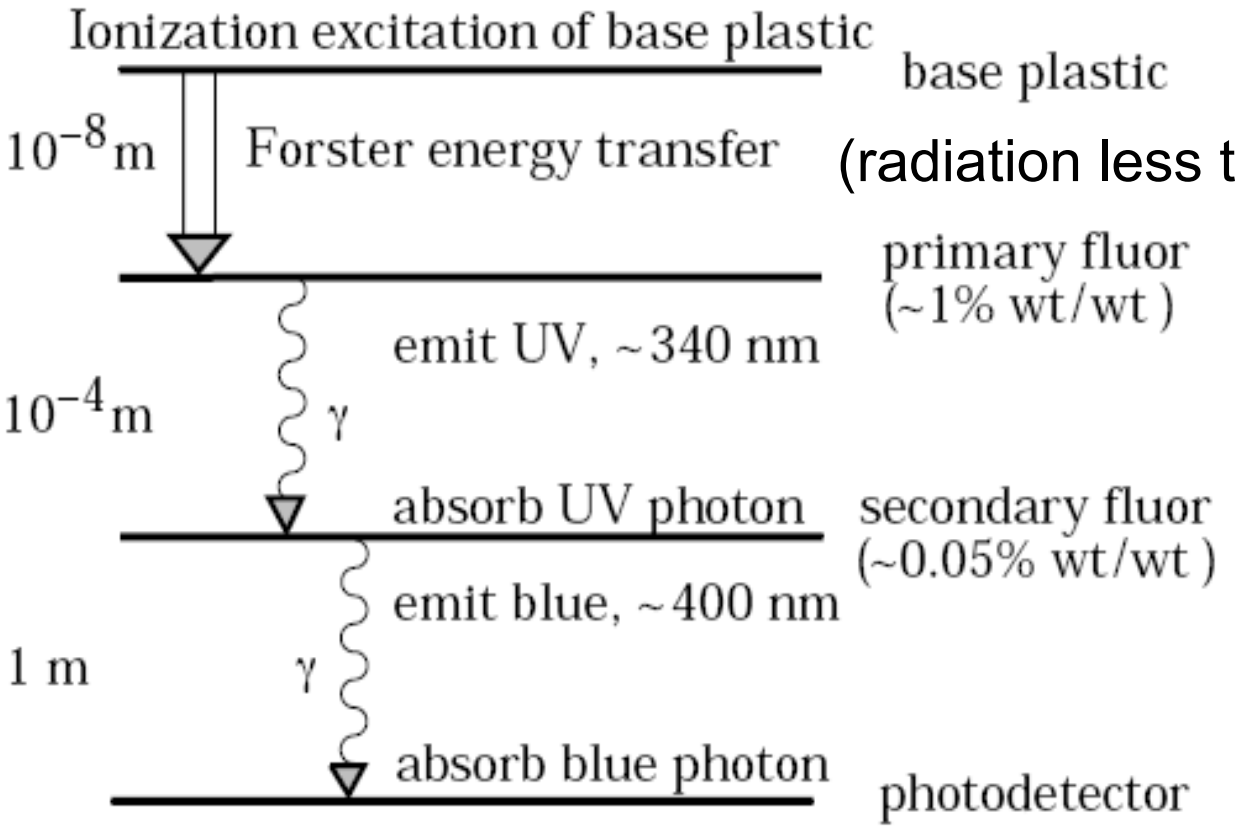

Figure 28.1: Cartoon of scintillation "ladder" depicting the operating mechanism of plastic scintillator. Approximate fluor concentrations and energy transfer distances for the separate sub-processes are shown.

Absorption and emission

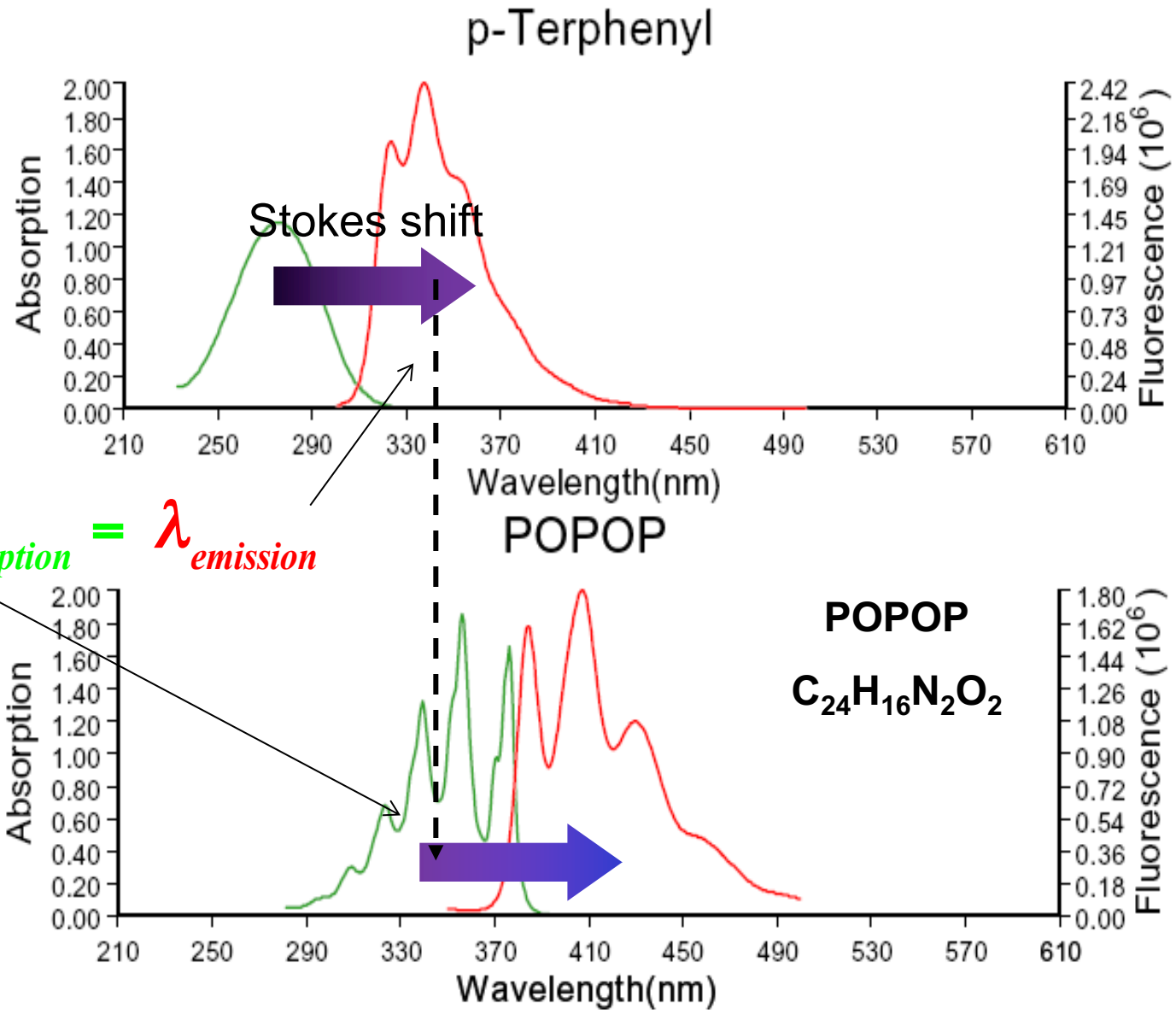

Light guides

Geometrical adaptation:

- Light guides: transfer by total internal reflection (+outer reflector)

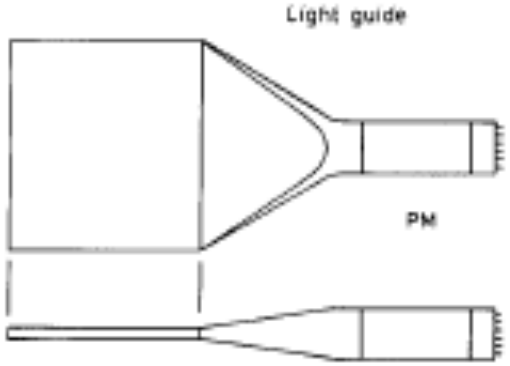

"fish tail"

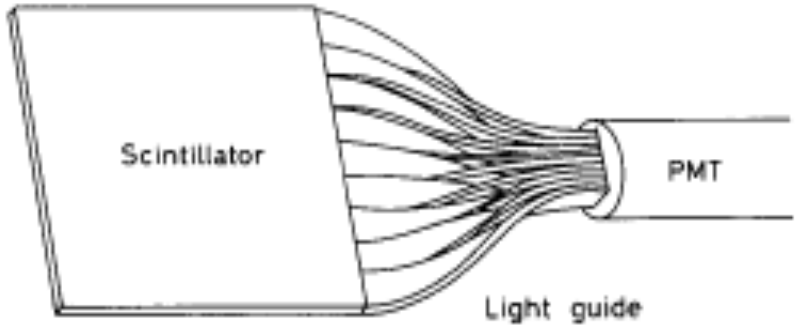

adiabatic

- wavelength shifter (WLS) bars

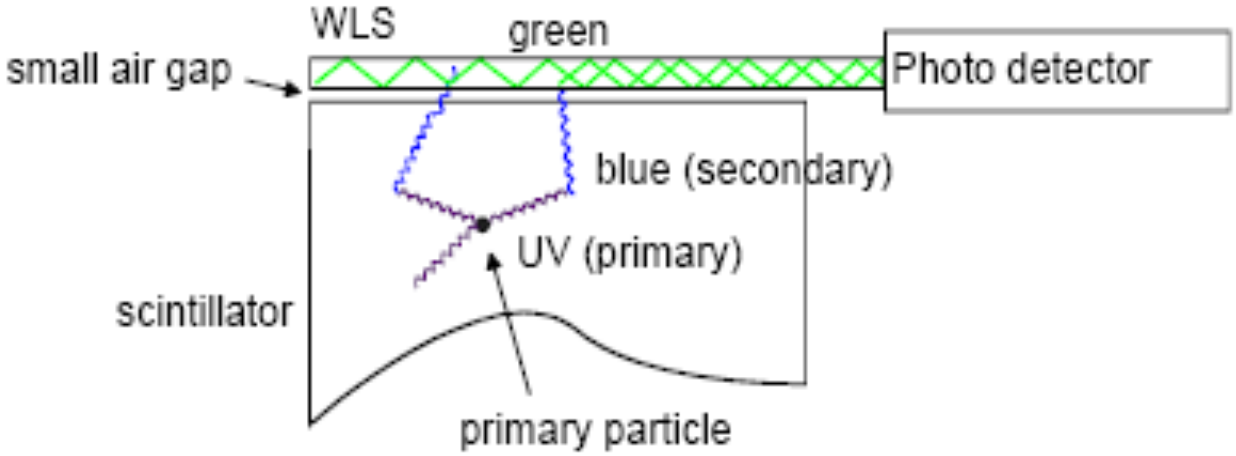

Adiabatic light guides

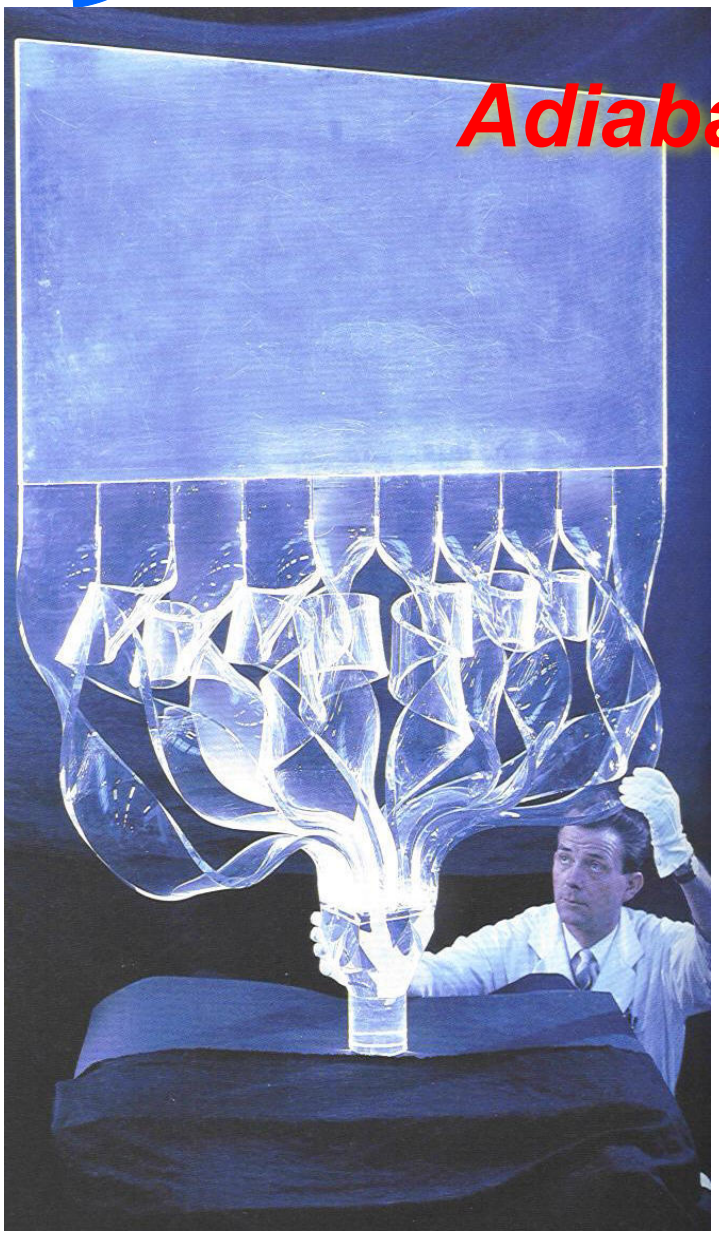

Scintillating fibers

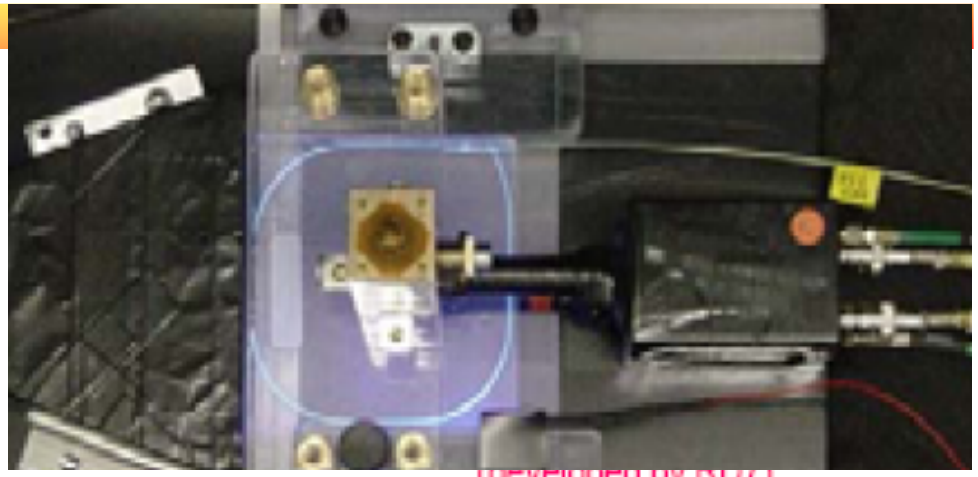

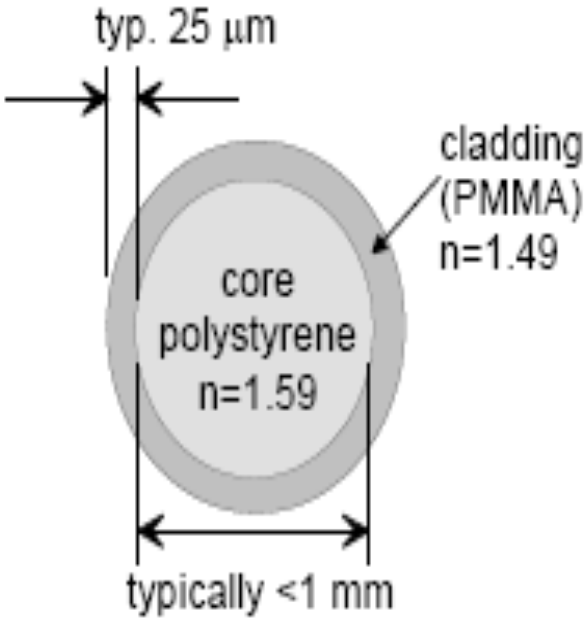

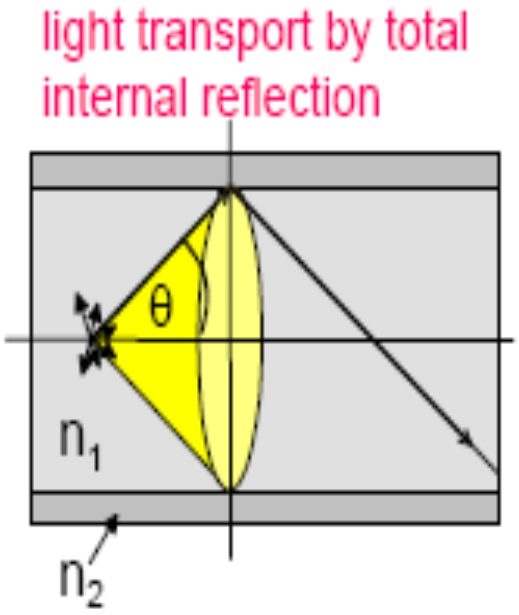

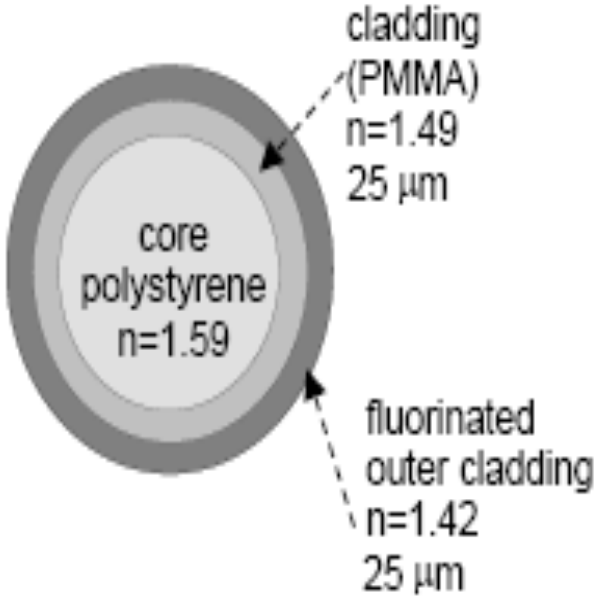

$$\cos\theta = \sin\alpha_1 = \frac{n_2}{n_1} = 0.937 \Rightarrow \theta = 20.5°; \quad \frac{d\Omega}{4\pi} = \tfrac{1}{2}\sin^2\theta = \tfrac{1}{2}\left(1-\cos^2\theta\right) = 0.06$$

$$\mathbf{\frac{n_2}{n_1} = 0.893 \Rightarrow \theta = 26.7°; \quad \frac{d\Omega}{4\pi} = 0.10}$$

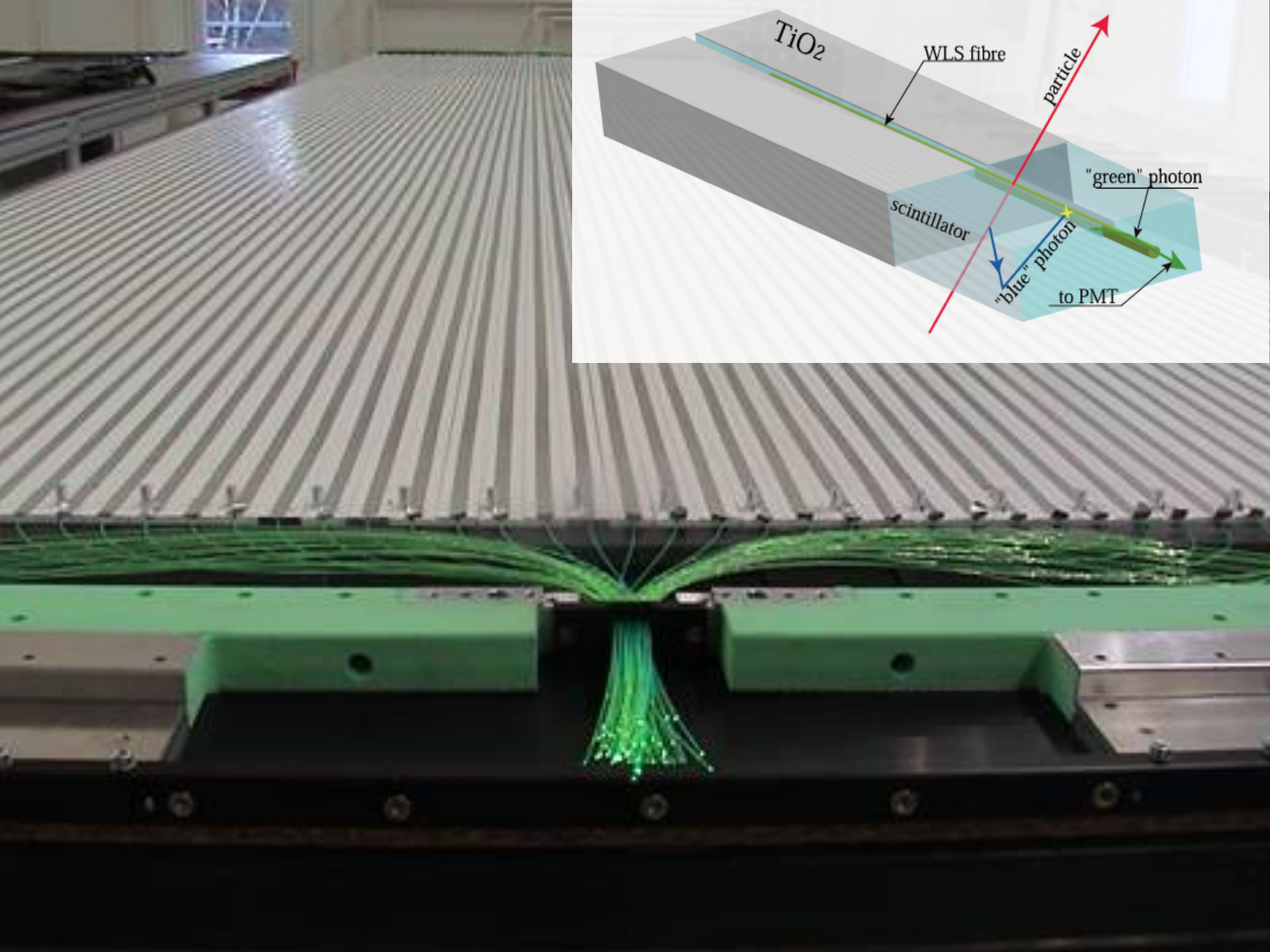
TiO_2
WLS fibre
particle
"green" photon
scintillator
"blue" photon
to PMT

Interaction of neutrinos

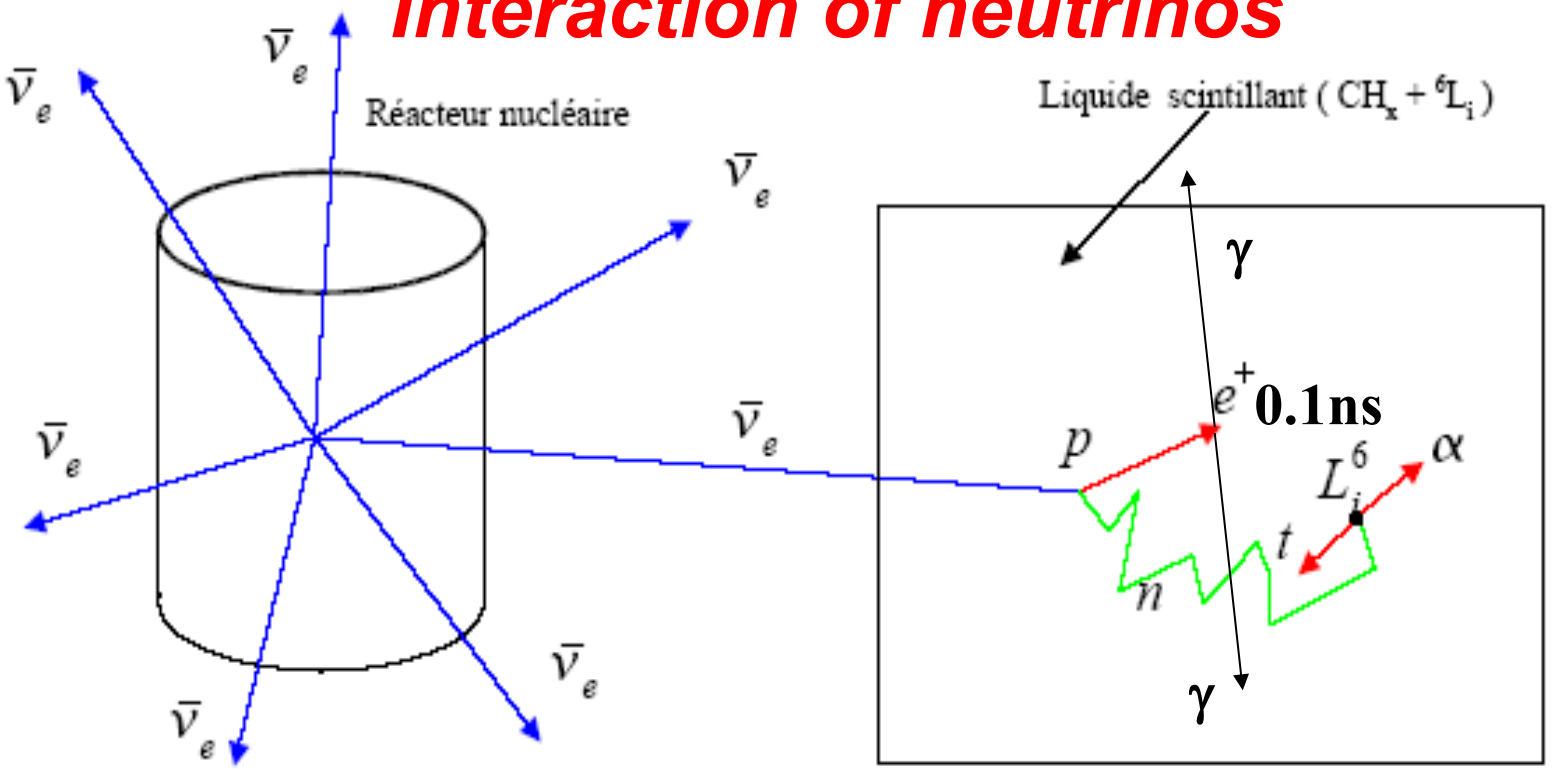

Reines & Cowan 1959

$\epsilon_\nu \sim 0$

La réaction de détection est : $\bar{\nu}_e + p \rightarrow n + e^+$, qui est rapidement (100 µs) suivie de la capture du neutron sur un noyau de L_i^6 selon la réaction : $n_{th} + L_i^6 \rightarrow \alpha + t + 4{,}8\,MeV$. Les particules chargées produisent des impulsions de scintillation en coïncidence . La signature de détection d'un neutrino correspond à l'enregistrement de deux impulsions lumineuses induites par le positon et la paire $\alpha - t$.

Liquid scintillator for the Double Chooz experiment

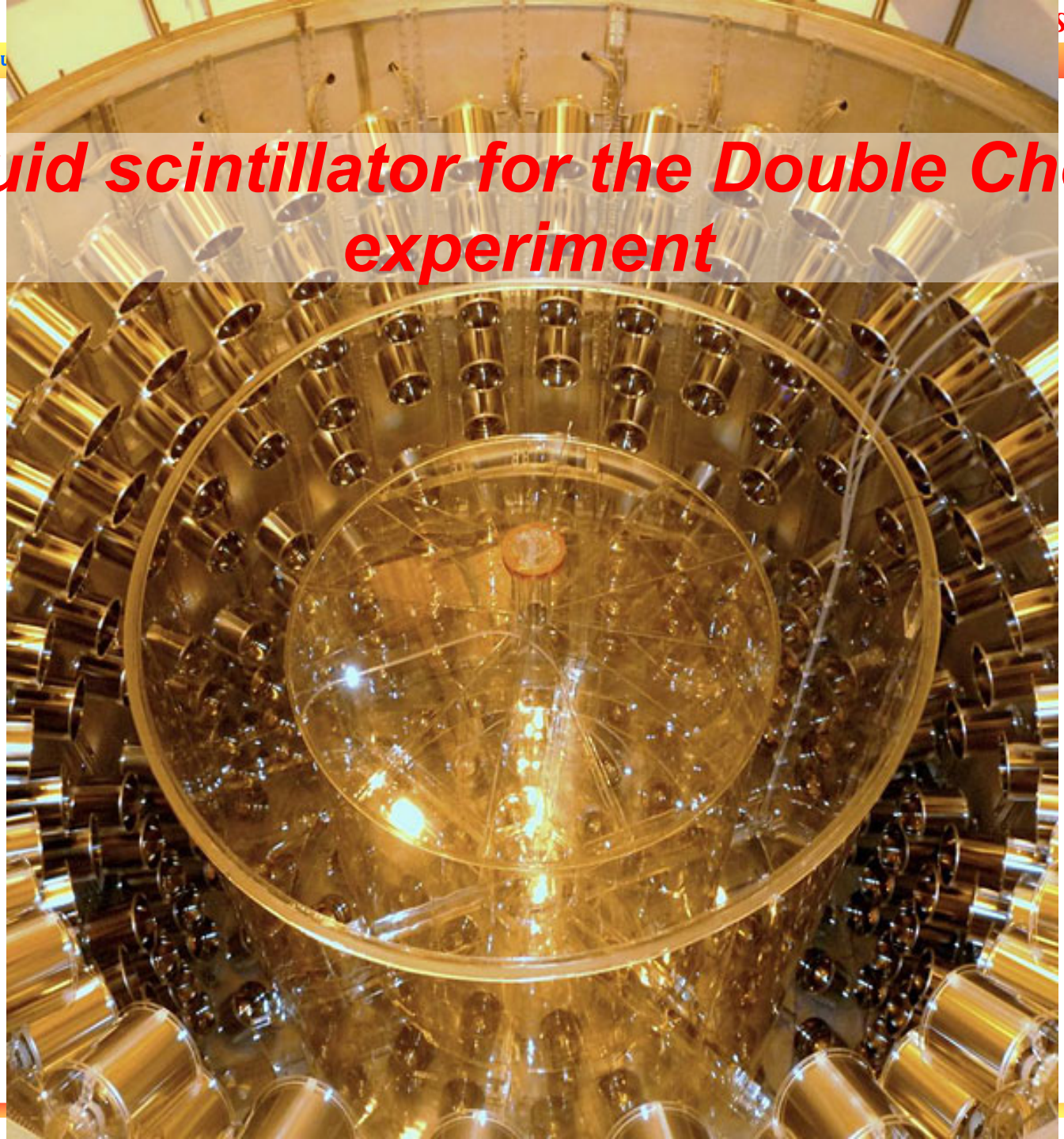

Calorimetry

Tracking a particle in a magnetic field

At high momentum you loose precision!

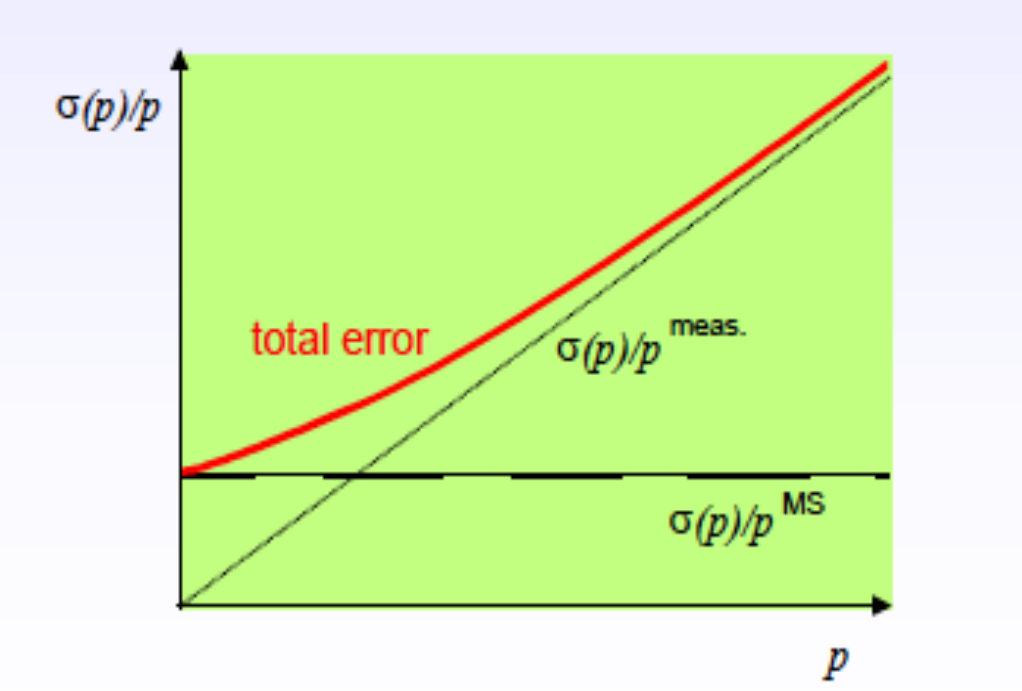

➔ **Measure energy !**

Calorimeters at high energy

- At very high energies the momentum resolution of any magnetic spectrometer will deteriorate rapidly
- Calorimeters measure the energy of the particles
  - The energy of the incident particle is transformed into a large number of secondary particles which can be measured
  - The number of secondary's is proportional to the energy
  - Ionisation, scintillation Cerenkov…
  - Electromagnetic showers (electrons, gammas, π^0…
  - Hadronic showers, all hadrons!
- Electromagnetic showers :
  - Conversion of photons into e^+e^- and Bremsstrahlung
- Hadronic showers:
  - nuclear interactions, fragmentation of nuclei

Showers in calorimeters

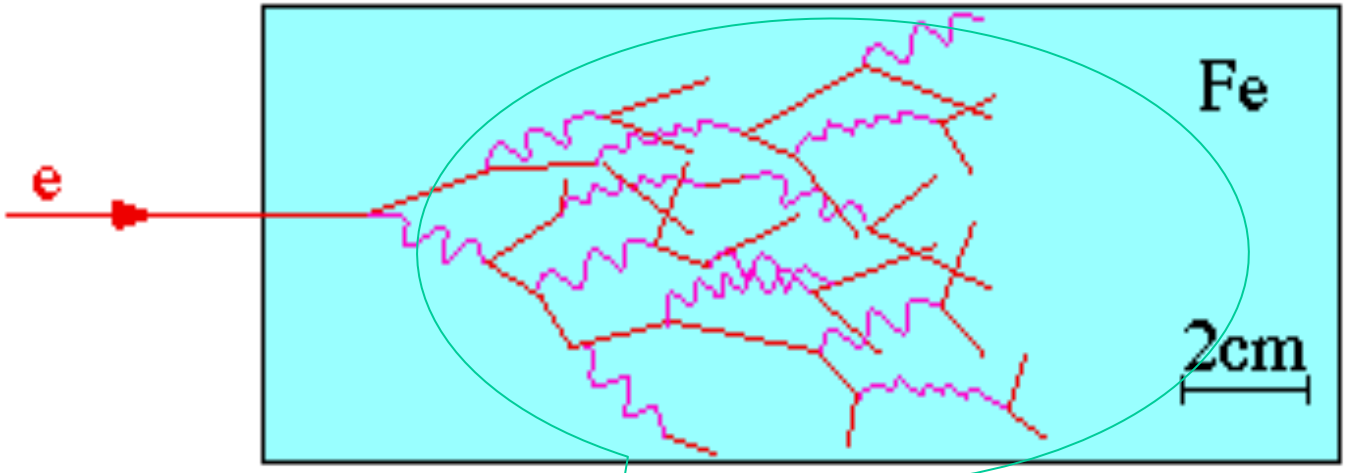

Electromagnetic shower

radiation length X_0

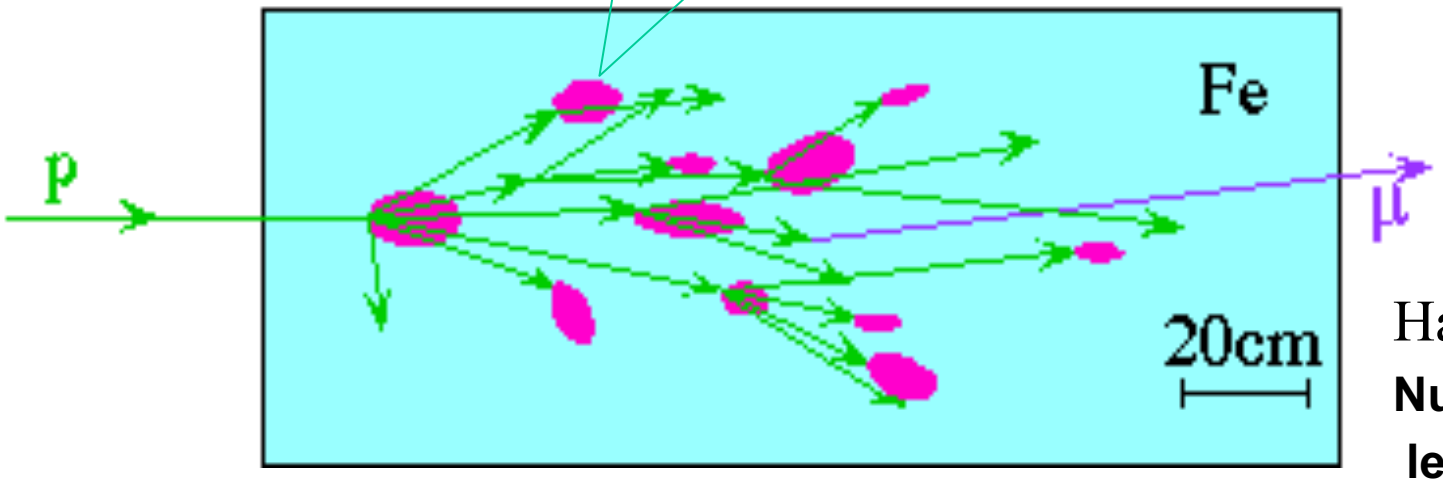

Hadronic shower

Nuclear interaction length Λ

Hadronic showers

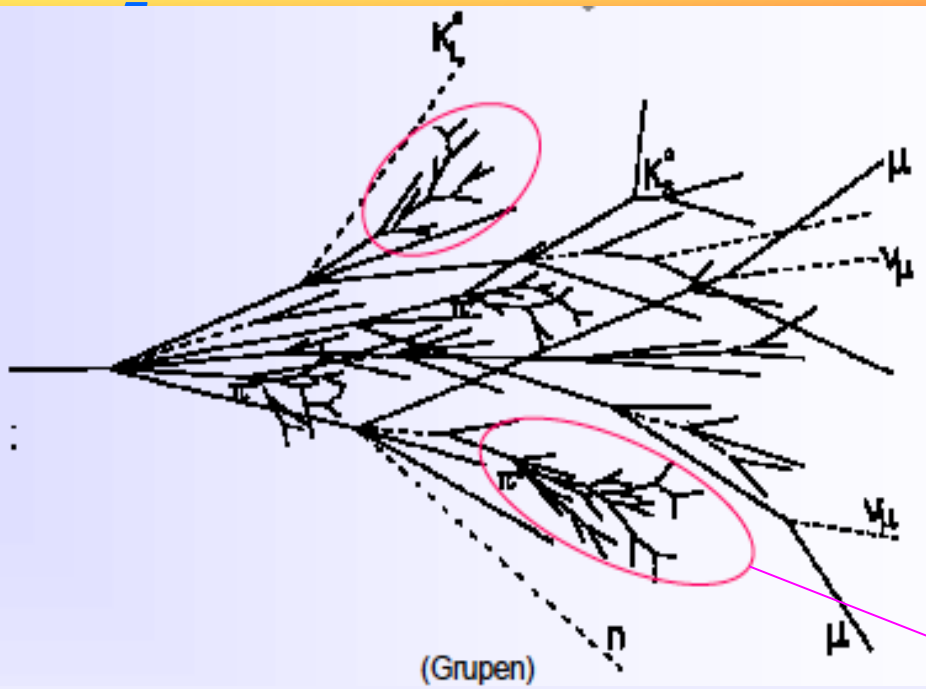

(Grupen)

hadronic + **electromagnetic**

- charged hadrons p,$\pi^{\pm}$,$K^{\pm}$,
- nuclear fragmets ….
- breaking up of nuclei (binding energy)
- neutrons, neutrinos, soft γ's, muons

→ invisible energy → large energy fluctuations → limited energy resolution

neutral pions → 2γ

→ electromagnetic cascades

$$n(\pi^0) \approx \ln E(GeV) - 4.6$$

example $E = 100$ GeV: $n(\pi^0) \approx 18$

CMS homogeneous elm Calorimeter

$PbWO_4$ Scint. Crystal Calorimeter

Entire shower in active detector material

- " **High density crystals (28 X_0)**
- " **Transparent, high light yield**
- " **No particles lost in passive absorber**
- " **High resolution: ~3%/$\sqrt{E}$ (stochastic)**

Granularity

- " **Barrel: $\Delta\eta \times \Delta\phi = 0.017^2$ rad**
- " **Longitudinal shower shape unmeasured**

Read out with avalanche photo diodes

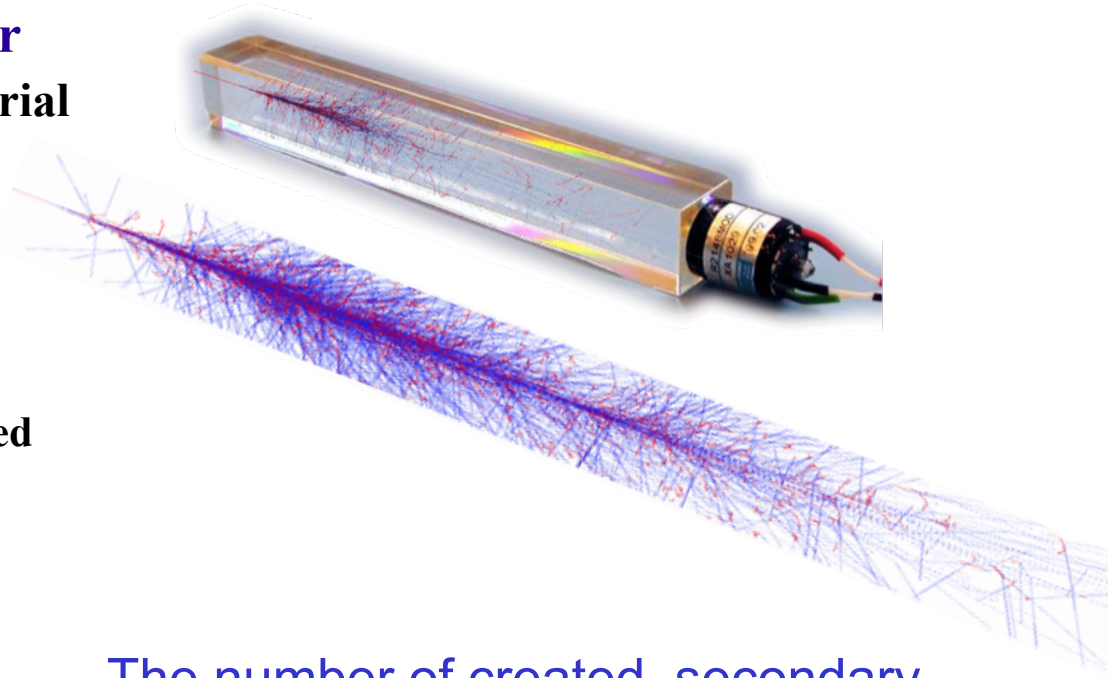

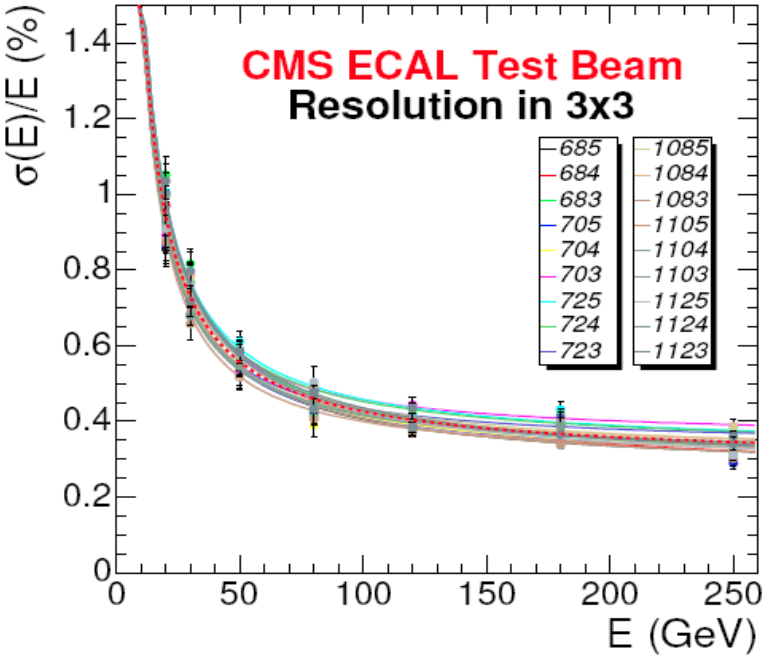

The number of created secondary particles is proportional to the energy $E \sim N$, $\sigma_{RMS} \sim \sqrt{N} \sim \sqrt{E}$

$$\frac{\sigma_E}{E} = \frac{2.8\%}{\sqrt{E\,(GeV)}} \oplus \frac{0.128}{E\,(GeV)} \oplus 0.3\%$$

The Electromagnetic Calorimeter - ECAL

Energy / momentum resolution

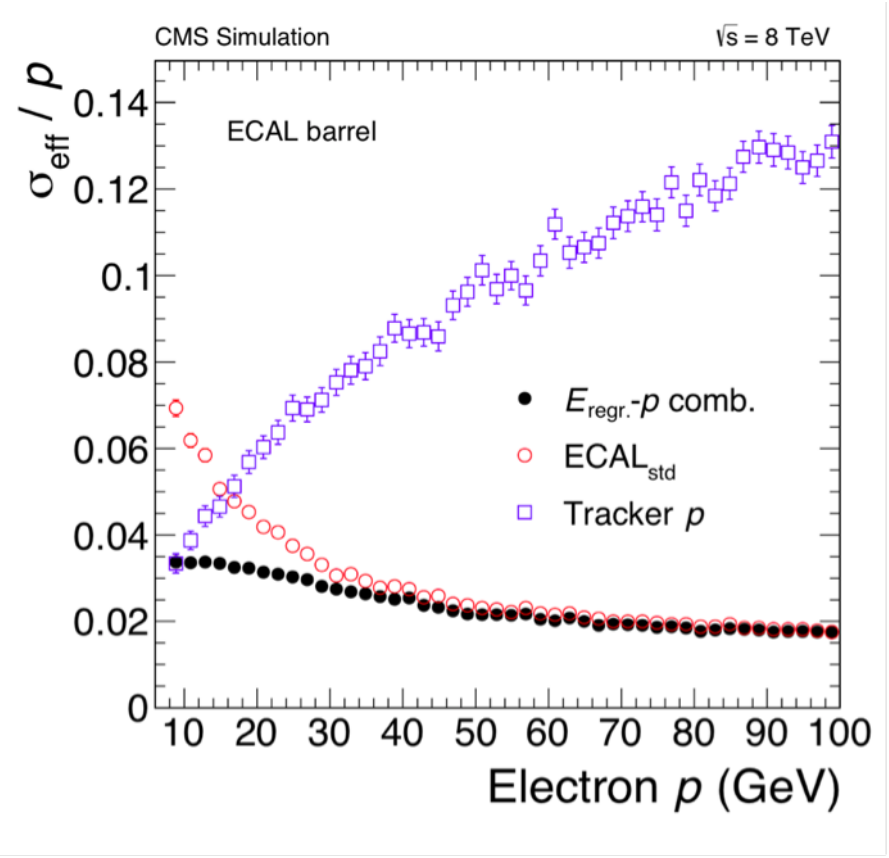

$$\frac{dE}{E} \sim \frac{1}{\sqrt{E}}; \quad \frac{dp_T}{p_T} \sim \frac{\Delta s}{BL^2} p_T$$

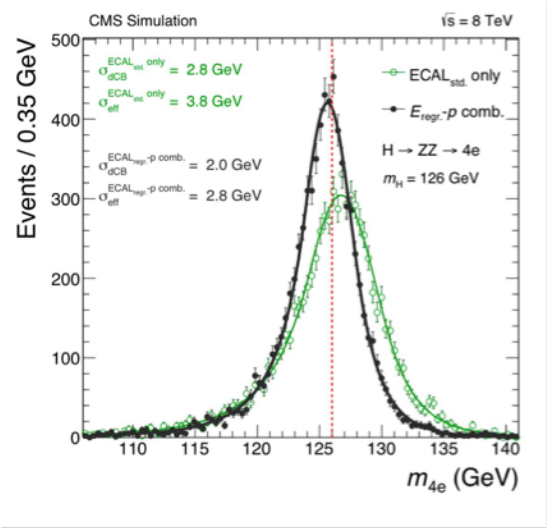

Sampling calorimeters

Absorber
Detector
Absorber
Detector
Absorber
Detector

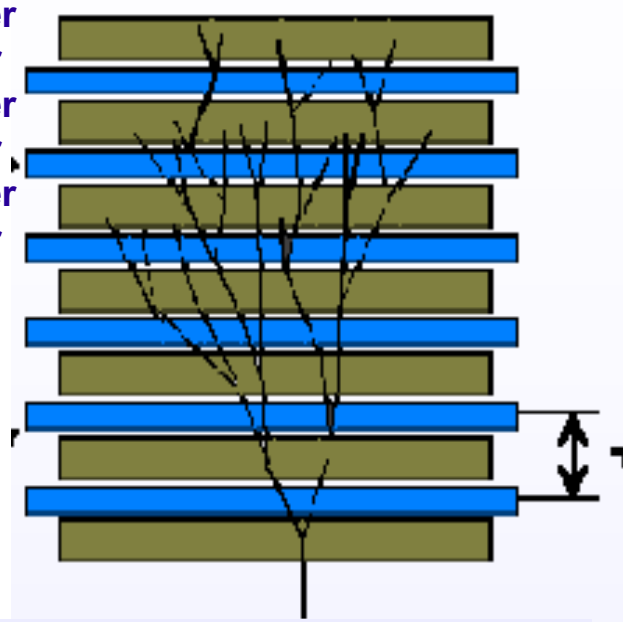

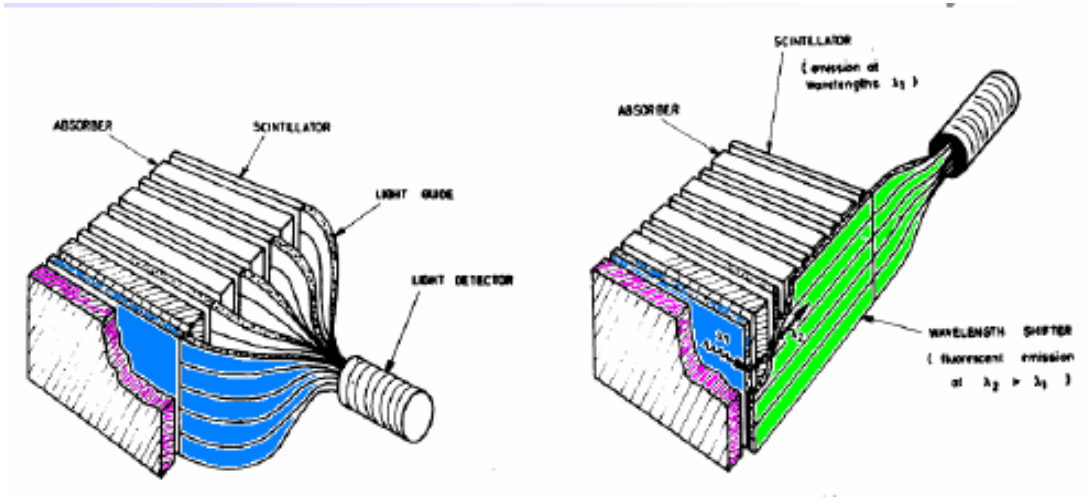

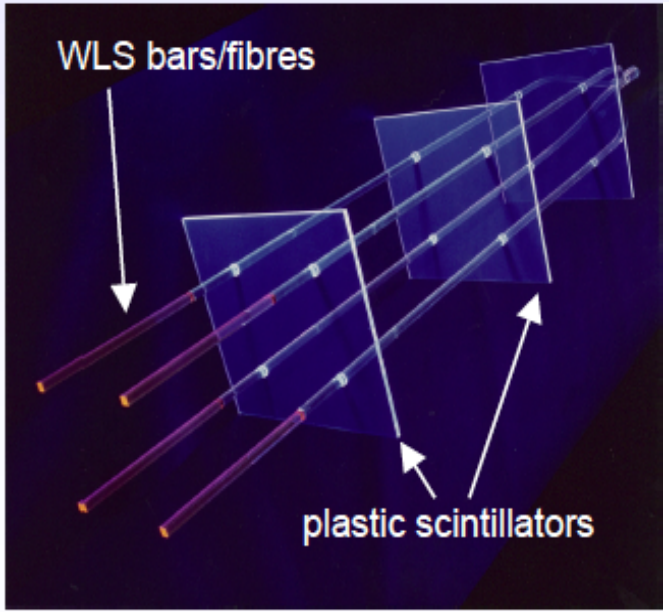

CMS Hadron calorimeter

Brass absorber + plastic scintillators

2 x 18 wedges (barrel)
+ 2 x 18 wedges (endcap)
~ 1500 T absorber
5.8 λ_i *at* $\eta = 0$.

Scintillators fill slots and are read out via WLS fibres by HPDs (B = 4T!)

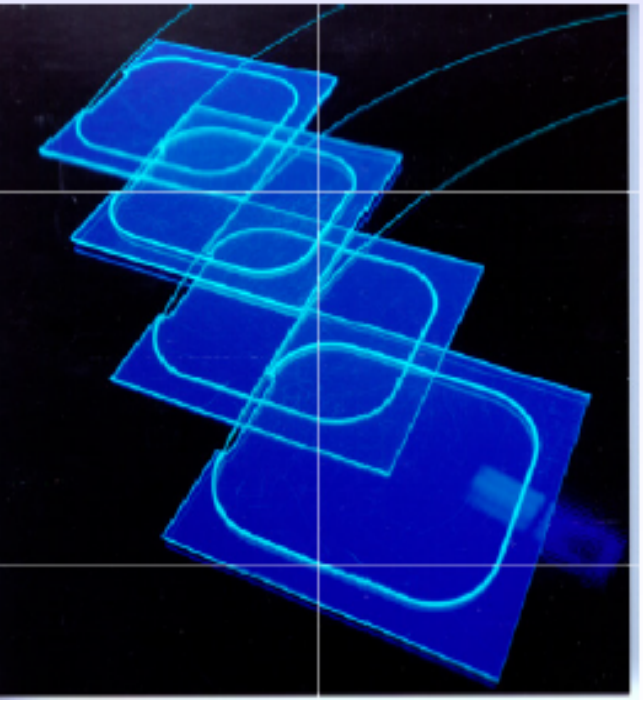

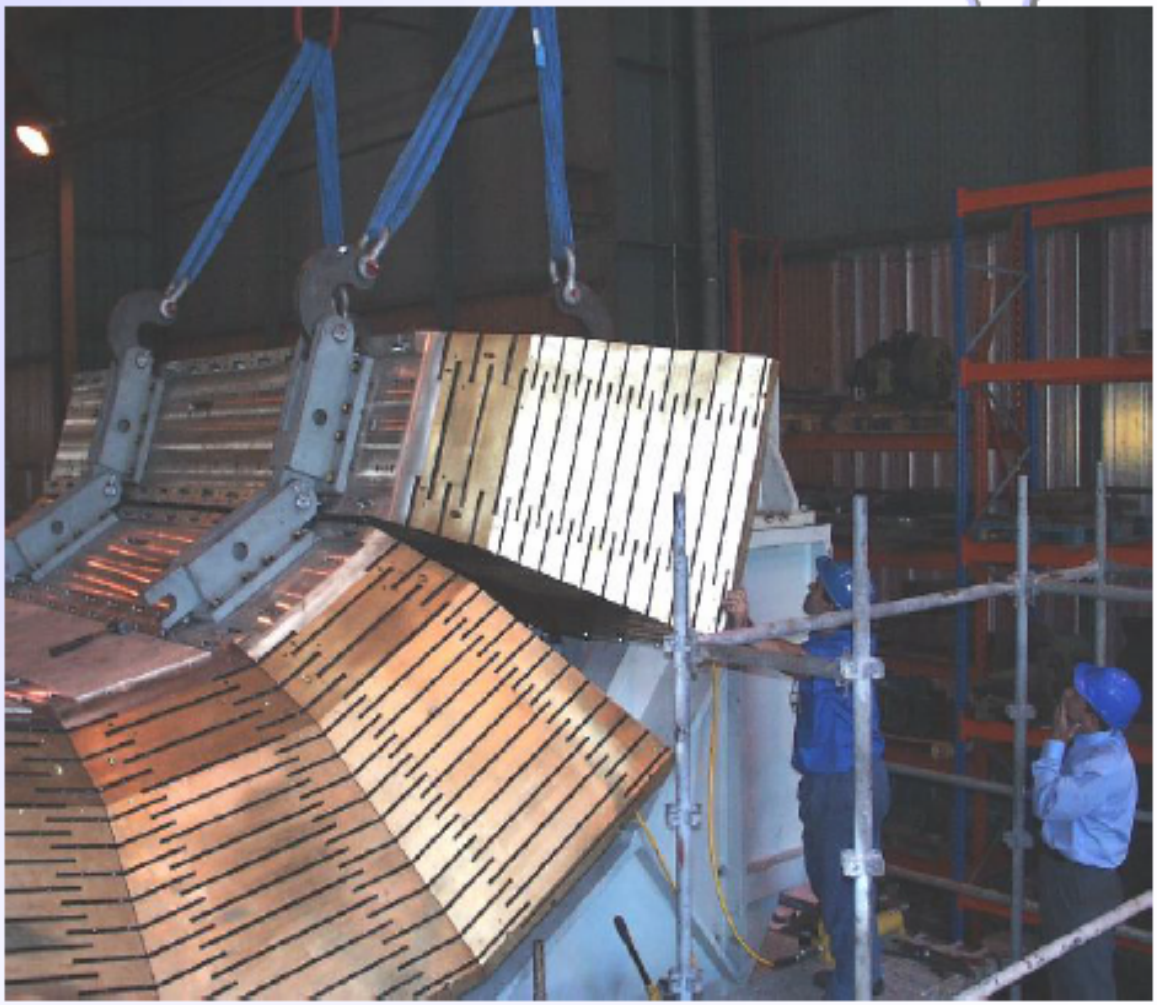

Test beam resolution for single hadrons

$$\frac{\sigma_E}{E} = \frac{65\%}{\sqrt{E}} \oplus 5\%$$

ATLAS Liquid Argon EM Calorimeter

LAr Sampling Calorimeter

- Passive, heavy absorber (Pb, 1.1–1.5 mm thick [barrel]) inter-leaved with active detector material (liquid argon)
  - Overall 22 X_0
  - Accordion structure for full ϕ coverage
  - Resolution: **~10% / $\sqrt{E}$** (stochastic)
- Granularity
  - Barrel: $\Delta\eta \times \Delta\phi = 0.025^2$ rad (main layer)
  - Longitudinal segmentation (3 layers)

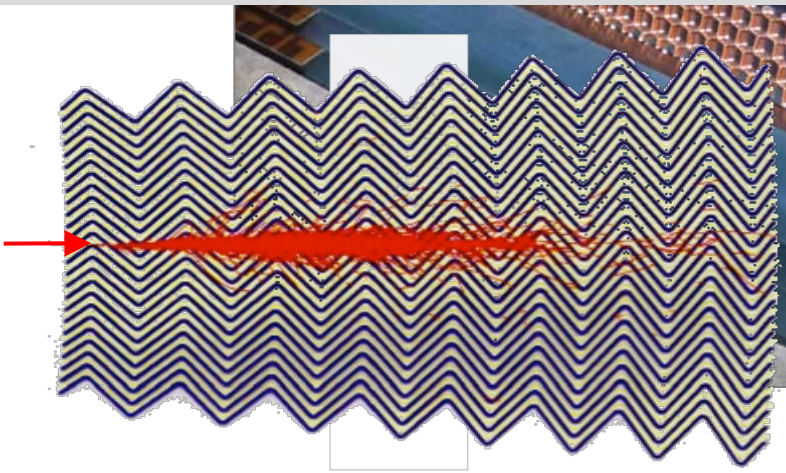

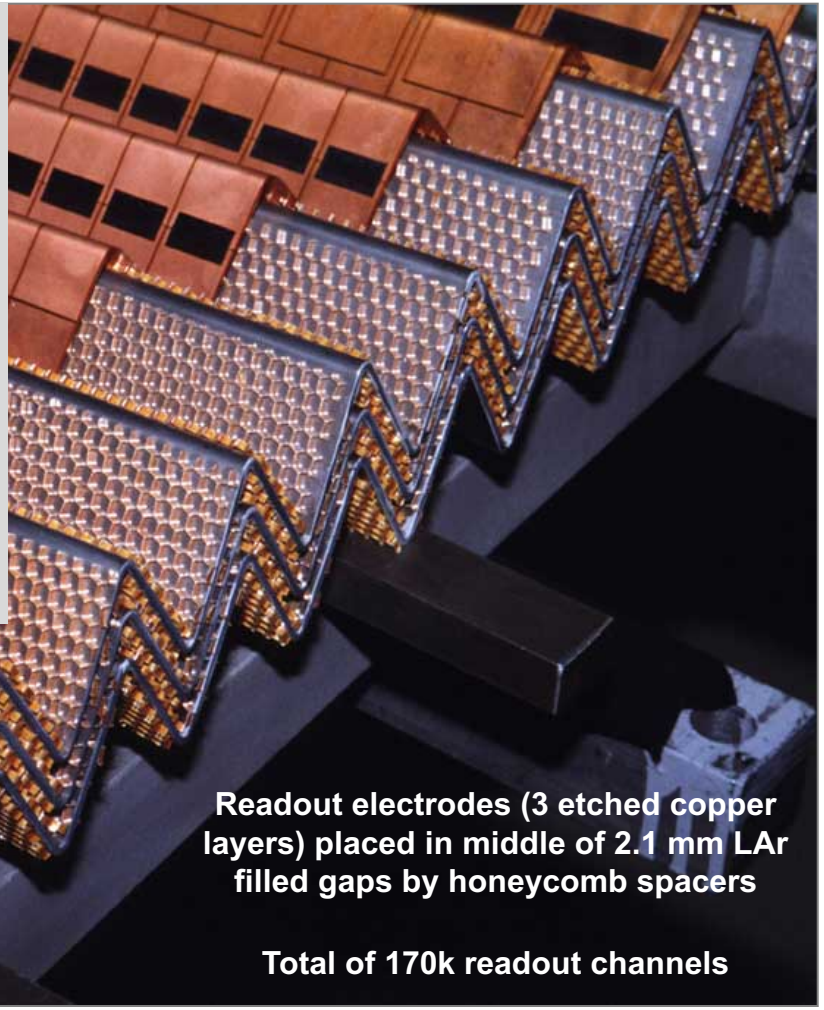

Readout electrodes (3 etched copper layers) placed in middle of 2.1 mm LAr filled gaps by honeycomb spacers

Total of 170k readout channels

Conclusions

- All particle detectors in nuclear, particle and astroparticle physics are based on the physics of the interaction of particles and radiation with matter
- It is possible to measure and reconstruct the interaction of elementary particles also in the very difficult environments of proton proton collisions at the LHC
- Many of the experiments today are large and complex, both in their concept and in the new technologies employed
- They are run by very large collaborations of scientists, engineers and also of students over periods of 10-20 years
- We live in exciting times and there is a lot more ahead of us, many opportunities for students

Message to students

- It is fun to work on these experiments and their data

Large colaborations: Where are the students?

- Sub divided in smaller groups
  - Detector, subdetector
  - Analysis: different topics
  - Students belong to instituts
- International environment
  - Communication skills !
  - Mobility
  - Good students become well known in the collaboration very fast!
- Management
  - Physicists are (generally) not trained for that
    changes with time...
  - Sometimes there are problems, one has to sort them out..
- Students are an extremely important factor
- job opportunities outside particle physics

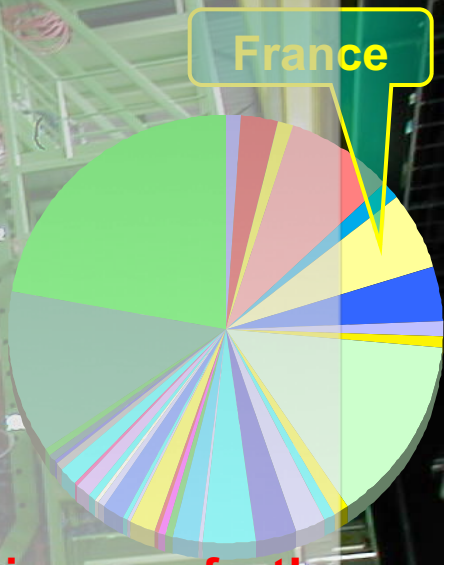

3300 Physicists and Engineers

39 Countries

172 Institutions

ATLAS and CMS EM Calorimeters

CMS: $PbWO_4$ Scint. Crystal Calorimeter

Entire shower in active detector material
- " High density crystals (28 X_0)
- " Transparent, high light yield
- " No particles lost in passive absorber
- " High resolution: ~3%/$\sqrt{E}$ (stochastic)

Granularity
- " Barrel: $\Delta\eta \times \Delta\phi = 0.017^2$ rad
- " Longitudinal shower shape unmeasured

Read out with avalanche photo diodes

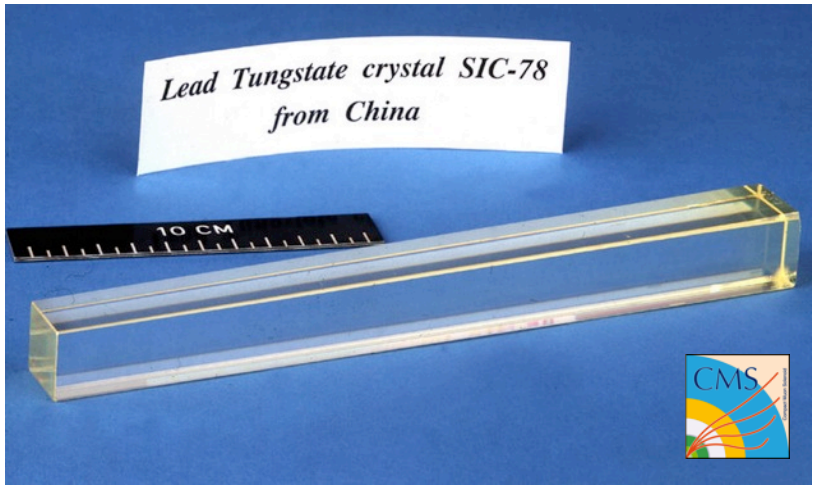

ATLAS: LAr Sampling Calorimeter

- Passive, heavy absorber (Pb, 1.1–1.5 mm thick [barrel]) inter-leaved with active detector material (liquid argon)
  - Overall 22 X_0
  - Accordion structure for full ϕ coverage
  - Resolution: ~10% / $\sqrt{E}$ (stochastic)
- Granularity
  - Barrel: $\Delta\eta \times \Delta\phi = 0.025^2$ rad (main layer)
  - Longitudinal segmentation (3 layers)

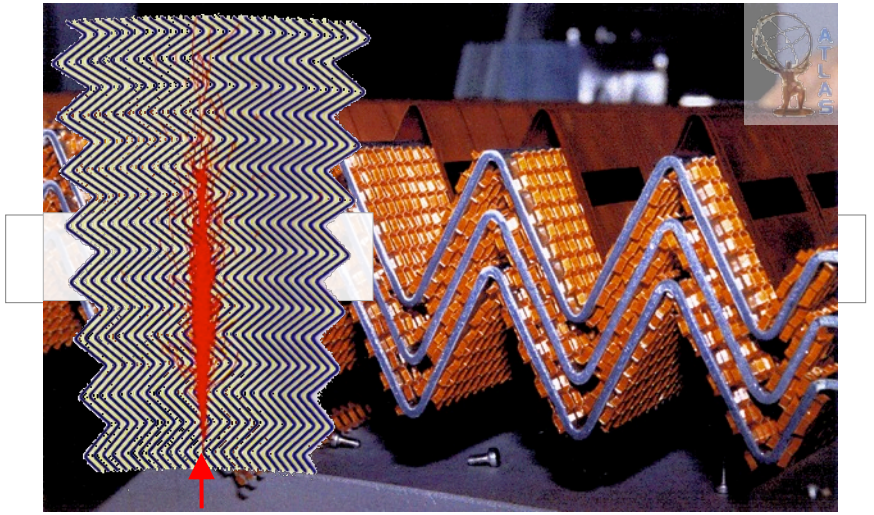

ATLAS electromagnetic Calorimeter

Accordion geometry absorbers immersed in Liquid Argon

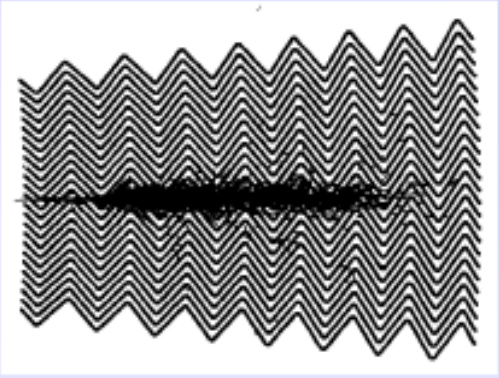

Liquid Argon (90K)

+ lead-steal absorbers (1-2 mm)

+ multilayer copper-polyimide readout boards

→ Ionization chamber.

1 GeV E-deposit → 5 x10^6 e^-

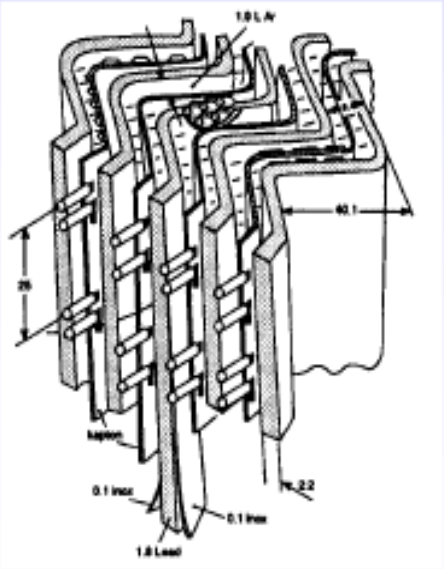

- Accordion geometry minimizes dead zones.
- Liquid Ar is intrinsically radiation hard.
- Readout board allows fine segmentation (azimuth, pseudo-rapidity and longitudinal) acc. to physics needs

Test beam results $\sigma(E)/E = 9.24\%/\sqrt{E} \oplus 0.23\%$

Spatial resolution ≈ 5 mm / √E

Two-dimensional read-out via cathodes

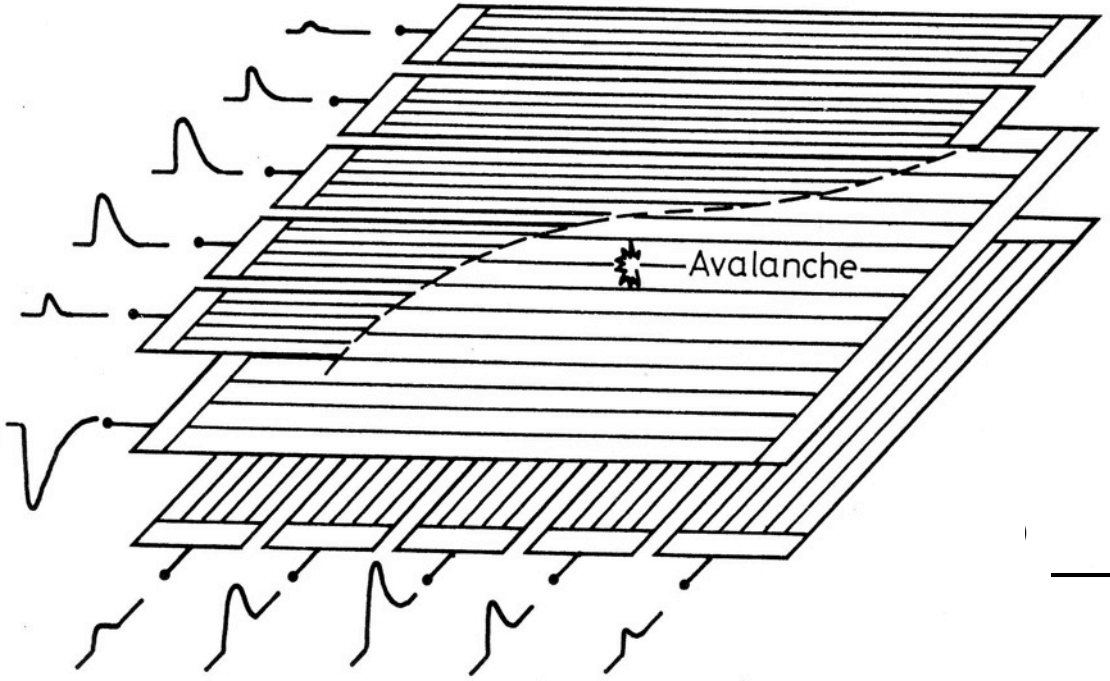

Fig. 6.11. Bidimensional readout using cathode strips (from *Breskin* et al. [6.18]). The signals from each strip are stored and the center of gravity of the distribution calculated to yield the position of the avalanche

$$y = \frac{\sum (Q_i - b) y_i}{\sum (Q_i - b)} ,$$

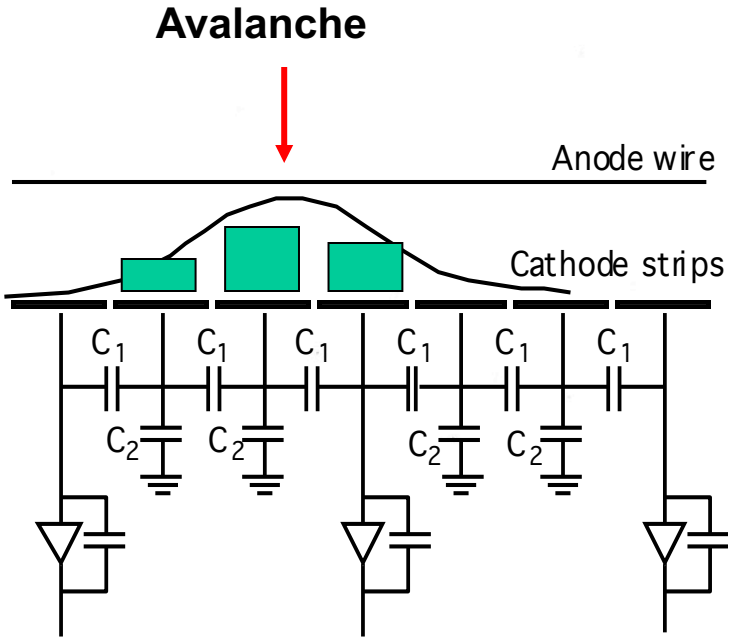

RPC – Resistive Plate Chamber

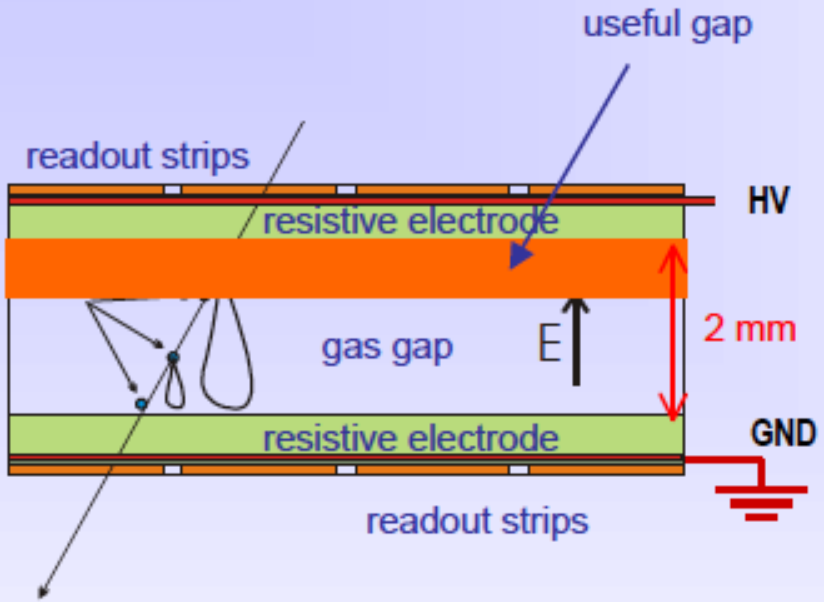

MRPC

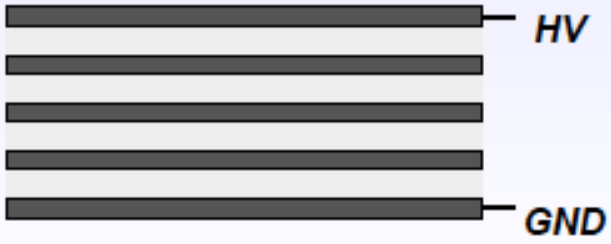

Multigap RPC - exceptional time resolution suited for the trigger applications

Rate capability strong function of the resistivity of electrodes in streamer mode.

A. Akindinov et al., NIM A456(2000)16

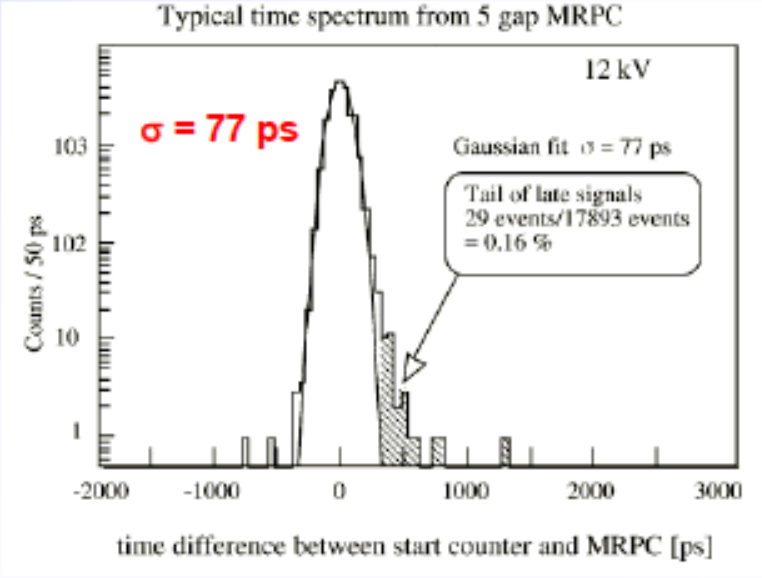

Time resolution

CERN Academic Training Programme 2004/2005

Ge ionization – phonon detectors I

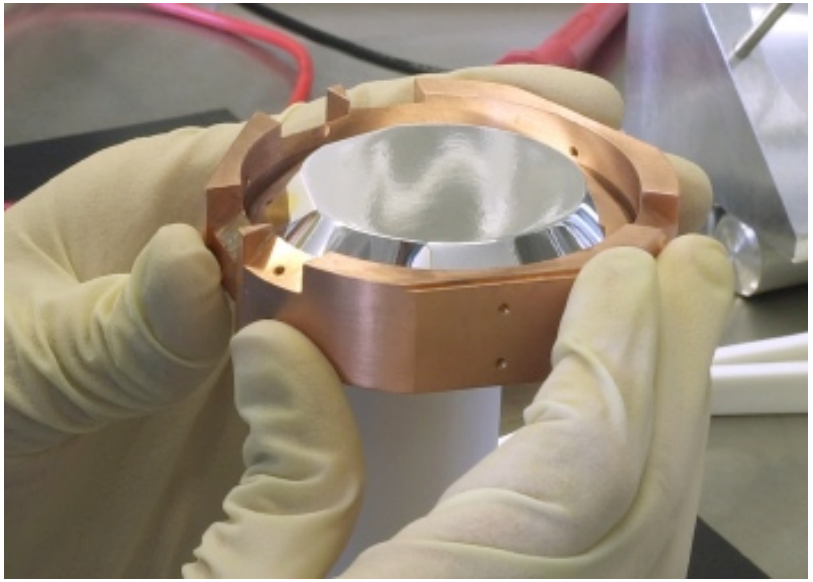

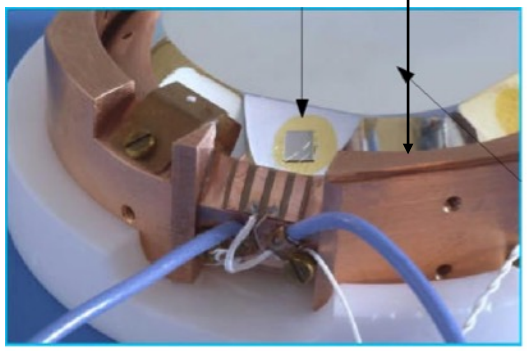

- bolometer mass: 320 g
- 100nm sputtered Al layer as electrode (center + guard ring)
- 60nm Ge(Si) amorphous layer below electrode
- NTD sensor glued on sputtered gold pad on guard ring electrode
- electrical contacts/heat links via gold wire bonding (Ø=25µm)
- **operating temperature T=17.00±0.01mK**

Charged Coupled Device (CCD)

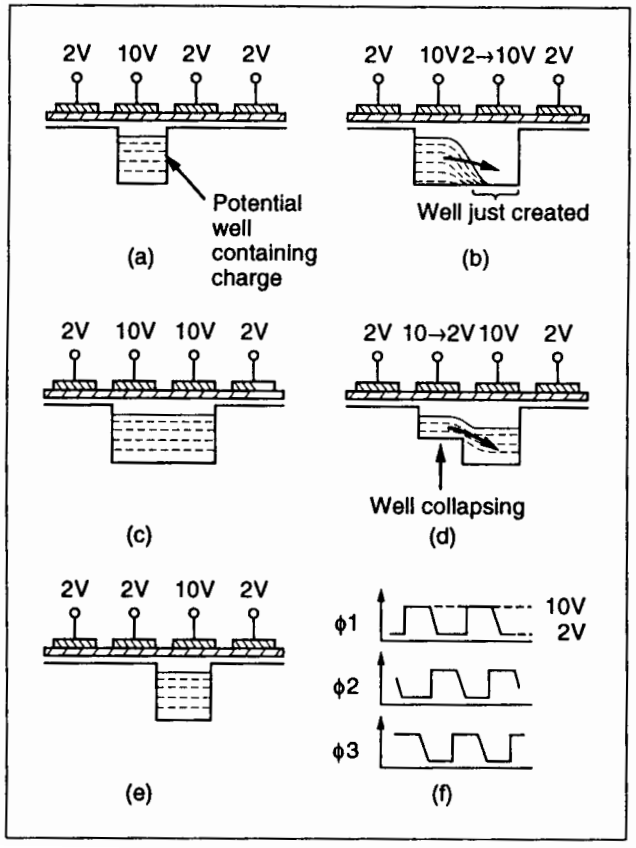

CCD detector : movement of potential well and associated charge packet by clocking of gate voltages

Principe :

- Le CCD est un dispositif qui assure en même temps les fonctions de conversion photoélectrique, d'accumulation de charge électrique du signal et de transmission de la charge du signal.
- Lorsqu'une charge est créée dans un pixel, elle est maintenue dans le substrat grâce au potentiel appliqué sur la grille (colonne) de lecture.
- Après un temps d'intégration fixe, les charges de tous les pixels d'une même colonne sont transférées simultanément vers le convertisseur Analogique Numérique.
- Le mouvement des puits de potentiels est donné par un jeu d'horloges décalées.
- Ils ont les avantages de la miniaturisation, légèreté, solidité et durabilité.
- Leurs applications progressent rapidement vers les capteurs de vision des robots intelligents, caméra vidéo etc...

IPHC
Institut Pluridisciplinaire
Hubert CURIEN
STRASBOURG

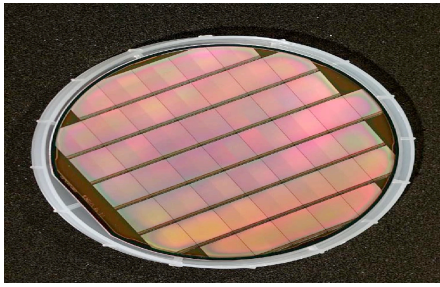

Monolithic Active Pixel Sensors IPHC

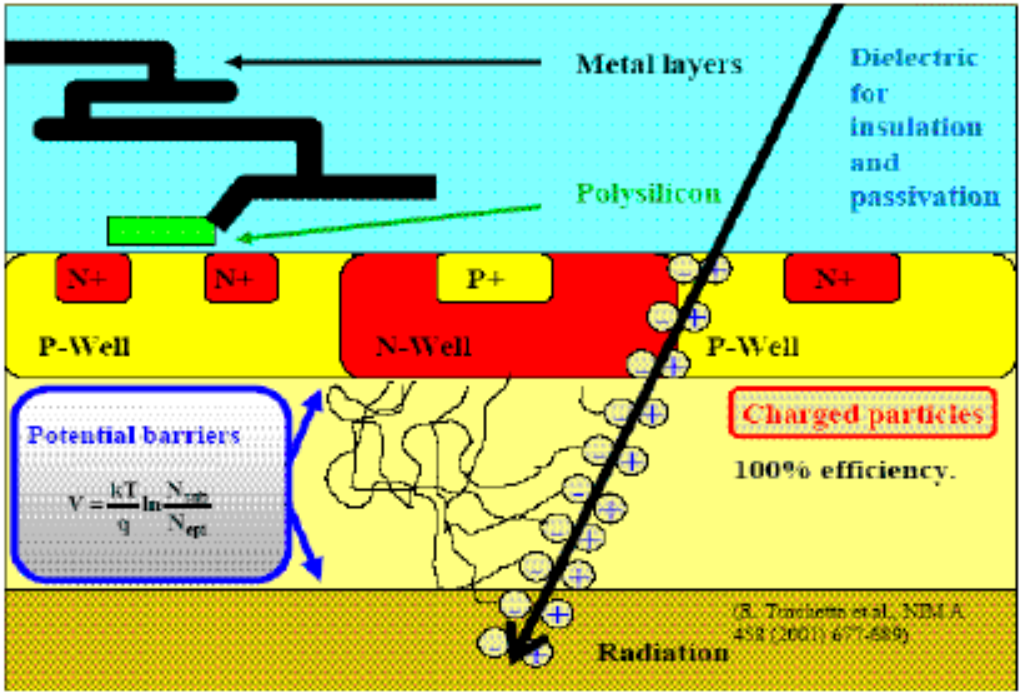

- charge collected at n-well / p-epi diode
- thermal diffusion of free charge
- reflection at potential barriers between areas with different doping concentration
- no depletion voltage applied
  ⇒ potential formed by different doping concentrations only

Détection des photons par un semi-conducteur: Les photodiodes

- Dans le silicium (E_g≈1.1eV) l'efficacité quantique η est proche de 100% pour des photons de 200- 900 nm
- Pas d'amplification,
- Grande stabilité
- Bruit électronique par le courant de fuite thermique
- Résolution en énergie pire que pour un photomultiplicateur
- Utilisation en spectroscopie gamma limité

$$\eta = \frac{\text{Courant généré (Amp)}}{\text{Puissance incidente (Watt)}}$$

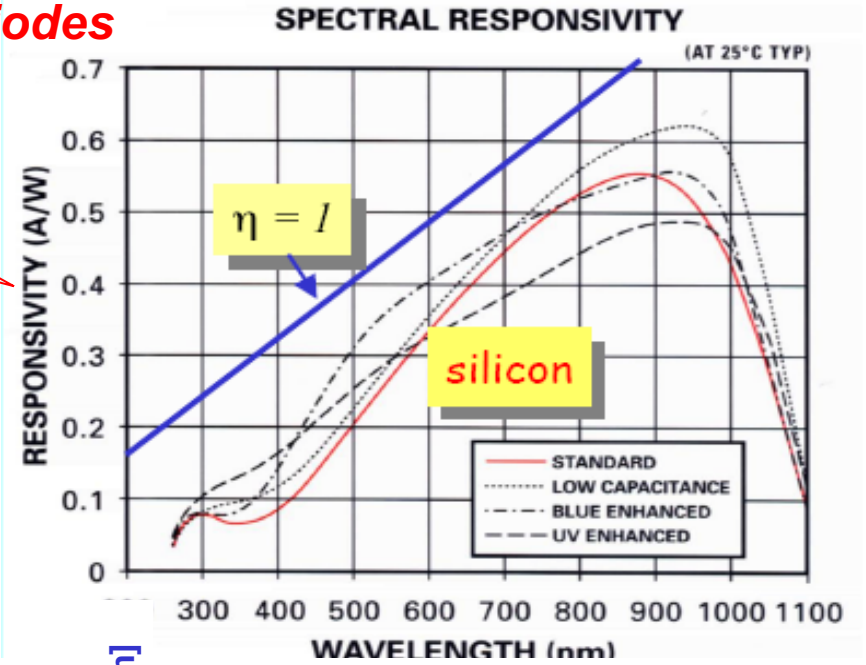

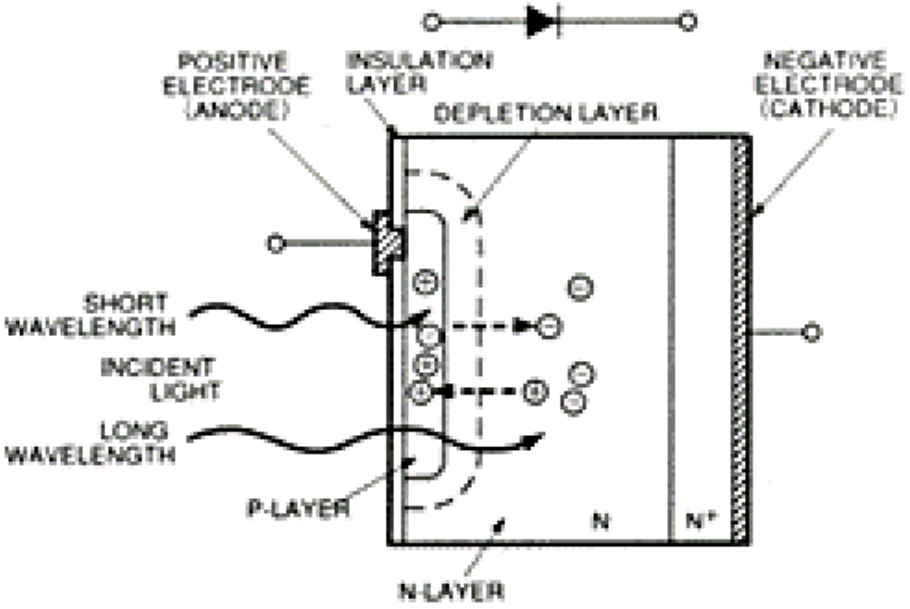

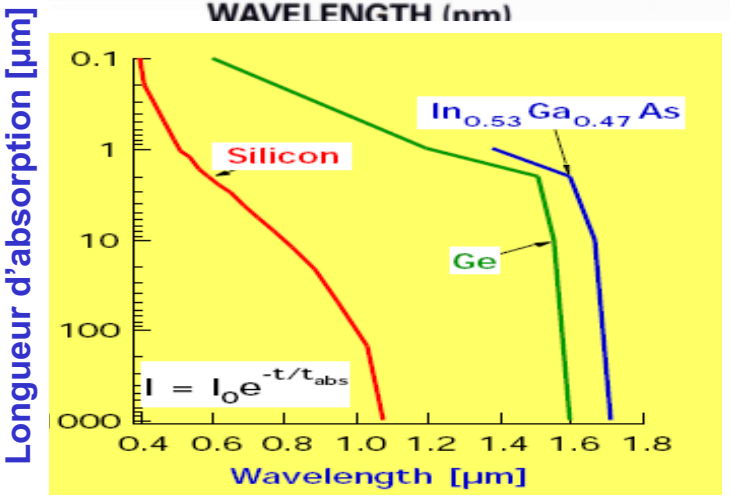

Avalanche photodiodes

- **p-n diode**
  - Champ électrique est maximal à la jonction
  - Au-dessous de seuil pour ionisation par l'impact
  - Emax » 2V /d ~ kV/cm
- **APD**
  - le profile est donné par la dopage, des champs plus important

Pro

  - Gain, important pour les signaux faibles
  - Reponse rapide (champ élevé)
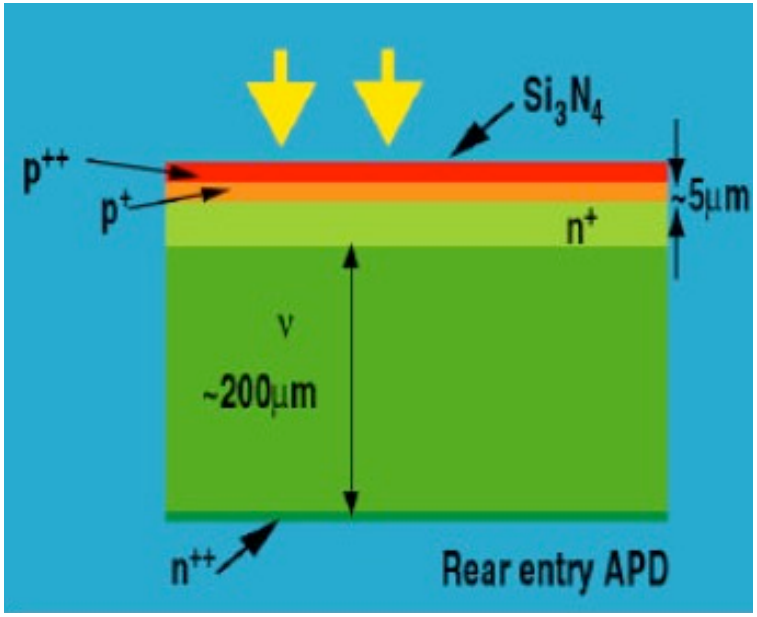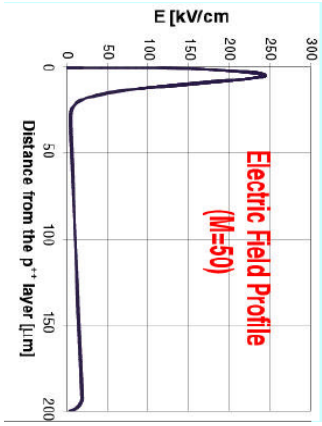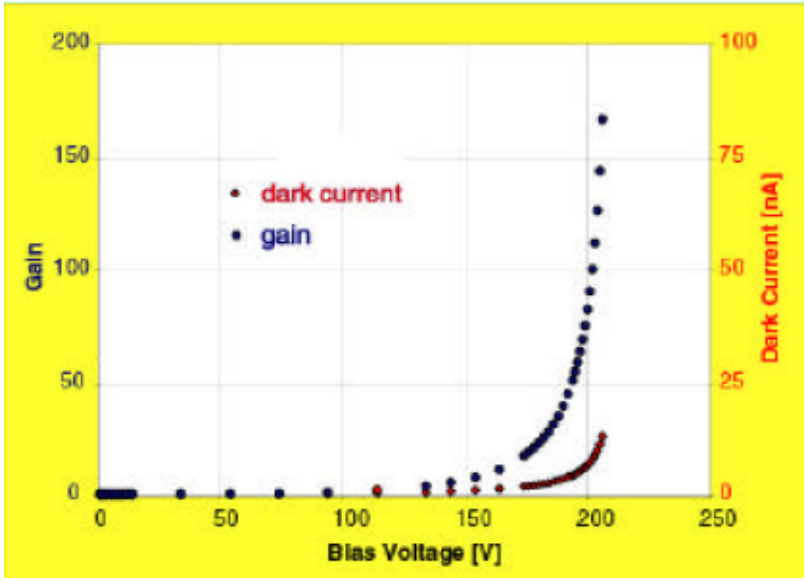
- **Con**
  - Risque d'instabilité
  - Courant de fuite est amplifié également (bruit)